

# Plant Plasticity in Intercropping: Mechanisms and Consequences

Junqi Zhu

## **Thesis committee**

### **Promotor**

Prof. Dr N.P.R. Anten

Professor of Crop and Weed Ecology

Wageningen University

### **Co-promotor**

Dr J.B. Evers

Assistant professor, Centre for Crop Systems Analysis

Wageningen University

Dr W. van der Werf

Associate professor, Centre for Crop Systems Analysis

Wageningen University

### **Other members**

Prof. Dr L.F.M. Marcelis, Wageningen University

Dr R. Pierik, Utrecht University

Dr D. Makowski, INRA, Thiverval-Grignon, France

Dr J. van Ruijven, Wageningen University

This research was conducted under the auspices of the C.T. de Wit Graduate School for Production Ecology and Resource Conservation

# **Plant Plasticity in Intercropping: Mechanisms and Consequences**

**Junqi Zhu**

## **Thesis**

submitted in fulfilment of the requirements for the degree of doctor  
at Wageningen University  
by the authority of the Rector Magnificus  
Prof. dr M.J. Kropff,  
in the presence of the  
Thesis Committee appointed by the Academic Board  
to be defended in public  
on Thursday 8 January 2015  
at 11 a.m. in the Aula.

Zhu, J. (2015)

Plant plasticity in intercropping: mechanisms and consequences,  
196 pages.

PhD thesis, Wageningen University, Wageningen, NL (2015)  
With references, with summaries in English, Dutch and Chinese

ISBN: 978-94-6257-219-5

## Abstract

Diverse agricultural system such as intercrop is practised widely in developing countries and is gaining increasing interest for sustainable agriculture in developed countries. Plants in intercrops grow differently from plants in single crops, due to interspecific plant interactions and heterogeneous resource distribution, but adaptive plant morphological responses to competition in intercrops have not been studied in detail. This thesis aims to link the performance of an intercropping system with plasticity in plant traits.

Grain yield of border-row wheat of an intercrop was 141% higher than in sole wheat. The yield increase was mainly associated with plasticity in tillering and leaf sizes. Compared to maize in monoculture, maize in intercrops had lower leaf and collar appearance rates, larger blade and sheath sizes at low ranks and smaller ones at high ranks. The data suggest many of those changes are linked to each other through feedback mechanisms both at plant level and at phytomer level. A model of maize development was further developed based on three coordination rules between leaf emergence events and dynamics of organ extension. Flexible timing of organ development can emerge from the model as well as the distribution of leaf sizes over ranks. A wheat-maize architectural model was developed for quantifying the role of architectural trait plasticity in light capture in intercrop. Simulated light capture was 23% higher in intercrop with plasticity in traits than the expected value weighted from the light capture in sole crops. Thirty-six percentage of the light increase was due to intercrop configuration alone and 64% was due to plasticity.

Overall, this thesis clearly shows the importance of plasticity in architectural traits for overyielding in wheat-maize intercropping and probably in diversified cropping systems in general. Thus it points to a previously under-appreciated mechanism driving the relationship between species diversity and overyielding of plant communities.



# Contents

Chapter 1	General introduction	1
Chapter 2	Overyielding of wheat in intercrops is associated with plant architectural responses that enhance light capture	15
Chapter 3	Early competition shapes maize whole-plant development in mixed stands	39
Chapter 4	Towards modelling the flexible timing of shoot development: simulation of maize organogenesis based on coordination within and between phytomers	63
Chapter 5	The contribution of plastic architectural traits to complementary light capture in plant mixtures	87
Chapter 6	General discussion	109
	References	127
	Appendix I	143
	Appendix II	147
	Appendix III	151
	Appendix IV	161
	Summary	177
	Samenvatting	181
	摘要	185
	Acknowledgements	187
	Publication list	191
	PE&RC Training and Educational Statement	193
	Curriculum vitae	195



# CHAPTER 1

## General introduction

## Overall objectives

One of the most important challenges facing society today is to produce enough food to meet the demand of a growing and more affluent world population, while simultaneously reducing agriculture's environmental impact. Increasing the area of land used for agriculture entails the conversion of natural habitats, and thus leads to losses in biodiversity, and carbon storage, and is therefore not a sustainable means of increasing food production. Most of this increase will therefore need to be achieved by agricultural intensification on the current cultivated area. Both ecological and agricultural literature show that productivity, nutrient retention by soil, and resilience to stress (diseases and pests) tend to increase with the number of species in one field. Thus, diverse agricultural systems such as intercrops (i.e., a situation where different crop species are grown together in a field) could contribute to sustainable intensification. Yet, contrary to decades of crop improvement in sole cropping, little quantitative research has been done to determine the traits of cultivated species that drive the positive effects that have been shown for intercropping. There is, therefore, ample scope to further increase the advantages of intercropping systems, by optimizing crop traits in relation to the specific conditions in intercrop systems. Inter-cropping inherently entails growing plants in a heterogeneous environments, i.e., intra- and interspecific interaction occurring in different plant arrangements. Phenotypic plasticity, the ability of a genotype to adjust their phenotype under different environmental conditions (Sultan, 2000; Pigliucci *et al.*, 2006) is likely to play an important role in this regard. The overall objective of this thesis therefore is to understand how plant growth in intercrops differ from that in monocrops, and how plasticity in plant development and growth contributes to the performance of an intercrop.

This introductory chapter aims to provide context and articulate the relevant research questions on: (i) intercropping; (ii) plant responses to environmental cues; (iii) nature and regulation of plastic responses; (iv) the role of plant plasticity in resource capture. I integrate these issues through a combination of experiments and modelling.

## Intercropping as a sustainable agricultural system

Despite a substantial increase in food production over the past half-century, one of the most important challenges facing the world today is still how to feed a rapidly growing population (Fischer *et al.*, 2014). The global population is projected to reach ~9.3 billion by 2050 (FAO, 2011), which is considerably more than the current population of slightly over 7 billion. In the light of population growth and economic progress, Alexandratos and Bruinsma (2012) projected that the demand for cereals will rise by 44%, while demands for meat, sugar and vegetable oil will increase by 70-90% between 2005-07 and 2050 (including expansion of bioenergy crops). However, the need for increased food production should be viewed in relation to the considerable environmental impact of agriculture. Agriculture is currently already a dominant cause of many environmental threats, including climate change, biodiversity loss, deforestation and degradation of land and freshwater (Foley *et al.*, 2011). Thus, the goal of agriculture is no longer simply to maximize productivity, but to simultaneously reduce its environmental impact (Pretty *et al.*, 2010). Foley *et al.* (2011) suggested a number of solutions to reach this goal, e.g. stopping the expansion of agriculture area, closing yield gaps, increasing agricultural resource efficiency, shifting diets towards less meat and reducing food waste. An alternative solution for reaching part of this goal could be the practice of intercropping, because of its proven advantages in productivity (Li *et al.*, 2001; Zhang *et al.*, 2007), climate resilience (Horwith, 1985; Rusinamhodzi *et al.*, 2012), suppression of pests and airborne diseases (Zhu *et al.*, 2000; McDonald and Linde, 2002), carbon storage and nitrogen retention in the soil (Makumba *et al.*, 2007; Cong *et al.*, 2014).

Intercropping is an old and commonly used cropping practice in Asia, Africa, and Latin America, and used to be a common practice in Europe and United States before the 1940s (Machado, 2009; Vandermeer, 2011). The relative reduction in the importance of intercropping in the past half century across the world is probably due to difficulties encountered in the mechanization of intercropping, and the availability of relatively cheap synthetic fertilizer and pesticides which make monocropping more economically efficient (Machado, 2009). However, intercropping still provides

~20% of world food supply especially in the most vulnerable areas such as sub-Saharan Africa and large parts of Latin America (Altieri, 2009; Chappell *et al.*, 2013). Over the last decade, intercropping has drawn interest as a means for strengthening the ecological basis of agriculture both in developing and developed countries (Zhang and Li, 2003; Eichhorn *et al.*, 2006; Knörzer *et al.*, 2009; Lichtfouse *et al.*, 2009; Lithourgidis *et al.*, 2011).

The most common advantage of intercropping is higher productivity per unit of land than the weighted (by their relative density in intercrop) mean of sole crops (Loreau and Hector, 2001)(Eq.1.1):

$$\Delta Y_i = Y_{o,i} - Y_{e,i} = Y_{o,i} - RD_i \times M_{o,i} \quad (\text{Eq. 1.1})$$

where  $Y_{o,i}$  is the observed yield of species  $i$  in intercrop.  $Y_{e,i}$  is the expected yield of species  $i$  in intercrop, calculated as the product of its yield in monoculture ( $M_{o,i}$ ) and its the relative density in intercrop ( $RD_i$  defined as density of species  $i$  per unit intercrop land area, divided by density in monoculture).  $Y_{e,i}$  is calculated under the null hypothesis that each individual plant in intercrop performs the same as plants in monoculture.  $\Delta Y_i$  larger than zero means species  $i$  is overyielding in intercrop compared to monoculture. Otherwise it is underyielding. When the sum of  $\Delta Y_i$  for all species is larger than zero, then the intercrop has a higher productivity per unit of land area compared to sole crops. The same formula can also be used to calculate resource capture, e.g. light and nitrogen. The overyielding of species in intercrops is attributed mainly to complementarity in resource capture, e.g. light, nitrogen and phosphorus (Morris and Garrity, 1993a; Li *et al.*, 2001; Zhang, 2007; Zhang *et al.*, 2008a).

Moreover, intercropping suppresses pests and diseases through increasing biodiversity and environmental heterogeneity at local scale which reduces the rate of dissemination (McDonald and Linde, 2002; Ratnadass *et al.*, 2012). For instance, mixtures of different rice varieties were found to reduce the severity of rice blast by 67%-94% compared to monoculture (Zhu *et al.*, 2000; Zhu *et al.*, 2005). Kimani *et al.* (2000) showed that airborne volatiles from *Melinis minutiflora* repelled oviposition by the spotted stem borer on intercropped maize. Intercropping may improve soil fertility through biological nitrogen fixation with the use of legumes (Fujita *et al.*, 1992; Giller and

Cadisch, 1995), and enhance soil organic carbon content through larger input of root biomass as compared to monoculture (Makumba *et al.*, 2006; Cong *et al.*, 2014). In addition, intercropping reduces the risk of crop failure associated with drought or unpredictable rainfall because it has multiple crops with different temporal profiles of water requirement in one field (Ghosh *et al.*, 2006; Rusinamhodzi *et al.*, 2012; Mulugeta, 2014).

Yet, while the advantages of intercropping have long been known, the underlying mechanisms are still poorly understood because of their complex nature. The success of an intercrop system depends on the understanding of the physiology and growth habits of the species to be cultivated together, their canopy and root architecture, and their resource acquisition (light, water and nutrient). The complex interactions between those factors make it hard to interpret the mechanisms underlying the advantages of intercropping. Thus, most research on intercropping has been rather descriptive simply documenting the extent to which intercropping results in yield advantage, than trying to understand how intercropping systems exactly work and testing hypotheses about the mechanisms that result in the advantage of intercropping (Connolly *et al.*, 2001).

Recent studies however started to delve into these mechanisms. For instance, Li *et al.* (2007) showed that maize roots avoided those of wheat in intercrop, but grew near roots of faba bean due to better phosphorus availability near faba bean roots. They further characterized this as a nutrient-mobilization-based facilitative interaction (Li *et al.*, 2014), that is, maize roots grow away from a neighbour with which it competes (wheat) but towards one that provides facilitation (bean). Zhang *et al.* (2008b) found that increased radiation interception by wheat and cotton in wheat-cotton intercrop fully explained the high land-use efficiency of this system. However, no detailed studies have been done on individual plant development throughout the development cycle in intercrop. Hence the role of plant plasticity in enhancing the productivity of an intercrop is largely unknown (Connolly *et al.*, 2001). In this thesis I aimed to fill this knowledge gap by addressing the following three research questions: (1) how do plants in intercrops grow? (2) how are plant responses to the conditions in intercrops regulated? (3) what are the consequences of plastic responses for resource capture and productivity?

Information on these questions is crucial for optimizing intercropping systems in terms of crop trait selection, system design and yield benefits. To this end, I use wheat-maize relay strip intercrop as a model system (Fig. 1.1).

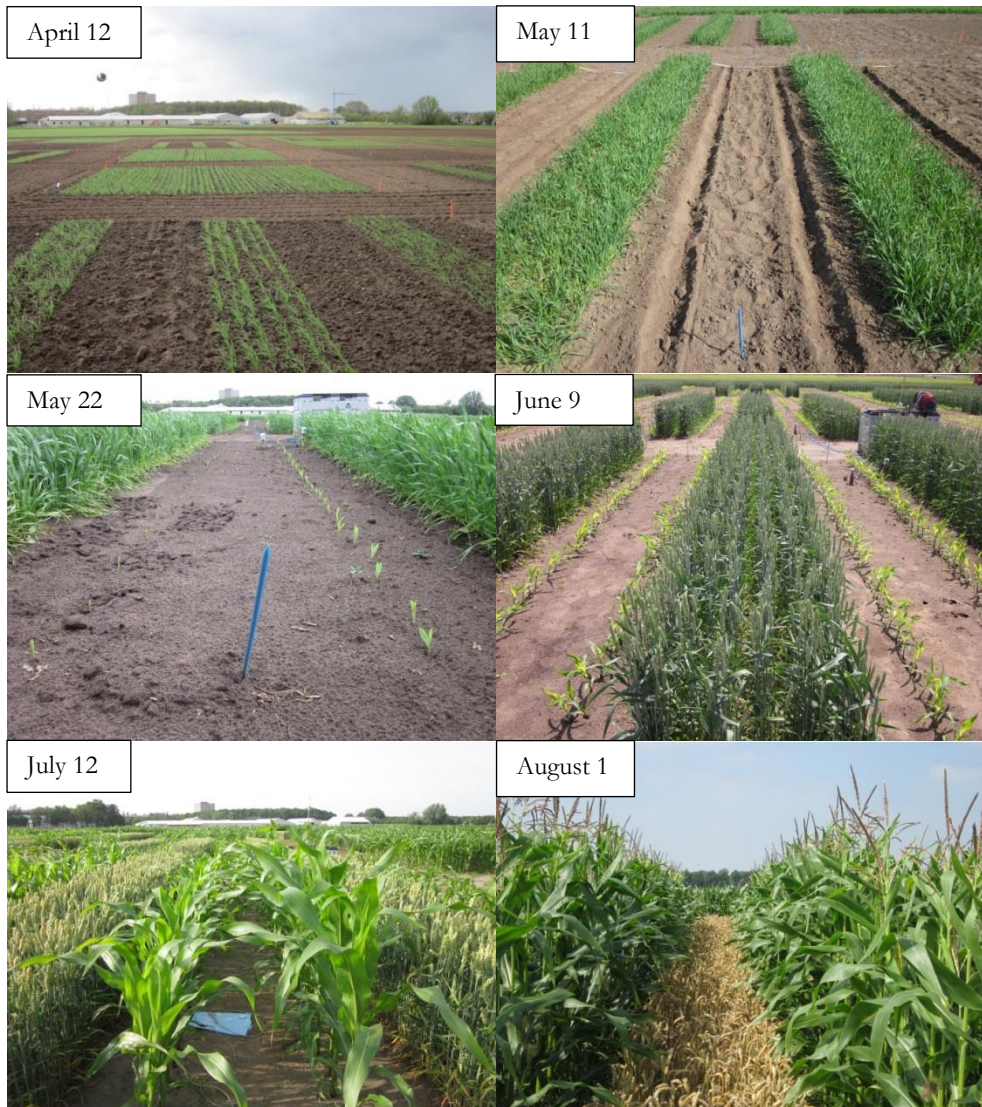


Fig. 1.1 Field views of wheat-maize relay intercropping with alternating strips of 6 rows of wheat or two rows of maize throughout the growing season in Wageningen in 2011. Wheat was sown on March 9, and harvested on August 10, while maize was sown on May 11, and harvested on October 14.

## Wheat-maize intercropping system

Wheat and maize are two of world's three biggest cereals besides rice (Fischer *et al.*, 2014). Together, wheat and maize account for ~40% of the annually harvested area globally, and directly provide ~30% of world food calories (Fischer *et al.*, 2014). Intercropping of wheat and maize is a common practice in North-Western China (including the autonomous regions of Xinjiang and Ningxia and the provinces of Shaanxi, Gansu, and Qinghai). For instance, 43% of the total cereal yields are derived from this type of intercropping in Ningxia province (Li *et al.*, 2001). In this region, the part of the year that is suitable for crop production extends beyond the duration of a single crop, from sowing to harvest, but is too short to grow two crops in succession. This provides an incentive for wheat-maize relay strip intercropping. In this system, strips of spring wheat are sown in March, with a strip of bare soil between the wheat strips. Maize is inter-sown in these bare strips in late April. After wheat harvest in early July, maize continues to grow as a sole crop until its harvest on early October (Fig. 1.1). The yield advantage of this system may vary with relative density of wheat and maize. Li *et al.* (2010) showed that this system can produce approximately 70% of the wheat yield of a sole wheat and 48% of the maize yield of a sole maize at a relative density 0.48 for wheat and 0.52 for maize.

In this thesis, I hypothesized that enhanced light capture explains most of the yield advantage of a wheat-maize intercropping system under well-managed conditions (fertilization, irrigation, weed and disease control). This hypothesis is based on the realization that under well-managed conditions, competition for water and nutrients between species is probably weak because they are abundantly available in the soil. This is because competition for water and nutrient is 'size symmetric' with smaller and larger individuals acquiring proportional amounts of resources (Weiner, 1990). In contrast, shoot competition for light is generally believed to be 'size asymmetric' as taller individuals shade shorter ones and can therefore capture more than light relative to their size (Dybzinski and Tilman, 2009). The enhancement in light capture is in part related to the relay aspect of the system: wheat is sown before maize, and maize keeps growing after wheat is harvested. Thus, over the entire

year, the intercrop system can capture more light, as compared to single crop systems. However, this temporal niche differentiation between the two crop species may not be sufficient to account for the productivity advantage in intercrops. A further mechanism that may play an important role is plasticity of plants in response to the available space and resources. Plants adapt their structure and function to the available space and resources. That is: individual plants in intercrops are likely to be phenotypically different from those in sole crops as a result of functional and structural plasticity in response to the different light environment in intercrop as well as other cues. These plastic responses influence and determine the share of the light captured by the components in an intercrop system, and can putatively enhance the total resource acquisition and productivity.

### Plant morphological responses to light quantity and quality

Plants display plastic responses to a wide variety of ecological conditions including variation in the abiotic environment, disturbance, herbivory, parasitism, mutualistic relationships, and the presence, absence or identity of neighbours (Bradshaw *et al.*, 1965; Schlichting, 1986; Chen *et al.*, 2012). Competition for light to drive photosynthesis is a key process determining the growth of plants in dense communities (Mohr, 1964). The amount of light captured affects all aspects of plant development and growth through a positive feedback between light capture, assimilate production and organ growth. In addition to providing energy (light quantity), the quality of light also conveys important environmental information to plants, enabling the prediction of the season and the determination of spatial orientation (Franklin and Whitelam, 2007). In particular, the ratio of red to far-red radiation (R: FR) is an important cue by which plants can detect environmental variation in vegetation shade, both from overstory foliage and from neighbours (Smith, 2000). This cue is specifically important for plants grown in dense stands since a decrease in R: FR serves as an indicator of competition with neighbours for light. In competition for light, plants adjust their architecture to bring the leaves higher in the vegetation where more light is available than in the lower strata. These architectural responses include accelerated elongation of the hypocotyl, internodes and petioles, upward leaf movement (hyponasty), and

reduced shoot branching are collectively referred to as the shade avoidance syndrome (Pierik and de Wit, 2013). In gramineous species, e.g. wheat (*Triticum aestivum*) and maize (*Zea mays*), typical shade avoidance responses include an increase in height (internode and sheath length) (Fournier and Andrieu, 2000b), an increase in blade length (Casal *et al.*, 1985), a reduction in tillering (Evers *et al.*, 2006), a higher shoot/root ratio (Kasperbauer, 1986), and a change in leaf orientation towards gaps (Maddonni *et al.*, 2002). In addition, radiation in the blue and ultraviolet A (UVA) wavelengths can also trigger a wide range of responses, including phototropism, chloroplast migration (reallocating of nitrogen) and stomatal opening (Briggs and Christie, 2002). These plastic responses play an important role in optimizing photosynthetic rate (Drouet and Bonhomme, 1999). Furthermore, plants display various responses to the same environment signal depending on their development stage. Novoplansky *et al.* (1994) show that the annual legume *Onobrychis squarrosa* responds to light conditions in early season by adjusting the number of branches, while it responds to light conditions in late season by changing the number of leaves and fruits. In this thesis, regarding plants growth in intercrop and their plastic responses, I address the following research question.

RQ 1: *What are the main responses of wheat and maize assemblies to a heterogeneous light environment in intercrop (chapters 2 and 3)?*

### Coordinated plant development

To understand plant plastic responses to environmental change such as those created by intercropping, it is important to realise that many of those plastic responses are coordinated (Schlichting, 1986). A plant is built by the repeated formation, expansion, and (partial) senescence of phytomers (Forster *et al.*, 2007). A phytomer of gramineous species consists of an internode with an axillary bud at the bottom, and a node, a leaf sheath, and blade at the top. Like all organisms, plants are highly integrated systems in which the growth of one organ (blade, sheath and internode) is strongly correlated with the growth of other organs (Xu *et al.*, 2013). Thus a local plastic response by an organ may alter the response of the plant to later conditions. However, the extent to which such sequential dependencies play a role in determining plant growth and development is still largely unclear as little is known about how local

plastic responses shape and influence the development of whole plant architecture (Beemster *et al.*, 2003; de Kroon *et al.*, 2005). This lack of knowledge hampers a systematic evaluation of the effects of local plastic response on the performance at plant and community level.

Experimental results indicate that plant growth is partly controlled by the architecture itself (Fournier *et al.*, 2005; Verdenal *et al.*, 2008). During the vegetative stages of maize and rice, blade tip appearance is synchronized with the initiation of the sheath at the same phytomer (Andrieu *et al.*, 2006; Parent *et al.*, 2009). In maize, emergence of the leaf collar is associated with a decline in elongation rate of the sheath and an increase in elongation rate of the internode, with the sum of the two remaining the same (Fournier and Andrieu, 2000b; Fournier and Andrieu, 2000a). Furthermore, in cereals and grasses, the depth of the sheath tube formed by preceding sheaths influences the elongation rates and final lengths of the blades and sheaths that grow within it (Davies *et al.*, 1983; Wilson and Laidlaw, 1985; Casey *et al.*, 1999). Thus, early growth processes, by affecting the depth of the sheath tube, affect later growth processes. Because of the positive effect of the length of one sheath on the length of the next (Andrieu *et al.*, 2006), changes in the length of lower sheaths would continue to propagate to upper sheaths and thus also to blades.

Understanding how these coordination rules (e.g. synchrony between emergence events and dynamics of organ extension) scale to structural development of whole plant requires a structural plant growth model that is based on these rules. However, such a modelling approach has not been developed. In this thesis, with regard to coordination between plastic responses, I address therefore the following research question.

RQ 2: *How and to what extent can whole-plant structural development in maize emerge from coordination rules at organ level (chapters 3 and 4)?*

### **The role of plant plasticity in complementary light capture**

Complementary strategies for resource capture have been regarded as a key factor driving the yield advantage of species-diverse plant communities (Tilman *et al.*, 2001; Cardinale *et al.*, 2007). The complementarity hypothesis states that because of niche differentiation and resource partitioning in space and time, e.g. difference in rooting depths or phenology, individuals in a mixture on average

experience less niche overlap in resource use than in the corresponding monocultures, resulting in an increase in biomass production of the system as a whole (Yachi and Loreau, 2007). Plants in intercrops or mixtures are likely to adjust their traits such as leaf appearance rate and organ size to the local environment they grow in, and result in a different phenotype as compared to a monoculture. Plant plastic responses to spatially varying resource availability in intercrops could strengthen the complementary exploitation of resources and thus strengthen overyielding potential in crop mixtures. However, such plasticity in plant morphological traits has not been considered in the complementary resource use theory. Thus, it is largely unknown how overyielding in mixed stands is associated with plasticity in traits. In other words, is this overyielding mainly due to inherent differences in growth habits and morphological traits between species or because of the ability of species to plastically adjust to environment in a mixture.

Phenotypic plasticity enables plants to alter morphological, physiological and developmental traits to match their phenotypes to the composition of the communities and abiotic environments they are growing in (Ballaré *et al.*, 1994; Price *et al.*, 2003; Sultan, 2010). Poorter and Lambers (1986) found that with increasing frequency of fluctuations in nutrient level, a highly plastic genotype of annual dicot *Plantago major* outcompeted a less plastic genotype, supporting the hypothesis that plastic individuals are superior competitors in temporally variable environments. In a physiological manipulation experiment with the annual dicot *Impatiens capensis*, Dudley and Schmitt (1995; 1996) found that phytochrome-mediated elongation is advantageous when competing in dense stands with plants of similar size. Therefore, plasticity in plant morphological development is expected to increase plant performance as well as canopy photosynthesis and productivity in heterogeneous environment (Silvertown and Gordon, 1989; Stuefer *et al.*, 1994; Pearcy, 2007). However, in ecological studies, the effects of phenotypic plasticity on community performance are implicitly included in the overall complementarity effect (Loreau and Hector, 2001; Tilman *et al.*, 2001), and are thus not explicitly considered.

In this thesis, I split the complementarity effect into a ‘configuration effect’ and a ‘plasticity effect’, and I quantify the contribution of phenotypic

plasticity to the overall complementarity effect. The configuration effect strictly quantifies the effect of diversity-induced variation in the spatial and temporal dynamic of the community caused by the component species being inherently different in phenology, root and shoot architecture, nutrient requirement, etc., in intercrop as compared to sole crop. The plasticity effect quantifies to which extent plastic responses of each species enhance resource capture beyond the level expected from monoculture phenotypes. Thus, I address the following research question:

RQ 3: *What is the relative contribution of plasticity in shoot development and configuration in time and space to the complementary light capture in intercropping (chapter 5)?*

### **Functional-structural plant model (FSPM)**

In this study, I use functional-structural plant model (FSPM) to test the hypothesis that enhanced light capture of the whole system provides a sufficient quantitative explanation for overyielding in wheat-maize intercrop, as compared to sole crops. Functional-structural plant models, also known as virtual plant models, are models explicitly describing the three-dimensional (3D) plant architectural development over time as governed by physiological processes which, in turn, depend on environmental factors and the resource capture and growth processes shaped by previous growth and developmental responses (Vos *et al.*, 2010). FSPM was used in this study since it constitutes an effective tool for evaluating the light capture by the component plants under a heterogeneous environment and for assessing the influence of local architectural change on the performance of the whole system. FSPM combines the representation of 3D plant structure with selected plant physiological functions, and is able to take into account their interactions (Evers *et al.*, 2005). The plant structure part deals with (i) the types of organs that are initiated and the way these are connected (topology), (ii) co-ordination in organ expansion dynamics, and (iii) geometrical variables (e.g. leaf angles, leaf curvature). The process part may include any physiological or physical processes that affects plant growth and development (e.g. photosynthesis, carbon allocation). In spite of its potential strength in this respect, relatively little work has been done to use FSPM to analyse the adaptive significance of variation in plasticity to changes in light conditions (Franca *et al.*, 2014). Furthermore, to my knowledge

FSPM has rarely been applied to analyse inter-specific interactions. FSPM was used in this study since it constitutes an effective tool for evaluating the influence of local architectural change on the performance of the whole system. FSPM also allows the implementation and study of different hypotheses drawn from experimental data. Finally, it is an ideal tool to capture the heterogeneous structure of intercrops.

## Outline of the thesis

In this thesis, I aim to link the performance of an intercropping system with plasticity in plant traits. The general methodological steps can be summarized as: *First* explicitly describe the plant development in a field experiment, including both intercrop and sole crops, and obtain data on final yield from all these cropping types; *Second* build up an FSPM based on the experimental data; *Third* analyse the contribution of configuration in time and space and plasticity in plant traits to the performance of whole system. The content of each chapter is summarized below:

In **chapter 2**, I describe the plastic responses of wheat when intercropped with maize, and test the hypothesis that mixed cultivation triggers plastic responses of wheat that have the potential to increase light capture and result in overyielding. The results show that plasticity in tillering is strongly associated with overyielding of wheat in intercrop.

In **chapter 3**, I describe the plastic responses of maize when intercropped with wheat. A wide range of effects, including changes in the rate of leaf initiation and appearance, in leaf length and width, and in sheath length were found. I conclude that many of the changes were linked to each other through feedback mechanisms, and that changes in light quality and quantity may have initiated these differences. A conceptual model is constructed to explain the development of maize plants in pure and mixed stands.

In **chapter 4**, I show that flexible timing of maize organ development can emerge from coordination rules. A structural development model of maize was built based on a set of coordination rules at organ level. In this model, whole-plant architecture is shaped through initial conditions that feed a cascade of coordination events. The modelling shows that a set of simple rules for

coordinated growth of organs is sufficient to simulate the development of maize plant structure when assimilates are not a limiting factor.

In **chapter 5**, I evaluate the respective roles of configuration in time and space and plasticity in plant traits to the light capture of a wheat-maize intercropping system, using a wheat-maize FSPM. The quantitative results clearly show the importance of developmental plasticity in explaining overyielding in this two-species system. I further argue that plasticity can have a large contribution in driving the potential benefits of niche differentiation in diversified plant systems.

In **chapter 6**, I reflect on the results of the study and answers to the three questions that I raised in the *general introduction*. I further provide future perspectives for linking plant plasticity with the performance of the community and for optimizing intercropping systems through a combination of experiments and modelling.

## CHAPTER 2

Overyielding of wheat in intercrops is associated  
with plant architectural responses that  
enhance light capture

Junqi Zhu, Wopke van der Werf, Jan Vos, Niels P. R. Anten, Peter E. L. van  
der Putten, Jochem B. Evers

Centre for Crop Systems Analysis, Wageningen University, PO Box 430, 6700  
AK, Wageningen, the Netherlands

---

This chapter has been submitted.

**Abstract**

Mixed cultivation of crops results in increased production per unit land, but the underlying mechanisms are poorly understood. Here we test the hypothesis that mixed cultivation triggers plastic responses of wheat (*Triticum aestivum*) that maximize light capture. We compared leaf development, tiller dynamics, final leaf sizes on main stem and tillers, leaf chlorophyll concentration, photosynthetically active radiation, red:far-red ratio, and yield components of wheat grown in two cultivation systems: sole wheat and intercrops with maize (*Zea mays*). Within the intercrop, wheat is grown in strips of six wheat rows, that are alternated with two maize rows. In our analysis, we contrast traits of wheat plants in border rows of those strips with traits of plants in the first and second inner rows within the strip, and traits of plants in sole wheat. Plants in border rows of an intercrop experienced more favourable light conditions and exhibited the following plastic responses: (i) more tillers due to increased tiller production and survival, (ii) larger top leaves on main stem and tillers, and (iii) higher chlorophyll concentration in leaves. Grain yield per meter row length of border rows was 141% higher than in sole wheat. Together these results clearly indicate the importance of plasticity in architectural traits for overyielding in multi-species cropping systems, and thus point to a previously under-appreciated mechanism driving the relationship between species diversity and overyielding of plant communities.

**Keywords:** plasticity, overyielding, wheat-maize intercropping, tiller dynamics, leaf size, border row effect

## Introduction

There is an increasing consensus that the performance of natural plant communities and associated ecosystem functions increase with species diversity (Loreau *et al.*, 2001; Hooper *et al.*, 2005). Similarly, diverse agricultural systems such as intercrops (consisting of multiple crop species growing together) have clear agro-ecological advantages over systems in which only one crop species is grown (hereafter). Advantages include: up to 40% higher production per unit land (Li *et al.*, 2013), higher resource-use efficiencies of water and nutrients (Vandermeer, 1989; Vandermeer, 2011), suppression of pests, diseases and weeds (Trenbath, 1993; Wolfe, 2000; Zhu *et al.*, 2000), and more carbon sequestration in the soil (Makumba *et al.*, 2006; Makumba *et al.*, 2007; Cong *et al.*, 2014). Intercropping is the dominant form of agricultural in many parts of the world and provides an estimated 20% of world food supply especially in the most vulnerable areas (Altieri, 2009; Chappell *et al.*, 2013). Yet, contrary to decades of crop improvement in sole cropping and in spite of the enormous potential of intercropping, little research has been done to determine the traits of cultivated species that drive these positive effects in intercropping. Fundamental information needed to improve these highly valuable systems is still lacking.

Plants in intercrops typically grow in close proximity to neighbours with differences in architecture (e.g. tall vs. short), light-use efficiency (e.g. sun vs. shade species), length of the growth period (e.g. in relay intercropping), and rooting depth (e.g. shallow vs. deep). Such differences result in complementary strategies for resource capture which are regarded as a key factor driving the yield advantage of species-diverse plant communities (Yachi and Loreau, 2007), including intercropping (Lithourgidis *et al.*, 2011). However, there are very few studies that analyse how resource-capture traits and plasticity in those traits contribute to the functioning in multi-species systems. Ground-breaking work in intercrops include the studies of Li *et al.* (2006) and Li *et al.* (2007) who showed that maize roots avoided those of wheat in intercrop, but grew near roots of faba bean due to better phosphorus availability near faba bean roots. Zhang *et al.* (2008b) found that increased radiation interception by wheat and cotton in wheat-cotton intercrop fully explained the high land-use efficiency of

this system. Furthermore, plasticity in plant development and architecture should be expected to result in 'gap filling' in heterogeneous leaf canopies such as intercrops and hence maximize plant performance as well as canopy photosynthesis and productivity (Silvertown and Gordon, 1989; Werner and Peacor, 2003). Analysing and quantifying these effects will be crucial to identify which traits and plasticity therein are responsible for overyielding in intercrops. Such information would help optimizing intercropping systems in terms of crop trait selection and plant configuration. However, no information on above-ground responses is available. While it is known that plants in intercrops usually produce more yield than plants in sole crop, we do not know which above-ground plant traits are responsible for these greater yields. As radiation interception is a key process in crop growth and yield formation, we focus here on above-ground traits that may be associated with radiation interception.

We use wheat grown in a relay strip intercrop with maize as a model system. In this system, strips of spring wheat are sown in March, with a strip of bare soil between the wheat strips. Maize is inter-sown in these bare strips in late April. After wheat harvest in early July, maize continues to grow as a sole crop until its harvest on early October (Fig. 1.1). The light conditions in this system are highly dynamic and spatially heterogeneous. Wheat experiences a favourable light environment at early stages of development because of the absence of maize which is sown later, but it will be shaded by the much taller maize plants during its grain filling stage. Plasticity in tillering, leaf growth and the number and size of reproductive organs enables wheat to adjust to the environment and maximize the acquisition of resources and production of yield (Fischer, 1985; Fischer and Stockman, 1986; Nelson, 2000; Evers *et al.*, 2006). Due to the differences in light environment between inner and border rows and the associated plastic responses, substantial differences between inner and border plant performance are to be expected. Indeed, Li *et al.* (2001) showed that wheat plants in border rows greatly overyield the plants in inner rows of the wheat strips when intercropped with maize.

To assess the contribution of plastic responses of wheat to the overyielding in the relay-strip intercropping with maize, we analysed the wheat development and yield in three situations: (i) wheat grown as a sole crop, (ii)

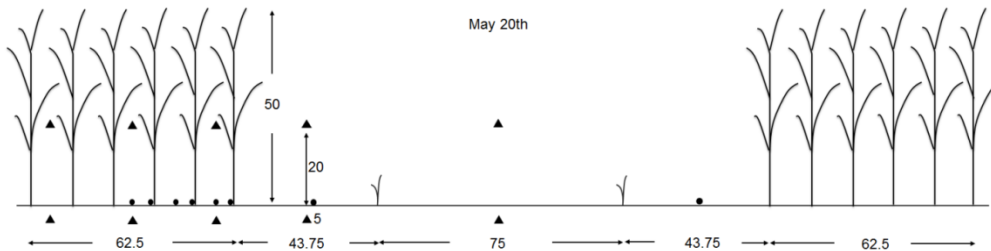


Fig. 2.1 Cross-row profile of a wheat-maize intercrop on May 20, 2011 (unit: cm). Wheat was grown in strips of six rows at 12.5 cm row distance. Maize was grown in strips of two rows at 75 cm distance. Following a replacement design, one maize row replaces exactly six wheat rows. Distance between adjacent wheat and maize rows equal to half of the row distances of wheat plus half the row distance in maize ( $6.25 + 37.5 = 43.75$  cm). Wheat was sown on March 9, and harvested on 10 August, while maize was sown on May 11, and harvested on October 14. Closed circles indicate placement of the ceptometer parallel to crop rows; triangles represent placement of thermocouples.

wheat plants in the border rows (rows one and six) of the wheat strips in a wheat-maize intercropping system with alternating sets of six rows of wheat and two rows of maize, and (iii) wheat plants from the inner rows of the wheat strips in the intercropping system. Wheat development was characterized by leaf development, tiller dynamics and final size of leaf blades (referred to as leaves hereafter) on the main stem and on each tiller. Leaf chlorophyll concentration and light environment were quantified throughout the growing season. The yield components as well as the nitrogen concentration of each component were determined in each row of intercropped wheat and in sole wheat.

## Materials and Methods

### Field experiments

Two field trials on growth and yield of wheat in intercrop were conducted on a sandy soil at the experimental farm of Wageningen University, the Netherlands ( $51^{\circ}59'20''\text{N}$ ,  $5^{\circ}39'16''\text{E}$ ), from March to October 2011. One experiment was designed to determine yield in wheat-maize intercrop as compared to sole wheat crop (yield trial), and the other to determine growth and development (development trial). The yield trial had six replicates with a plot size of  $8 \times 8$  m

for both sole crops and intercrop. The development trial had three replicates with a plot size of  $6 \times 6$  m. The two trials were simultaneous and the fields were adjacent to each other.

Wheat cultivar Tybalt was sown on 9 March 2011 at a row distance of 12.5 cm and a density of approximately 250 plants  $m^{-2}$ . Wheat was harvested on 10 August 2011. Maize cultivar LG30208 was sown at a row distance of 75 cm and a population density of approximately 10 plants  $m^{-2}$  on 11 May and harvested on 14 October. Intercropped wheat was grown by alternating strips of six wheat rows with strips of two maize rows, with plant distances within the strip the same as in sole crops, and the distance between adjacent wheat and maize rows set at half the row distance in wheat plus half the row distance in maize ( $6.25\text{ cm} + 37.5\text{ cm} = 43.75\text{ cm}$ ) (Fig. 2.1 and Fig. 1.1). The relative density of plants in intercrop as compared to sole crop is 1/3 for the wheat and 2/3 for the maize, i.e. a replacement design. Intercrop plots included two maize strips, three wheat strips, and a maize guard row at each side. Row direction was north-south. The height of maize was measured throughout the growing season. It is defined as the distance from the soil surface to the highest point at which the whorl of growing leaves still forms a complete tube before the appearance of the tassel, and measured till the tip of the tassel afterwards. To avoid drought stress, irrigation was done six times in May and June with approximately 15 mm each time. Further details are given in chapter 3.

The development, growth and yield of wheat plants in three growing conditions were compared: (I) in sole crop; (II) in intercrop border rows; (III) in intercrop inner rows.

#### *Temperature measurements and calculation of thermal time*

Temperature was recorded in sole crop and intercrop to determine whether growth responses were caused by temperature differences between crop systems. Measurements were made with shielded thermocouples (type T, TempControl Industrial Electronic Products, the Netherlands) connected to a data logger (Datataker DT600, Datataker Data Loggers, Cambridgeshire, UK) at 10 minute intervals. Thermocouples were placed at 5 cm depth, and at 20 cm above the soil surface within the canopy. Six thermocouples, three in the

canopy and three in the soil, were placed at three locations in the wheat strip (triangles in Fig. 2.1). In sole wheat, two thermocouples were placed between the rows, one in the canopy and one in the soil. Since only slight differences in temperature were found between treatments and positions, average soil temperature over positions and treatments was used for calculating the temperature sum till the first internode is distinguishable (10 May), when the apex was still below the soil surface. Thereafter, average canopy temperature over positions and treatments was used. Thermal time ( $^{\circ}\text{Cd}$ , degree days) was calculated on an hourly basis from sowing, considering a base temperature for wheat development of  $0\text{ }^{\circ}\text{C}$ .

#### *Yield*

Wheat plants were harvested by hand separately for each row in the intercrop. In each intercrop plot, four meter row length was sampled in each row to determine fresh weight (after drying on a drying floor; see below) and two separate row sections of 50 cm length were used to take subsamples for determining dry weight. Rows 1 and 6 are named border rows (Fig. 2.1). Rows 2 and 5 are named ‘inner rows I’, and rows 3 and 4 are named ‘inner rows II’. For sole wheat, the total sampling area was four meter row length times 1 m row width (8 rows). The subsample procedure in each row was the same as in intercrop plot. After harvest, samples were first dried on a drying floor with forced ventilation at  $25\text{ }^{\circ}\text{C}$  (ACT-20, Ommivent Co., the Netherlands) to a standard moisture content ( $\sim 15\%$ ). After this, samples were measured and further oven-dried at  $70\text{ }^{\circ}\text{C}$ .

Non-reproductive tillers with green or no ears at harvest were separated from the subsample and counted. The remaining reproductive tillers were subdivided into shoot and ear. Ears were counted and were subdivided into grain and chaff (including everything except the kernels). The oven-dry weights of grain, shoot, chaff, and non-reproductive tillers were determined by drying to constant weight at  $70\text{ }^{\circ}\text{C}$ . Grain number per square meter and per ear, as well as grain and ear weight, were determined.

Yield comparisons within the intercrop, and between intercropped wheat and sole wheat, are made on the basis of yield per meter row length. This unequivocally assigns responses to the position in the crop. Subsequently,

crop yields per unit area of intercrop (area of wheat per unit intercrop area) and expected wheat yields per unit area of intercrop are compared. The expected yield is calculated as the wheat yield per unit area in sole crop, multiplied by the relative density of wheat in intercrop as compared to sole crop. This expected yield is thus calculated under the null hypothesis that an individual wheat plant has the same yield in intercrop and sole crop (Loreau and Hector, 2001).

Pairwise comparisons between treatments, or between rows within intercrop, were made with ANOVA ( $P = 0.05$ ) in the ‘stas’ package of R programming language (R Core Team, 2014). Block effects were fitted as a fixed effect.

#### *Nitrogen yield*

The total nitrogen concentration of each oven-dried sample was determined by the Kjeldahl method (Novozamsky *et al.*, 1983). The oven-dried samples were ground, and a small subsample was digested in a mixture of concentrated  $\text{H}_2\text{SO}_4$  and  $\text{H}_2\text{O}_2$ . The digests were analysed by a Kjeldahl device (KDY 9820, Tongrunyuang, China). The nitrogen yield for each yield component, defined as the total nitrogen uptake per unit land area at final harvest, was calculated by multiplying the nitrogen concentration of the component with its biomass.

#### *Plant selection and sampling time*

To monitor plant development, 24 wheat plants in each intercrop plot were tagged when leaf 2 was visible, eight in each of rows 6 (Fig.1, counting from left to right, border row), rows 5 (inner row I) and rows 4 (inner row II). Twelve of these plants were used for destructive sampling on 6 May (667 °Cd since sowing) when there were five mature leaves on the main stem in intercrop wheat. The other twelve were used for non-destructive observations on development, and they were used for the final destructive sample on 13 July (1862 °Cd since sowing) when there were five senescent leaves on main stem in intercrop wheat. In sole wheat, four plants in each plot were chosen for non-destructive observations, and no destructive sampling was done. Two plants died and were excluded from analysis of leaf and tiller dynamics.

#### *Leaf and tiller dynamics*

Leaves were numbered from bottom to top (acropetally). The number of

visible tillers and leaves, including mature and dead leaves, were measured twice per week. Events such as leaf appearance were considered to occur midway between the last observation date at which the event had not occurred and the first observation date on which the event was recorded. Tip appearance was defined as the moment the leaf tip visibly appeared out of the whorl. A leaf was considered mature when its collar had emerged from the sheath tube formed by preceding phytomers. A leaf was considered dead when at least half of the leaf area had turned yellow. Phyllochron (i.e. the thermal time between successive tip appearances) was estimated as the slope of the linear relationship between thermal time at tip appearance and phytomer rank ( $^{\circ}\text{Cd leaf}^{-1}$ ). Regressions were made using the linear mixed effects model function (`lme`) in the 'nlme' package (Jose *et al.*, 2013) of the R programming language with plot and plant (nested in plot) as random effects.

A tiller was recorded as "appeared" when its first leaf had appeared from the encapsulating sheath on the parent shoot. A tiller was considered to be senescing, when the youngest leaf had not increased in length since the last measurement (Kirby and Riggs, 1978).

#### *Leaf area*

To obtain individual leaf area, leaf dimensions (length and width) and leaf shape were measured. The dimensions of all leaves were measured destructively on two destructive sampling occasions. Leaf width was measured at the point of greatest width. Leaf shape was assessed by measuring width at five to ten locations along the length of each of ninety fully grown leaves chosen randomly. It was further fitted using the following relationship (Evers *et al.*, 2006):

$$W = \left( \frac{-L \times (L - 2L_m)}{L_m^2} \right)^C \quad (\text{Eq. 2.1})$$

where  $W$  is the normalized margin to midrib distance (where normalization is achieved by dividing by half the greatest leaf width) as a function of normalized leaf length ( $L$ ).  $L$  is the distance from leaf tip to the measured point divided by final leaf length.  $L_m$  is the distance of the point of maximum margin-midrib distance to the leaf tip as a fraction of the final length ( $0.5 < L_m < 1$ ), and  $C$  is a curvature coefficient ( $0 < C < 1$ ). Parameters  $C$  and  $L_m$  were estimated by

minimizing the root mean square error using the ‘solver’ function in Microsoft Excel 2010 (Supplementary Fig. S2.1). Finally, normalized leaf area was calculated as leaf length  $\times$  leaf width  $\times$  shape coefficient  $S$ . The value of  $S$  was 0.786, obtained by integration of Eq. 2.1 through the ‘integrate’ function in the ‘stats’ package of the R programming language (R Core Team, 2014). For brevity, individual leaf area is only shown for leaves on the main stem and tiller 1 (i.e. the tiller which appeared from the sheath of the first leaf).

Leaf area per meter row length was calculated for the two destructive samplings by determining whole-plant leaf area (summing up all individual leaf areas for each sampled plant) and multiplying average plant leaf area by the number of plants in one row ( $31.25 \text{ plants m}^{-1}$ ). For a m length of strip, we have six rows of wheat, representing  $6 * 12.5 = 75 \text{ cm width}$ . The leaf areas per meter row length can be added up, and multiplied by  $8/6$  to get wheat leaf area in the strip.

#### *SPAD measurement*

Leaf greenness, as a proxy for chlorophyll content, was measured once per week on main stem leaves 3, 5, 7 and 9, using a SPAD 502 Plus Chlorophyll Meter (SPAD-502, Minolta Camera, Tokyo, Japan). Measurements were made on two plants per row, which were also selected for non-destructive observation, at border rows, inner rows I and inner rows II in intercrop. On each leaf, measurements were made on the top, middle and bottom part and then averaged. Only large enough and non-senescent leaves were considered. The measurements on a certain leaf number were discontinued as soon as one of the selected leaves started to senesce.

The effect of row position on leaf SPAD values was tested by mixed effects models with temporal pseudoreplication. Test were made using the lme function in the ‘nlme’ package of the R programming language (R Core Team, 2014) with thermal time, plant and plot as random effects. Thermal time was nested in plant and plot.

#### *Photosynthetically active radiation (PAR)*

Light intensity at soil level was measured once per week at eight positions in each plot using a ceptometer (SunScan Canopy Analysis System; Delta T Devices, Cambridge, UK) parallel to the crop rows. Measurements were made

around solar noon. Measurement positions in intercrop were immediately next to the border row, inner row I and inner row II, in the middle between rows, and in the middle between the wheat and maize row, as indicated in Fig. 2.1. Measurements in sole crop were next to the row and in the middle between rows, using three replicates per position per plot. A reference PAR sensor was placed just above the canopy.

#### *Red:far red ratio (R:FR)*

Weekly measurements of red : far red ratio (R:FR) were made at soil level around noon, using the Skye SKR100/116 Fibre Optic Probe Measuring System (Skye Instruments Ltd, Powys, UK). The device was equipped with a glass fibre probe that measured R:FR at its tip, with an angle of view of 40°. Measurements were made on two plants per row, which were the same plants used for SPAD measurement, at the border row, inner row I and inner row II in intercrop. Four measurements were made parallel to the soil surface with back of the sensor against the plant and the sensor facing east, south, west, and north.

## **Results**

### *Biomass and grain yield of wheat*

The observed grain yield per unit of land area in intercrop was 38% higher than the expected yield from sole wheat (Table 2.1). The relative yields per meter row length in border rows, inner rows I and inner rows II, as compared to sole wheat, were 241%, 85% and 89%, indicating massive overyielding in the border rows, and moderate underyielding in the inner rows in the intercrop. Patterns in total shoot biomass, chaff, N yield in grain and N yield in the shoot resembled those described for the grain yield (Table 2.1).

The density of ears was  $112.8 \pm 4.5$  ears per meter row length in border rows, 261% of sole wheat ear density per m row (Fig. 2.2). Density of ears in inner rows I and II amounted to 115 and 122% of sole wheat, respectively. Number of grains per ear in the border row was 108% of sole wheat, while that in inner rows I and II was 80% and 77% of sole wheat, respectively. Plants in sole wheat had the highest thousand-grain weight ( $46.4 \pm 0.6$  g), while plants in border rows had the lowest thousand-grain weight

Table 2.1 Dry matter weights and nitrogen yields of grain, shoot and chaff in sole and intercrop wheat

Treatment <sup>1</sup>	Grain	Chaff	Shoot <sup>2</sup>	Non-reproductive tillers	N yield of grain	N yield of chaff	N yield of shoot
<i>Yields per meter row</i>							
Sole wheat (g m <sup>-1</sup> row <sup>-1</sup> )	87.2 ± 2.6a	116.5 ± 3.3a	39.7 ± 1.0a	9.3 ± 0.9a	2.26 ± 0.09a	0.08 ± 0.003a	0.22 ± 0.01a
Border rows (g m <sup>-1</sup> row <sup>-1</sup> )	209.9 ± 7.9b	388.9 ± 11.8b	117.7 ± 6.4b	37.6 ± 5.4b	5.59 ± 0.18b	0.41 ± 0.03b	0.85 ± 0.06b
Inner rows I (g m <sup>-1</sup> row <sup>-1</sup> )	74.5 ± 3.3a	106.4 ± 5.5a	35.4 ± 2.1a	6.0 ± 1.4c	1.87 ± 0.06c	0.10 ± 0.01a	0.22 ± 0.01a
Inner rows II (g m <sup>-1</sup> row <sup>-1</sup> )	77.3 ± 2.7a	113.0 ± 11.3a	35.3 ± 2.2a	6.8 ± 1.7c	1.96 ± 0.05c	0.10 ± 0.02a	0.20 ± 0.02a
<i>Observed and expected yields, per m<sup>2</sup> intercrop</i>							
Expected yield <sup>3</sup> (g m <sup>-2</sup> )	232.5 ± 6.8a	38.8 ± 1.1a	106.0 ± 2.8a	24.7 ± 2.5a	6.02 ± 0.25a	0.22 ± 0.01a	0.59 ± 0.02a
Observed yield <sup>4</sup> (g m <sup>-2</sup> )	321.6 ± 8.4b	67.6 ± 2.4b	167.6 ± 8.1b	44.8 ± 7.0b	8.38 ± 0.11b	0.55 ± 0.05b	1.13 ± 0.08b

<sup>1</sup>The statistical comparisons between crop rows in sole wheat and intercrop, between expected yield and observed yield of wheat at per square meter of intercropping area were done separately. Pairwise significant differences (ANOVA) between expected yield and observed yield are indicated with *a* and *b*. Pairwise significant differences (ANOVA) between wheat rows are indicated with *a* and *b*. Different letters indicate significant ( $P < 0.05$ ) differences between means based on ANOVA.

<sup>2</sup>Shoot weight is for reproductive tillers only and excludes the weight of the ears. The total biomass of non-reproductive tillers is given separately. The weight of ears is divided over grains (kernels) and chaff (ear exclude kernels).

<sup>3</sup>The expected yield is calculated by multiplying the yield of sole wheat per square meter with the relative density of the wheat in intercropping under the null hypothesis that individual wheat plants have the same yield in intercrop as in sole crop

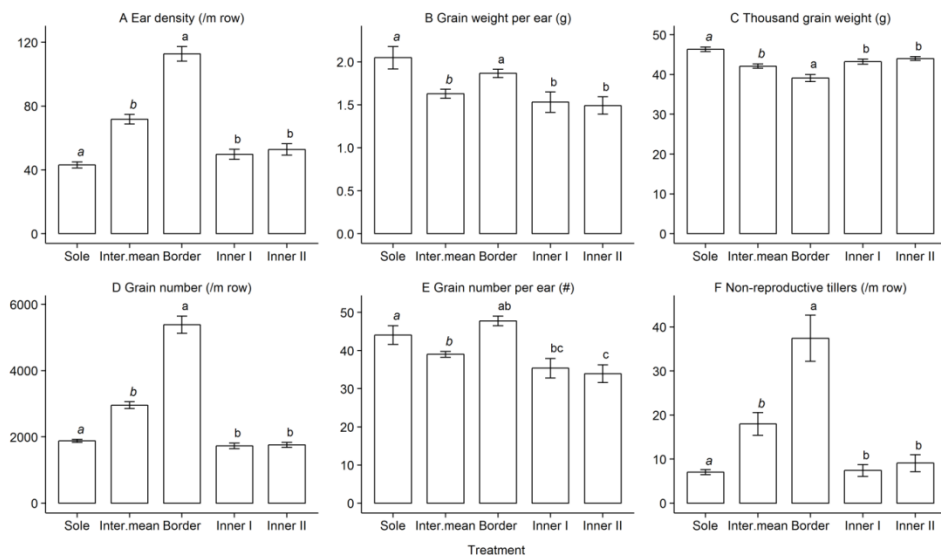


Fig. 2.2 The ear density per meter row length (A), grain weight per ear (B), thousand grain weight (C), grain number per meter row length (D), grain number per ear (E), number of non-reproductive tillers per meter row length (F) of sole and intercrop wheat in the yield trial. Inter.mean represent the mean value of border row and inner rows. Yield per meter row length can be calculated as ear density  $\times$  grain weight per ear, or as thousand grain weight  $\times$  grain number per meter row length  $\div$  1000. The statistical comparisons between sole wheat and inter.mean, and between rows within intercrop were done separately. Pairwise significant differences (ANOVA) between sole wheat and inter.mean are indicated with *a* and *b*. Pairwise significant differences (ANOVA) between crop rows in intercrop wheat are indicated with *a* and *b*. Different letters indicate significant ( $P < 0.05$ ) differences between bars based on ANOVA.

( $39.1 \pm 0.9$  g), 84% of sole wheat. The thousand-grain weights in inner rows I and II was 93 and 95% of sole wheat, respectively. The reduced thousand-grain weight in intercropping was an indication of severe competition with maize during grain filling in the border rows and inner rows. Plants in the inner rows I and II showed the lowest grain weight per ear ( $1.5 \pm 0.1$  g), while no significant differences in grain weight per ear were found between border-row and sole wheat (mean  $1.9 \pm 0.1$  g).

### Phenology

Development proceeded synchronously in all treatments. Wheat emergence

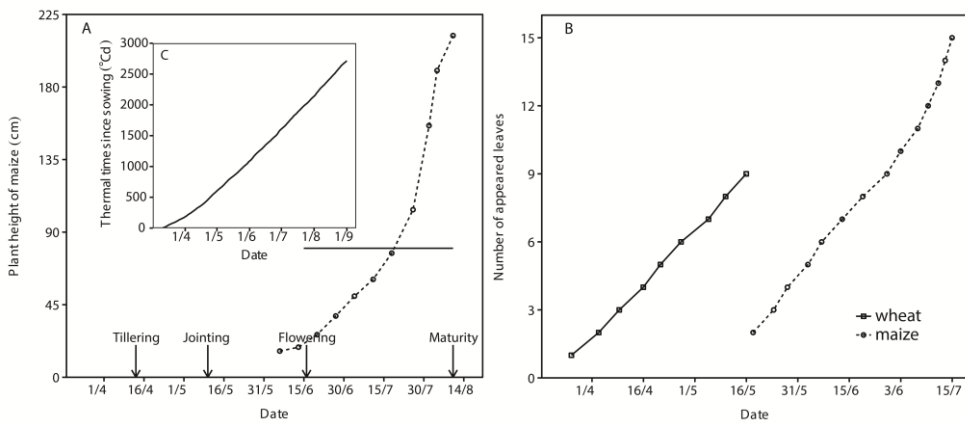


Fig. 2.3 The temporal dynamic of maize height (panel A) and number of appeared leaves (panel B). Mean number of appeared leaves of wheat over rows and treatments and of maize in intercrop were presented. Panel C represented the conversion between date and thermal time. Horizontal line in panel A represented the final height of wheat from soil to the top of the ear. Arrows from left to right indicate the wheat tillering on 13 April ( $337\text{ }^{\circ}\text{Cd}$ ), jointing on 10 May ( $750\text{ }^{\circ}\text{Cd}$ ), flowering on 16 June ( $1350\text{ }^{\circ}\text{Cd}$ ), and maturity on 10 August ( $2321\text{ }^{\circ}\text{Cd}$ ). Error bars are omitted because they would be smaller than the symbols in most cases.

occurred on 28 March ( $150\text{ }^{\circ}\text{Cd}$  since wheat sowing), tillering occurred on 13 April ( $337\text{ }^{\circ}\text{Cd}$ ), stem elongation occurred on 10 May ( $750\text{ }^{\circ}\text{Cd}$ ), flowering occurred on 16 June ( $1350\text{ }^{\circ}\text{Cd}$ ), and maturity occurred on 10 August ( $2321\text{ }^{\circ}\text{Cd}$ , see field views in Supplementary Fig. 1.1). Maize emerged at approx.  $900\text{ }^{\circ}\text{Cd}$  after wheat sowing, when the wheat was in the stem elongation stage and approx. 50 cm high (Fig. 2.1). Final plant height of wheat was 80 cm. Maize in intercrop started to grow above the wheat during wheat grain filling on 20 July ( $1950\text{ }^{\circ}\text{Cd}$  since wheat sowing, Fig. 2.3A). The final height of maize in the intercrop was 210 cm from soil to the tip of the tassel.

#### *Leaf appearance*

The mean phyllochron was  $90.8 \pm 0.6\text{ }^{\circ}\text{Cd}$  for leaves on main stem and  $98.1 \pm 1.7\text{ }^{\circ}\text{Cd}$  for leaves on the tiller 1, both averaged across rows and treatments (Fig. 2.3B and Supplementary Fig. S2.2). The mean duration of leaf expansion from appearance to maturity was  $101.3 \pm 1.8\text{ }^{\circ}\text{Cd}$  for main stem leaves and  $112.1 \pm 4.0\text{ }^{\circ}\text{Cd}$  for leaves on tiller 1. On average, main stem leaves 1 to 4

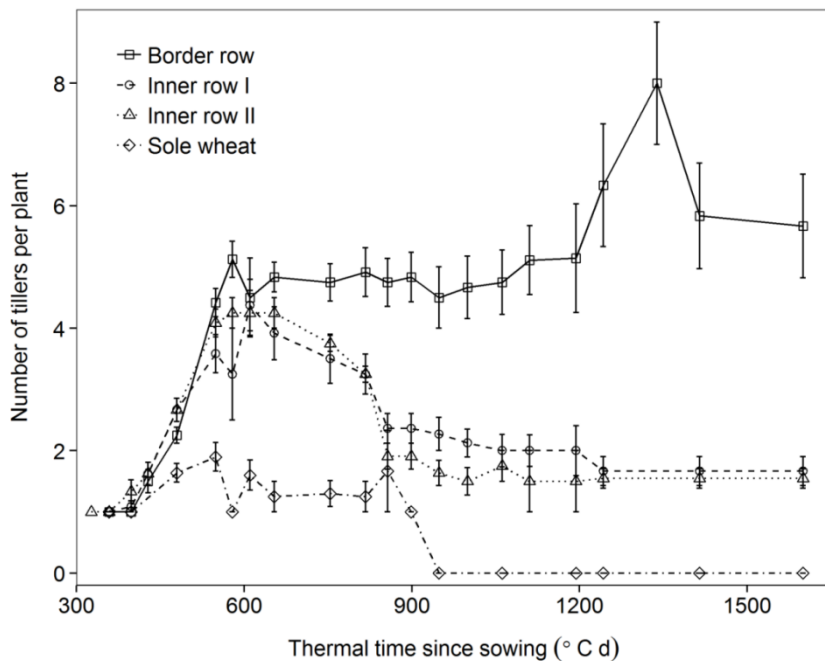


Fig. 2.4 Number of tillers per plant against thermal time since wheat sowing in border rows (squares and solid line), inner rows I (circles and dashed line), and inner rows II (triangles and dotted line) in strip intercropping, and in sole wheat (diamonds and dash-dotted line). Error bars represent the standard error of the mean in each treatment.

stayed green longer ( $88.6\text{ }^{\circ}\text{Cd}$ , i.e. approximately one week) in border rows than in inner rows and sole wheat. No significant differences between sole wheat and intercrop rows were found in the longevity of later appearing leaves on the main stem or most leaves on tillers.

#### *Tiller dynamics*

The number of tillers produced per plant in intercrop (approximately five per plant) far exceeded the number of tillers produced per plant in sole wheat (less than two) (Fig. 2.4). Initially, the dynamics of tillering were similar among the rows in intercrop, but from approximately  $550\text{ }^{\circ}\text{Cd}$  after sowing onwards, tiller

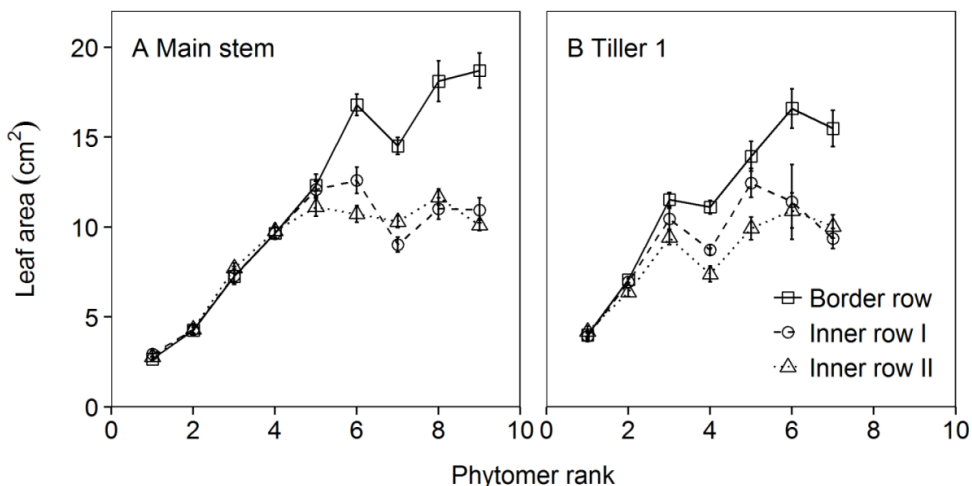


Fig. 2.5 The surface area of individual leaves along phytomer rank on the main stem (A) and on the tiller 1 (the tiller which appeared from the sheath of the first leaf) (B) in border rows (squares and solid line), inner rows I (circles and dashed line) and inner rows II (triangles and dotted line) in wheat maize relay strip intercropping. Error bars represent the standard error of the mean.

senescence started in both inner rows in intercrop, whereas the number of tillers in the border rows remained steady until approximately 1200 °Cd and then increased again. Most of the second-flush tillers appearing at 1200 °Cd bore an immature ear at harvest and therefore did not contribute to grain yield. The number of tillers in inner rows stabilized around 1.6 tillers per plant at maturity. In the sole crop, all tillers died. Similar differences in the final tiller number between rows and treatments were also found in the yield trial, but with more surviving tillers in sole wheat.

#### *Leaf area*

No differences in area per leaf were found between plants in border rows, inner rows I and inner rows II in intercrop up to leaf 5 on the main stem (Fig. 2.5A). Thereafter, divergences occurred. Significant differences in leaf size were found between plants in the border row, which had consistently larger leaves, and those in the inner rows, without a significant difference between the inner rows I and II. A similar pattern of divergence of leaf area between

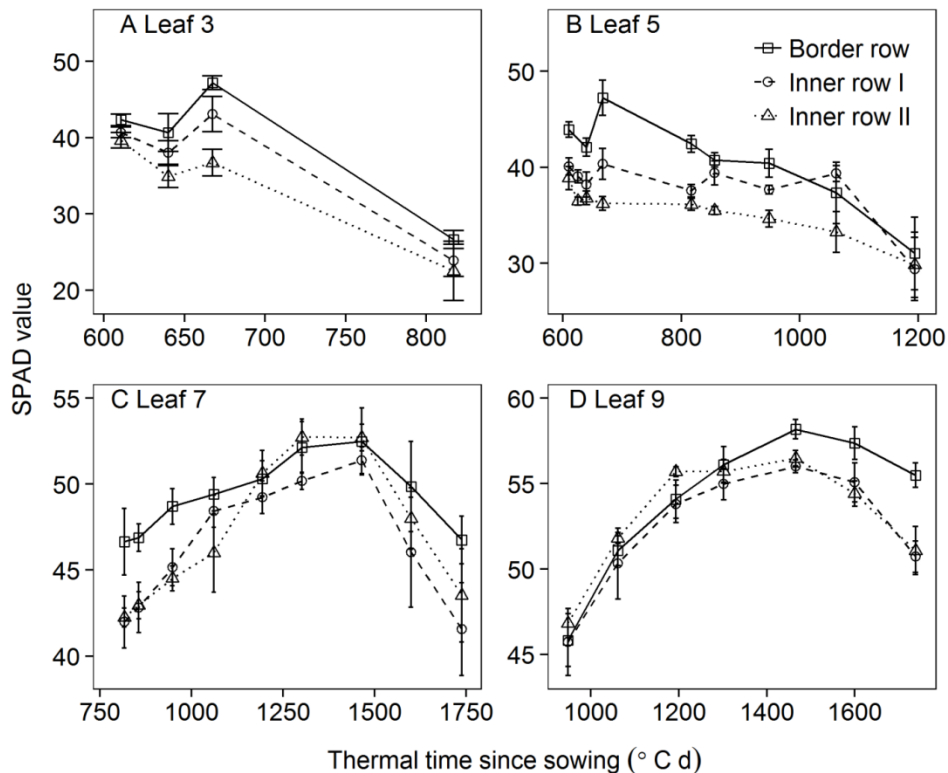


Fig. 2.6 Chlorophyll concentration as measured using SPAD values versus thermal time since wheat sowing of leaf 3 (A), leaf 5 (B), leaf 7 (C) and leaf 9 (D) in border rows (squares and solid lines), inner rows I (circles and dashed lines) and inner rows II (triangles and dotted lines) in wheat maize relay strip intercropping. Error bars represent standard error of the mean.

rows was observed on tiller 1, starting from a lower leaf rank (Fig. 2.5B).

The combined effects of tiller dynamics and individual leaf area were reflected in leaf area ( $\text{m}^2$ ) per m row. Border row showed a moderately higher leaf area per meter row ( $0.29 \pm 0.03$ ) compared to inner row I ( $0.21 \pm 0.04$ ) and inner row II ( $0.17 \pm 0.02$ ) on 4 May ( $653 \text{ }^{\circ}\text{Cd}$ ). The leaf area index on 15 July ( $1870 \text{ }^{\circ}\text{Cd}$ ) was much larger in border row ( $0.66 \pm 0.18$ ) compared to inner row I ( $0.09 \pm 0.01$ ) and inner row II ( $0.11 \pm 0.04$ ).

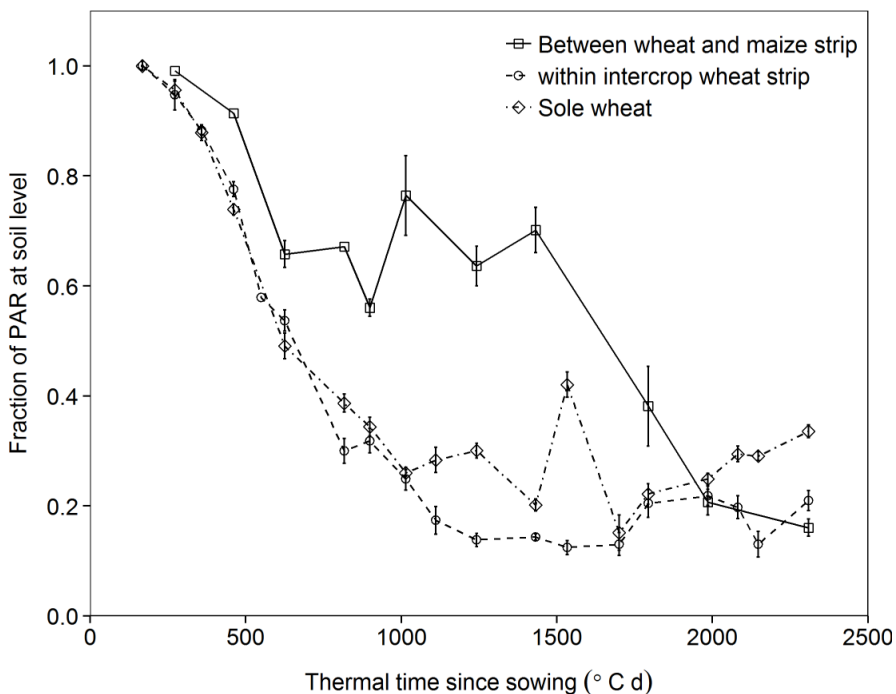


Fig. 2.7 Fraction of PAR at the soil level as a function of thermal time since wheat sowing between wheat and maize strip in intercrop (squares and solid line), within the wheat strip in intercrop (circles and dashed line) and in sole wheat (diamonds and dash-dotted line). Error bars indicate standard error of the mean.

#### *Chlorophyll concentration*

Leaves of plants in border rows have higher chlorophyll concentration compared to inner rows, as shown by SPAD measurements (Fig. 2.6). The differences between border row and two inner rows were significant for leaf 5 (mean  $P = 0.0020$ ) and leaf 7 (mean  $P = 0.0036$ ).

#### *Interception of photosynthetically active radiation (PAR)*

No significant differences in fraction of PAR penetrating to ground level around solar noon were found between the six positions in sole wheat and within intercrop wheat strip (Fig. 2.7), therefore means over the six positions were used for further analysis. Sole wheat and intercrop had similar PAR at soil level until approx. 1000 °Cd. Subsequently, at a time that maize plants were still

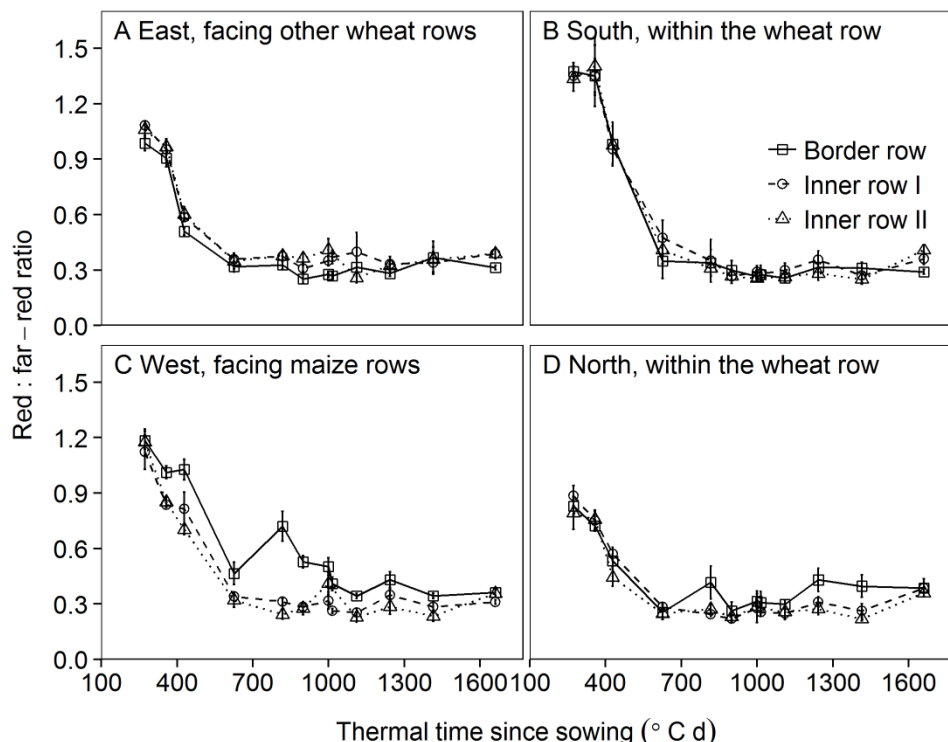


Fig. 2.8 Red: far red ratio measured at soil level as a function of thermal time since wheat sowing in border rows (squares and solid lines), inner rows I (circles and dashed lines), and inner rows II (triangles and dotted lines) for the sensor facing east (A, facing the other wheat rows), south (B, within the row facing towards the sun), west (C, facing the maize strip), and north (D, within the row facing away from the sun). Errors bars denote standard error of the mean.

very small, PAR at ground level decreased further in the wheat strip in fraction in the middle between the wheat and maize strips showed a two-step decrease: the PAR fraction dropped to 0.65 and stabilized until 1500 °Cd, after which the value decreased rapidly due to the growth of maize.

#### Red-far red ratio

The R:FR values averaged over the four wind directions stabilized at approx. 0.35 in border rows, and 0.31 in inner rows I and inner rows II (Fig. 2.8). The biggest difference in R:FR between border rows and inner rows was found for

the sensor facing west, i.e. in the direction of the maize strip where maize was initially absent and emerged at 900 °Cd since wheat sowing. Thereafter R:FR dropped at the border row and stabilized at a value similar to the inner rows.

## Discussion

The aims of this study were to identify plant responses in intercropping that contribute to high light capture and overyielding, using the wheat-maize relay intercrop as a model system. We assessed the developmental responses of wheat, and found several responses that contribute to increasing light capture, in particular an increased number of tillers in border rows and inner rows as compared to sole crops, and larger leaves on border row plants as compared to plants in inner rows. Wheat in border rows of the intercrop experienced favourable light conditions (PAR, R:FR) early in their growth cycle because of the initial absence of neighbouring plants at one side, but it experienced progressively more shading during the grain filling stage, as maize overgrew the wheat.

Wheat plants have several options to adjust their structural development to the resources that are available. Some of these options are sequential, (e.g. first the number of tillers, then the number of ears, then number of grains per ear, and later grain size) and some are synchronous, e.g. tillering and leaf expansion. Intercropped wheat both in border row and in inner row showed a suit of plastic responses as compared to sole wheat. Responses entailed a production of more tillers at early growth stage both in border-row and inner-row plants. Plants in border rows further showed a higher tiller survival rate, higher number of kernels per ear, larger size of top leaves and higher N yield compared to plants in inner rows and sole wheat. The late shading during grain filling stage resulted in a significant reduction of thousand grain weight in both border-row and inner-row wheat. However, the early plastic responses in border-row wheat fully compensated for the yield-reducing effect of shading by maize during grain filling. Ultimately, the grain yield per meter row was 141% higher in border-row wheat than in sole wheat. To our knowledge this is the first study that has explicitly associated overyielding in intercropping to plasticity in individual aboveground structural traits.

### *Yield components of border rows*

Overyielding responses in our study confirm earlier work in a similar wheat-maize intercropping system in Northern China (Li *et al.*, 2001; Zhang *et al.*, 2007), even though the climate, varieties and designs differed between the studies. Overyielding in wheat could be attributed to a much higher grain number per square meter in the border rows, even though the thousand-grain weight of the border row plants was lower (Fig. 2.2). The number of grains per ear and per square meter is related to incident solar radiation in the 30 days preceding flowering (Fischer, 1985). Thus, the higher grain number in border rows is a likely consequence of greater light availability before flowering as compared to inner rows and sole wheat. Grain weight is positively related with post flowering radiation (Fischer, 1975). Border rows were shaded by maize during grain filling, while their grain number was large due to the favourable conditions during early growth, explaining why thousand grain weight was lower in border row plants. The importance of shading by maize was confirmed in a pilot treatment in which maize was sown two weeks later while all other conditions were the same. The thousand grain weight in this pilot treatment was higher than that in any plot of the main intercrop treatment (Supplementary Fig. S2.3 and Table S2.1), indicating the role of shading by maize in reducing the thousand grain weight.

### *Higher tiller survival and productivity are the main determinants of border row yield advantage*

As border row plants were responsible for overyielding in the intercrop, we assessed the trait responses that underlie these effects. There were major differences in tiller dynamics between sole wheat and intercropped wheat, and between different row positions in intercrop. All row positions in the intercrop produced substantially more tillers than sole wheat, indicating that in all row positions, wheat plants experienced conditions more favourable for tillering during early growth than in sole crop. In due course, most tillers in the inner rows and in sole wheat died, while in the border rows most tillers survived. Ong *et al.* (1978) and Ong and Marshall (1979) suggested that adequate light for carbon acquisition by young tillers is critical for their survival, since tiller senescence is the result of competition between tillers for assimilates (Lauer

and Simmons, 1988; Nelson, 1988; McMaster *et al.*, 1999). Indeed, in our experiment, the majority of tillers in the inner rows and sole wheat died between 600 and 900 °Cd, but the border-row tillers did not die, probably due to high light penetration from the side of maize strip during that time. In addition, light quality (R:FR) may be responsible for tiller death in wheat (Lauer and Simmons, 1989; Sparkes *et al.*, 2006). In our experiment, this was supported by the fact that the R:FR at the side which facing the maize strip in intercrop was always higher for plants in border rows than for plants in inner rows.

A high plasticity in tiller production and senescence is therefore important for determining yield of wheat in intercrops. It is likely that tillering potential and plasticity in tillering are even more important in a heterogeneous canopy, such as an intercrop, than in a more homogeneous canopy such as a sole crop. In general, traits that allow optimum performance in intercrops may differ from those providing optimal sole crop yields. If, indeed, intercrops require genotypes with different traits than sole crops, it would pay off to select and breed varieties especially for use in intercrops. .

*Increase of the size of upper leaves contribute to improved light interception and assimilates production*

The green area above the node of flag leaf contributes 60 to 80% of the assimilates to the developing grains of wheat (Simpson, 1968; Gelang *et al.*, 2000), and the rate of grain filling is closely related to the photosynthesis of the flag leaves (Simpson, 1968; Sofield *et al.*, 1977; Verma *et al.*, 2004). Thus, an increase in the size of upper leaves could substantially contribute to grain yield. The size of the top four leaves was increased in the border-row plants. This effect was amplified by the greater number of surviving tillers in border rows and higher leaf chlorophyll concentration. However, the potential benefits were reduced by the shading of the neighbouring maize plants during the grain filling stage.

The increase in the size for top leaves must be attributed to an increase in leaf extension rate in both length and width, since leaf tip and collar appearance rates were constant across rows and treatments. An increase in leaf extension rate may be related to favourable nitrogen conditions (MacAdam *et*

*al.*, 1989). Consistent with Li *et al.* (2001), the N yields of grain, shoot and chaff were significantly higher in border-row plants than in sole wheat.

#### *Potential ecological implications*

The degree and direction of heterogeneity of light distribution within natural plant communities is strongly determined by the density, species composition and growth rates of the constituent plants, all of which differ substantially in time and space (Grime, 1994). This suggests that plants must have evolved fine-tuned detection mechanisms and transduction pathways that enable them to respond to the thus produced variation in light cues such that they can optimize their light capture. Physiological research indeed indicates that such mechanisms exist (Smith, 2000; Stamm and Kumar, 2010). However, few studies have analysed how the functional significance of plasticity in architectural traits, triggered by intra- and interspecific interactions, contributes to species performance in real plant communities. This study shows how a strong plasticity in tillering enables wheat to adjust its architecture strongly so as to improve its light acquisition in contrasting light environments. This may likely apply to other grasses as well. Tillering helps grasses to occupy space at an early time and maintain high rates of leaf area production which is essential in competition for light. In addition, the production of surviving tillers and the associated root production help to increase the uptake of available resources, as shown in higher N yields in the border row (Table 2.1). The senescence of tillers in dense canopies would balance the cost and benefits of tiller production (Fig. 2.4). In addition, the top leaves, which are vital for the production of grain filling, were larger (Fig. 2.5 A, B) and contained a higher chlorophyll concentration (Fig. 2.6). Together these results indicate the importance of plasticity in architectural traits for the success of tillering grasses.

## **Conclusions**

This study provides insight in the plastic responses of individual wheat plants in wheat-maize intercropping compared to sole crops throughout their lifetime, and confirms that the border row effect is a major factor in determining the advantage of wheat productivity in a wheat-maize relay strip intercropping system. The border row effect is shown here to be associated with a higher

number of reproductive tillers, larger top leaves on the main stem and on the tillers, and a greater number of grains per ear as compared to sole crop and inner rows. The potential yield advantage of border-row wheat in the mixture with maize is limited by the shade cast by maize during wheat grain filling, reducing the thousand-grain weight of wheat below its potential. A high degree of plasticity in tillering plays a crucial role in overyielding in intercrops while it may be less important in sole wheat if the sowing density is high. Insight in the determination of yield in intercropping can be used to optimize the strip arrangement and temporal overlap between the component species of intercrop systems by variety choice and management. Identification of the traits and plant responses that are associated with overyielding opens the way for assessing the genetic variation in these traits, and for subsequent breeding towards optimizing the yield benefits of intercropping. To further assess the relationships between plant development, crop architecture, intercropping design and light environment, experimental results may be combined with plant modelling. Functional-structural plant model (Vos *et al.*, 2010) which has been shown to be an effective tool for the evaluation of plant structural development and light interception (Evers *et al.*, 2007), can greatly help to quantify the contribution of plastic responses to the yield advantage of wheat in border rows.

## Appendix I

Fig. S2.1 The shape of a full-grown wheat leaf by plotting normalized margin to midrib distance versus normalized distance to leaf tip

Fig. S2.2 Moment of leaf tip and collar appearance on main stem and on tiller 1

Fig. S2.3 Thousand kernel weight versus number of kernels per square meter

Table S2.1 Yield components at different rows of intercrop with late sowing maize

## Acknowledgements

We thank Unifarm staff, Ans Hofman and Guohua Li for valuable help and contributions to the experiment, and Huub Spiertz for valuable comments. The financial support of the China Scholarship Council (CSC) and the Key Sino-Dutch Joint Research Project of NSFC (grant number: 31210103906) are gratefully acknowledged.

# CHAPTER 3

## Early competition shapes maize whole plant development in mixed stands

Junqi Zhu, Jan Vos, Wopke van der Werf, Peter E. L. van der Putten, Jochem  
B. Evers

Centre for Crop Systems Analysis, Wageningen University, PO Box 430, 6700  
AK, Wageningen, the Netherlands

## Abstract

Mixed cropping is practiced widely in developing countries and is gaining increasing interest for sustainable agriculture in developed countries. Plants in intercrops grow differently from plants in single crops, due to interspecific plant interactions, but adaptive plant morphological responses to competition in mixed stands have not been studied in detail. Here we describe maize response to mixed cultivation with wheat (*Triticum aestivum*). We provide evidence that early responses of maize (*Zea mays*) to the modified light environment in mixed stands propagate throughout maize development resulting in different phenotypes compared to pure stands. We compared photosynthetically active radiation (PAR), red:far-red ratio (R:FR), leaf development, and final organ sizes of maize grown in three cultivation systems: pure maize, an intercrop with a small distance (25 cm) between maize and wheat plants, and one with a large distance (44 cm) between the maize and the wheat. Compared to maize in pure stands, maize in the mixed stands had lower leaf and collar appearance rates, larger blade and sheath sizes at low ranks and smaller ones at high ranks, increased blade elongation duration, and decreased R:FR and PAR at plant base during early development. Effects were strongest in the treatment with short distance between wheat and maize strips. The data suggest a feedback between leaf initiation and leaf emergence at plant level and coordination between blade and sheath growth at phytomer level. A conceptual model, based on coordination rules, is proposed to explain the development of the maize plant in pure and mixed stands.

**Key words:** coordination of development, leaf development, phyllochron, plastochron, shade avoidance, wheat-maize intercropping

## Introduction

Intercropping is widespread in large parts of China, Africa and Latin America (Vandermeer, 1989; Vandermeer, 2011). It has important advantages compared to single crop systems: greater crop production per unit land (Li *et al.*, 2007), potential for improved water and nutrient capture (Morris and Garrity, 1993a; Morris and Garrity, 1993b), enhanced pest and disease suppression (Zhu *et al.*, 2000), and overall lower production risks (Rao and Singh, 1990). Adaptations in plant architecture and physiology are likely to contribute to the often reported overyielding (Lithourgidis *et al.*, 2011), but these adaptations have not been analysed (Connolly *et al.*, 2001). There is increasing interest for mixed cultivation systems in developed countries, to strengthen the ecological basis of agriculture and exploit the advantages of intercropping and agroforestry (Eichhorn *et al.*, 2006; Lichtfouse *et al.*, 2009; Pelzer *et al.*, 2012).

Light competition may be severe in mixed stands. Plants need to adapt to either tolerate (Gommers *et al.*, 2013) or avoid shading by neighbours (Franklin and Whitelam, 2007). For plants showing shade avoidance, alterations in both light quality and light quantity can invoke a suite of responses, including enhanced stem and petiole elongation, reduced branching, and more erect leaf angles (Sultan, 2010; de Wit *et al.*, 2012). Little is known about the consequences of local adaptation (e.g. enhanced sheath length) on later development and how this shapes and influences the development of whole plant architecture. Understanding the development of whole plant architecture (e.g. leaf appearance rate and final organ sizes) in mixed plant systems is of great importance for analysing whole-plant fitness and productivity of a component species in a mixed system and of the system as a whole.

A plant is built by the repeated formation, expansion and (partial) senescence of phytomers (Forster *et al.*, 2007). Growth responses of whole plants are realized by changes in the growth at phytomer level (Beemster *et al.*, 2003) with control at the plant level via hormones and sugar levels (de Kroon *et al.*, 2005; 2009). A phytomer of maize (*Zea mays*) consists of an internode with an axillary bud at the bottom, and a node, a leaf sheath and blade at the top. New phytomers are created at the shoot apex. Each component of the

phytomer unit differentiates, grows, appears and senesces with coordination among the components (McMaster, 2005).

During the vegetative stages of maize and rice (*Oryza spp*), blade tip emergence (defined as blade tip growing past the highest collar; collar marking the border between sheath and blade) is associated with the initiation of the associated sheath (defined as the moment when sheath length passes 1 mm) (Andrieu *et al.*, 2006; Parent *et al.*, 2009). In maize, collar emergence of a leaf, defined as its collar growing past the collar of the preceding leaf, is associated with a decline in elongation rate of the sheath and an increase in elongation rate of internode with the sum of the two remaining the same (Fournier and Andrieu, 2000a; Fournier and Andrieu, 2000b). It has been shown in grasses that blade and sheath length of a leaf are positively associated with the length of the whorl of mature sheaths through which the leaf grows (Davies *et al.*, 1983; Wilson and Laidlaw, 1985; Skinner and Nelson, 1994; Casey *et al.*, 1999). The length of the whorl affects several attributes of a leaf, such as final length, elongation rate, and length of the growing zone defined as the part in which cells divide and elongate (Durand *et al.*, 1995; Fournier *et al.*, 2005).

Leaf emergence rate in grasses is determined by the rate of leaf initiation at the apex, leaf elongation rate, and the whorl length of mature sheaths of previous phytomers through which this leaf emerges (Skinner and Nelson, 1995). In maize, high population density and low red: far-red ratio (R:FR) decelerate leaf emergence and increase sheath growth (Andrieu *et al.*, 2006; Page *et al.*, 2011), whereas leaf emergence rate increases with the daily sum of incident photosynthetically active radiation (PAR) (Birch *et al.*, 1998c; Padilla and Otegui, 2005). Conservative relationships between leaf emergence and leaf initiation have been found across hybrids and environments in wheat (*Triticum aestivum*) (Kirby, 1990), rice (Nemoto *et al.*, 1995), sunflower (*Helianthus annuus*) (Sadras and Villalobos, 1993) and maize (Kiniry *et al.*, 1983; Padilla and Otegui, 2005). The conservative relationship between the numbers of emerged and initiated leaves suggests coordination between the rates of leaf emergence, leaf growth and leaf initiation at the plant level.

All of these adaptive responses may be involved in the response of plants to mixed cropping but, as yet, ecophysiological research on intercrop performance has not considered the possibility of an effect of mixed cropping

on the regulation of plant development. We expect that plants in intercrops develop different structures in response to the changed light environment, while structural responses of different phytomers on the same plant are coordinated. What are these structural adaptations, and how are they coordinated between different phytomers on the same plant?

To answer these questions, we conducted a detailed analysis of maize development in three contrasting cultivation systems (henceforth: treatments): pure maize, an intercrop with a small distance (25 cm) between wheat and maize plants, and one with a large distance (44 cm) between the wheat and the maize. The structural development of the maize plants in the three systems was characterized by measuring leaf appearance, rate and duration of leaf elongation, collar emergence, and final sizes of blade and sheath of each phytomer. Generic coordination rules were inferred from the data.

## **Materials and Methods**

### *Experiment setup*

All measurements were made under ambient conditions in a field experiment in Wageningen, the Netherlands (51°59'20"N, 5°39'16"E) from March to October in 2011. Maize and wheat were grown in single and mixed stands on a sandy soil (N supply capacity: 96 kg N ha<sup>-1</sup> yr<sup>-1</sup>; organic matter: 5.9% with C/N ratio: 15; soil mineral N content before sowing (0-60 cm): 28 kg ha<sup>-1</sup>). Maize growth in three treatments was compared: (1) Monoculture maize at a row distance of 75 cm and a population density of 9.87 plants per m<sup>2</sup>. (2) Wide intercrop with 44 cm distance between adjacent wheat and maize rows. (3) Narrow intercrop with 25 cm between wheat and maize rows (Fig. 3.1). Intercropped maize was grown in strips of two rows, while intercropped wheat was grown in strips of six rows (Fig. S3.1). Row distance was 12.5 cm in wheat and 75 cm in maize. Intercrop plots included two maize strips, three wheat strips, and a maize border at each side. Plot size was 6 by 6 meters for both monoculture and wide intercrop. For narrow intercrop, the plot width was 4.9 meters (Fig. S3.1). Row direction was north-south. Each treatment was replicated three times.

Wheat 'Tybalt' was sown on 9 March 2011, and harvested on 10 August 2011. Maize 'LG30208' was sown on 11 May and harvested on 14

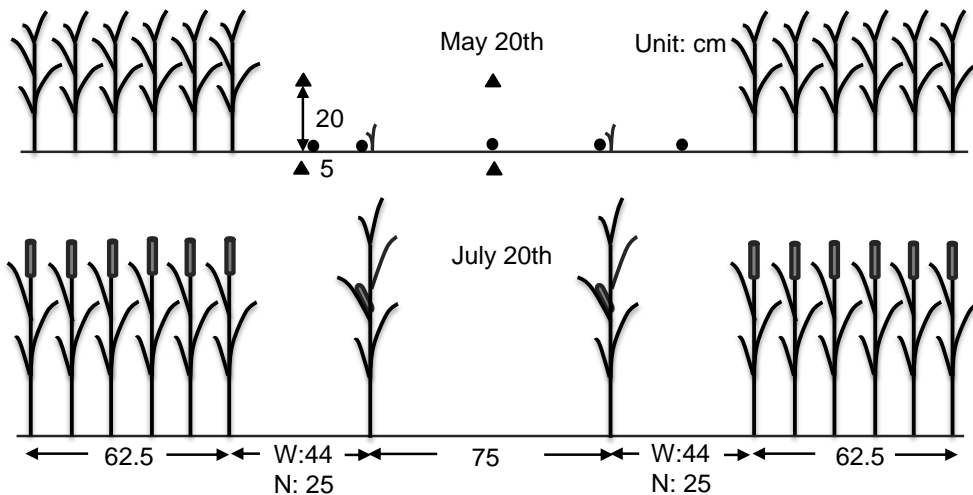


Fig. 3.1 Cross-row profile of a wheat-maize intercrop on May 20 and July 20 (unit: cm). Wheat was grown in 62.5 cm wide strips consisting of six rows at a distance of 12.5 cm. Maize was grown in strips of two rows, with 75 cm between the rows. The distance between maize and wheat was 44 cm (wide intercrop: W) or 25 cm (narrow intercrop: N), resulting in contrasting levels of interaction between wheat and maize. Wheat was sown on March 9, and harvested on 10 August, while maize was sown on May 11, and harvested on 14 October. On 20 July (675 °Cd), maize in wide intercrop reached the same height as the wheat. Dots indicate placement of PAR sensors, triangles represent placement of thermocouples. This figure is adapted from Fig. 2.1.

October. Fertilizer was applied homogeneously over the experiment. The first application was done on 5 April, after wheat emergence:  $15 \text{ kg P ha}^{-1}$ ,  $37 \text{ kg K ha}^{-1}$ ,  $14 \text{ kg Mg ha}^{-1}$  and  $46 \text{ kg N ha}^{-1}$ . Furthermore,  $75 \text{ kg N ha}^{-1}$  was top-dressed on 20 May shortly after maize emergence. An additional  $50 \text{ kg N ha}^{-1}$  was top-dressed on 10 June. Weeds were controlled mechanically after wheat emergence and chemically by 'primstar' and 'MCPA 500' on 27 April and by 'biathlon' and 'kart' on 3 June. Fungicide 'prosaro' and insecticide 'decis' were applied on 10 June in both wheat and maize.

#### *Temperature measurements and calculation of thermal time*

Temperature was recorded (Datataker DT600, Data taker Data Loggers, Cambridgeshire, UK) with shielded thermocouples (type T, TempControl Industrial Electronic Products, Voorburg, the Netherlands) at 10 minute

intervals. Thermocouples were placed at 5 cm depth, and at 20 cm above the soil surface within the canopy. Four thermocouples, two in the canopy and two in the soil, were placed at two locations in the maize strip, between the rows of maize and between the adjacent maize and wheat rows, in both intercrop treatments (triangles in Fig. 3.1). In monoculture maize, two thermocouples were placed between the rows, one in the canopy and one in the soil. Only slight differences in temperature were found between treatments and positions. Thermal time ( $^{\circ}\text{Cd}$ , degree days) was calculated on an hourly basis from sowing, considering a base temperature for maize development of  $8\text{ }^{\circ}\text{C}$  (Birch *et al.*, 1998a). Averaged soil thermal time for different positions from sowing to 1 July was  $8\text{ }^{\circ}\text{Cd}$  less in wide intercrop than in monoculture and  $28\text{ }^{\circ}\text{Cd}$  less in narrow intercrop than in monoculture. Average soil temperature over positions and treatments was used for temperature accumulation before jointing (1 July), when the apex was still below the soil surface, while average canopy temperature over positions and treatments was used for temperature accumulation after jointing.

#### *Plant selection*

In each plot, 12 similar maize plants were tagged when blade 2 was visible. Four of these were used for non-destructive observations. The remaining eight were used in two destructive samples, and their location was chosen such that sampling effects on plants used for non-destructive observations were minimized. To compare plants of similar developmental pattern, 49 maize plants with the predominant final leaf number in each treatment were selected from those initially tagged (see results for details) to analyse blade elongation and final organ size.

#### *Blade dynamics*

Leaves were counted acropetally starting from the bottom leaf. The number of visible, mature and dead leaves as well as the exposed length of all immature leaf blades were measured twice per week. Tip appearance and collar emergence were considered to occur midway between the last observation the event had not occurred yet and the first observation date on which the event had occurred. Emergence was defined as the moment a blade tip or collar had grown past the highest collar of the preceding sheaths. Tip appearance was

defined as the moment the blade tip had visibly appeared out of the whorl formed by preceding growing blades, when looking at a horizontal angle into the whorl. A blade was considered mature when its collar had emerged from the sheath tube formed by preceding phytomers. Phyllochron (i.e. the thermal time between appearances of successive leaf blades) was estimated as the slope of the linear relationship between thermal time at tip appearance and phytomer rank ( $^{\circ}\text{Cd leaf}^{-1}$ ). Regressions were made using the linear mixed-effects model (lme) in the ‘nlme’ package of the R programming language (R Core Team, 2014) with plot and plant (nested in plot) as random effects. The same method was used for analysing the relationship between final blade length and length of the encapsulating sheath.

### 3

#### *Blade elongation duration and elongation rate*

Blade dynamics data was further used for estimating the duration of blade elongation and calculate the average rate of elongation. Blade elongation duration was estimated by fitting the beta function (Eq. 3.1) (Yin *et al.*, 2003).

$$L(t) = L_{\max} \left( 1 + \frac{t_e - t}{t_e - t_m} \right) \left( \frac{t}{t_e} \right)^{\frac{t_e}{t_e - t_m}} \quad 0 \leq t_m < t_e \quad (\text{Eq. 3.1})$$

Where  $L(t)$  is measured blade length at thermal time  $t$  ( $^{\circ}\text{Cd}$ ) and  $L_{\max}$  is final blade length (cm).  $t_e$  is the time when final blade length was reached ( $^{\circ}\text{Cd}$ ) corresponding to the elongation duration from tip appearance to collar emergence in the measurement,  $t_m$  is the time when growth rate peaks ( $^{\circ}\text{Cd}$ ). Parameters  $t_m$  and  $t_e$  were estimated (Fig. S3.2) for each single blade using non-linear curve fitting with least squares (‘lsqnonlin’) in MATLAB 2012a (The MathWorks inc, Natick, Massachusetts, U.S.A.). The average elongation rate was calculated as the ratio of final blade length and estimated elongation duration ( $t_e$ ).

#### *Final organ size*

The sizes of all fully grown organs (blade, sheath and internode) of each maize phytomer were measured destructively on two sampling occasions. Blade width was measured at the widest cross-section. The first sampling (656  $^{\circ}\text{Cd}$ ) was at collar emergence of leaf 10 in monoculture maize; the second sampling (1261  $^{\circ}\text{Cd}$ ) was after maturity of the final leaf. Final blade length of phytomer

ranks 1 and 2 and final sheath length of rank 1 were not recorded due to their advanced senescence at the time of the first sampling.

#### *Red: far-red ratio (R:FR)*

We made weekly measurements of red : far-red ratio (R:FR) at approx. 2 cm above soil level around noon, using the Skye SKR100/116 Fibre Optic Probe Measuring System (Skye Instruments Ltd, Powys, UK). The device was equipped with a glass fibre probe that measured R:FR at its tip, with an angle of view of 40° relative to the soil surface. Measurements were made parallel to the soil surface with the sensor backing against the plant and facing north, east, south and west. The average of the four values was used for analysis.

A four-parameter logistic function (Eq. 3.2) was used to fit the data on R:FR versus thermal time using the ‘nlinfit’ function of Matlab.

$$\zeta(t) = \zeta_{\min} + \frac{\zeta_{\max} - \zeta_{\min}}{1 + \exp(k * (t - t_i))} \quad (\text{Eq. 3.2})$$

Where  $\zeta(t)$  is the R:FR measured at thermal time  $t$ .  $\zeta_{\min}$  and  $\zeta_{\max}$  are the lower and upper asymptotes (dimensionless),  $k$  is the slope at the inflection point ( $^{\circ}\text{Cd}^{-1}$ ),  $t$  is thermal time ( $^{\circ}\text{Cd}$ ) and  $t_i$  is the thermal time of the inflection point ( $^{\circ}\text{Cd}$ ).

#### *Photosynthetically active radiation (PAR)*

Light penetration at 2 cm above soil level was measured once per week around noon with a 1 m-long light-sensitive bar that was held parallel to the crop rows (SunScan Canopy Analysis System; Delta T Devices, Cambridge, UK). A reference PAR sensor was placed just above the canopy. Four fixed positions in each plot were measured in monoculture (two replicates in the middle of rows, and two directly adjacent to the plants with the row) and five in each of the intercrop treatments (dots in Fig. 3.1). A weighted mean fraction of PAR value of the four or five positions was used in further analysis. The weighting factors of different positions in the intercrop plots were calculated by their representative length; see Method S3.1 for details.

A four-parameter logistic function (Eq. 3.3) was used to model the fraction of incoming PAR reaching soil level as a function of thermal time:

$$f\text{PAR}(t) = f\text{PAR}_{\min} + \frac{f\text{PAR}_{\max} - f\text{PAR}_{\min}}{1 + \exp(k * (t - t_i))} \quad (\text{Eq. 3.3})$$

Where  $f\text{PAR}(t)$  is the fraction of PAR at soil level at thermal time  $t$ .  $f\text{PAR}_{\min}$

and  $fPAR_{\max}$  are the lower and upper asymptotes (dimensionless),  $k$  is the slope at the inflection point ( $^{\circ}\text{Cd}^{-1}$ ),  $t$  is thermal time ( $^{\circ}\text{Cd}$ ) and  $t_i$  is the thermal time of the inflection point ( $^{\circ}\text{Cd}$ ). The function was fitted to data using the 'nlinfit' function of Matlab.

#### *Tassel initiation and silking time*

Tassel initiation time, i.e. the switch from the vegetative to the generative phase, is estimated as the time when the final leaf was initiated at the apex. The timing of this switch cannot be observed macroscopically without dissection, and was therefore calculated from a linear regression between leaf initiation and leaf appearance (Table S3.2) (Padilla and Otegui, 2005). Silking time was defined as the time at which 75% of plants have silks visible (Hanway, 1963).

#### *Comparison of leaf initiation rate and leaf appearance rate between treatments*

Average leaf initiation rate (LIR) can be estimated by dividing the total number of initiated leaves by the thermal time from germination to tassel initiation. In order to assess the stability of the relationship between LIR of the monoculture and intercrop treatments, we calculated the ratio between LIR in monoculture and LIR in wide and narrow intercropping. As the thermal time to tassel initiation was similar among treatments, this ratio between LIR values could be estimated by simply taking the ratios of the number of initiated leaves (Eq. 3.4):

$$\frac{LIR_{MO}}{LIR_{WI}} = \frac{FLN_{MO} - 5}{FLN_{WI} - 5} \quad (\text{Eq. 3.4})$$

Where LIR is leaf initiation rate in monoculture (MO), wide intercropping (WI), or narrow intercropping (NI, not shown here).  $FLN_{MO}$ ,  $FLN_{WI}$  and  $FLN_{NI}$  represent the final leaf numbers in the three different treatments. We assume that 5 leaf initials are present in the embryo (Padilla and Otegui, 2005).

Leaf appearance rate (LAR) is the reciprocal of phyllochron. The ratio between LAR in monoculture and LAR in wide and narrow intercropping was calculated by taking the ratios of the reciprocal of phyllochron in each treatment.

#### *Statistics*

The data were analysed with linear mixed models to account for random effects and nesting in the data. The linear mixed model also takes into account

the fact that there were slightly different numbers of plant per plot, due to the random nature of our plant selection. We used in our analysis two types of linear mixed models, depending on the data structure. In the first type of analysis, there was only one measurement per plant. In this case, the plant was the unit of analysis, and the data were analysed with treatment as fixed effects and block and plot as random effects. This type of model was used for analysing final organ sizes, blade elongation durations and rates. In the second type of analysis, there were multiple measurements per plant included in the analysis. In this case, the data were analysed with phytomer rank and treatment as fixed effects and block, plot and plant as hierarchically nested random effects. This applies to the regression of phyllochron data. As none of the analyses with linear mixed models yielded a significant block effect, this effect was dropped from all models. The mixed effects model with plot and plant as random effects was used for analysing all data with multiple measurements per plant included in the analysis, and a model with only plot as random effect was used to analyse data with single measurement per plant. Multiple comparisons of treatments for final organ sizes, blade elongation durations and rates were done by means of least significant differences (LSD test,  $P = 0.05$ ) in the 'agricolae' package of R, after the treatment effects had been found significant using the mixed effects linear model. The mean square error and associated degrees of freedom required by the LSD function of R were obtained from the generalized least squares (gls) function with the restricted maximum likelihood (REML) method in the 'nlme' package in R. The experiment-wise rate of rejecting null hypotheses increases above the specified level  $\alpha$  when multiple comparisons are made. Use of LSD values here is justified due to the low number of treatments, and thus comparisons, but caution should nonetheless be used when interpreting marginally significant results.

## Results

### *Phenology*

Maize emerged approx. 60 °Cd after sowing, at which time the wheat was approx. 50 cm high. Maize in wide-intercrop treatment started to overtake

Table 3.1 Final leaf number distribution of three planting systems in non-destructive observation ( $n = 12$ ), destructive samples ( $n = 12$ ), and random count in field ( $n = 40$  for monoculture,  $n = 30$  for both wide and narrow-intercrop treatments)

Sample	Treatment	Number of leaves				
		12	13	14	15	16
Non-destructive samples ( $n = 12$ )	Monoculture				8(67%)	4(33%)
	Wide intercrop			9(75%)	3(25%)	
	Narrow intercrop	1(8%)	7(58%)	4(33%)		
Destructive samples ( $n = 12$ )	Monoculture				11(92%)	1(8%)
	Wide intercrop		1(8%)	7(58%)	4(33%)	
	Narrow intercrop		3(25%)	7(58%)	2(17%)	
Field random count ( $n = 40$ or 30)	Monoculture				24(60%)	9(22%)
	Wide intercrop		7(23%)	15(50%)	8(27%)	
	Narrow intercrop	3(10%)	10(33%)	12(40%)	5(17%)	

wheat in height at 675 °Cd (Fig. 3.1). At this time, the height of maize (measured from the soil surface up to the highest point at which the whorl of growing leaves still form a completely closed tube) was 125 cm in monoculture, 85 cm in wide intercrop and 70 cm in narrow intercrop. Maize in the narrow intercrop overtook wheat in height at 735 °Cd. The estimated tassel initiation time was 283 °Cd in monoculture, 295 °Cd in wide intercrop and 310 °Cd in narrow intercrop. Observed silking time was 780 °Cd in monoculture, 830 °Cd in wide intercrop and 864 °Cd in narrow intercrop.

Average final leaf number was  $15.3 \pm 0.08$  in monoculture,  $14.0 \pm 0.26$  in wide intercrop and  $13.6 \pm 0.35$  in narrow intercrop (Table 3.1). The most common number of leaves was 15 in monoculture, 14 in wide intercrop and 13 or 14 in narrow intercrop (Table 3.1). For subsequent analyses on the

characteristics of phytomers of individual plants, we used a subsample of plants with 15 leaves for monoculture, plants with 14 leaves in wide intercrop and an equal number of plants with 13 and 14 leaves in narrow intercrop, representing the modal leaf numbers in the three treatments. For the selected plants, the position of the subtending leaf of the cob was at rank 10 for monoculture, and rank 9 for both wide intercrop and narrow intercrop. The ratio between leaf initiation rates in monoculture and intercropping was 1.11 for wide intercropping and 1.25 for narrow intercropping.

#### *Leaf appearance and maturity*

From phytomer 4 onwards, blade tip appearance diverged among treatments (Fig. 3.2, solid lines). Average phyllochron from rank 2 onwards was  $44.2 \pm 0.5$  °Cd in monoculture,  $54.2 \pm 0.7$  °Cd in wide intercrop and  $62.8 \pm 0.8$  °Cd in narrow intercrop. The ratio between leaf appearance rates in monoculture and intercropping was 1.23 for wide intercropping and 1.42 for narrow intercropping. At the time of tip appearance of rank 14 in monoculture, plants in wide intercrop had approximately 12 leaves and plants in narrow intercrop had 10 leaves (Fig. 3.2).

Divergence of collar emergence occurred across treatments at low ranks (up to rank 8) (Fig. 3.2, dotted lines). The slope for rank 3 to 8 was  $67.4 \pm 1.3$  °Cd in monoculture,  $77.5 \pm 1.7$  °Cd in wide intercrop and  $85.1 \pm 1.6$  °Cd in narrow intercrop. For ranks beyond rank 8, collars emerged at similar thermal time intervals in the three treatments ( $27.6 \pm 1.1$  °Cd in monoculture,  $25.3 \pm 1.4$  °Cd in wide intercrop and  $28.9 \pm 2.0$  °Cd in narrow intercrop).

#### *Final size of organs*

Monoculture plants had the shortest blades in ranks up to 7 (Fig. 3.3A), but the longest blades in ranks beyond 8. Differences between treatments were significant for all ranks except 2 and 8 (LSD test at significance level of 0.05). However, for upper ranks this effect was confounded with differences in final leaf number between the treatments. Narrow-intercrop plants had smallest blade width for ranks up to 7. For ranks beyond 7, monoculture plants showed a significantly larger final blade width than the other treatments (Fig. 3.3B, significant for all ranks except rank 8). Leaf shape, represented by the ratio

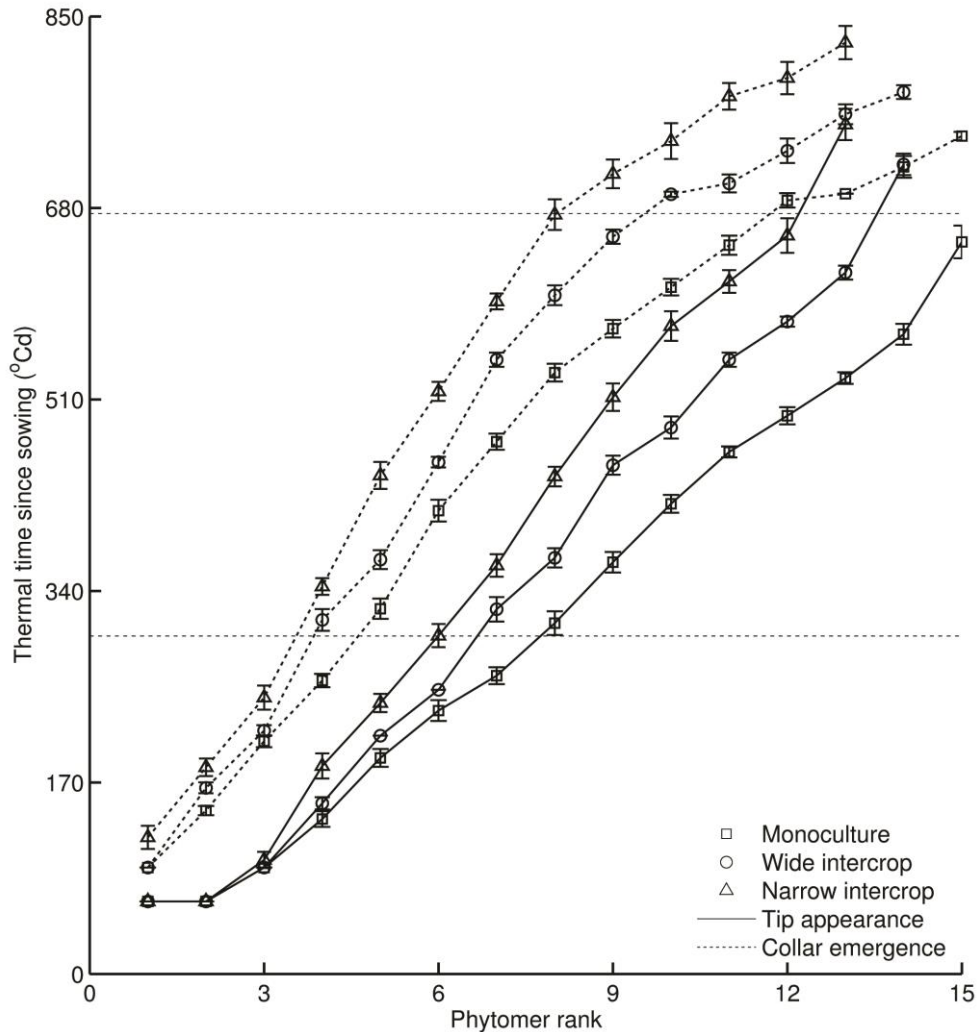


Fig. 3.2 Moment of blade tip appearance (solid lines) and collar emergence (dashed lines) of maize versus phytomer rank in monoculture (squares,  $n = 8$ ), wide intercrop (circles,  $n = 9$ ) and narrow intercrop (triangles,  $n = 7$ ). Upper dashed line ( $y = 675$  °Cd) indicates the time when maize in the wide intercrop became taller than wheat. Lower dashed line ( $y = 300$  °Cd) indicates tassel initiation time. Error bars indicate standard error (se).

between final blade length and width, showed significant differences between treatments for ranks up to 7 (Fig. 3.3C). In contrast, for ranks beyond 7, a

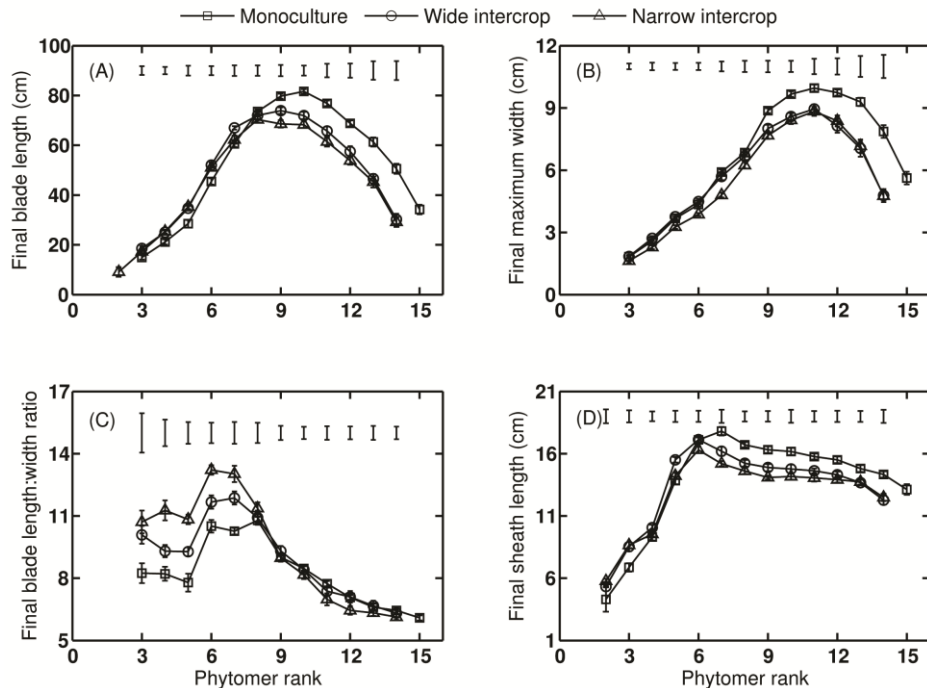


Fig. 3.3 Final blade length (A), final blade width (B), final blade length: width ratio (C), final sheath length (D) versus phytomer rank in monoculture (squares,  $n = 11$ ), wide intercrop (circles,  $n = 7$ ) and narrow intercrop (triangles,  $n = 7$ ). Error bars indicate one standard error (se). Top bars represent least significant difference ( $P < 0.05$ ) between treatments.

similar ratio was found across treatments, even though plants in monoculture and intercrops differed in their final dimensions. Across all treatments, monoculture plants had the smallest final sheath lengths in ranks up to 5 (Fig. 3.3D). Monoculture plants had the peak of sheath length at a higher rank (7) compared to wide and narrow intercrop (both 6). Beyond rank 6, monoculture plants had the largest sheath lengths (significant for all ranks).

The relationship between final blade length and the length of the encapsulating sheath (*i.e.* the sheath of the previous phytomer, which represents the length of the whorl that a blade grew through before maturity) was linear and independent of the treatment for ranks 3 to 7 (Fig. 3.4). Data for rank 1 and 2 were missing. No stable relationships were found between

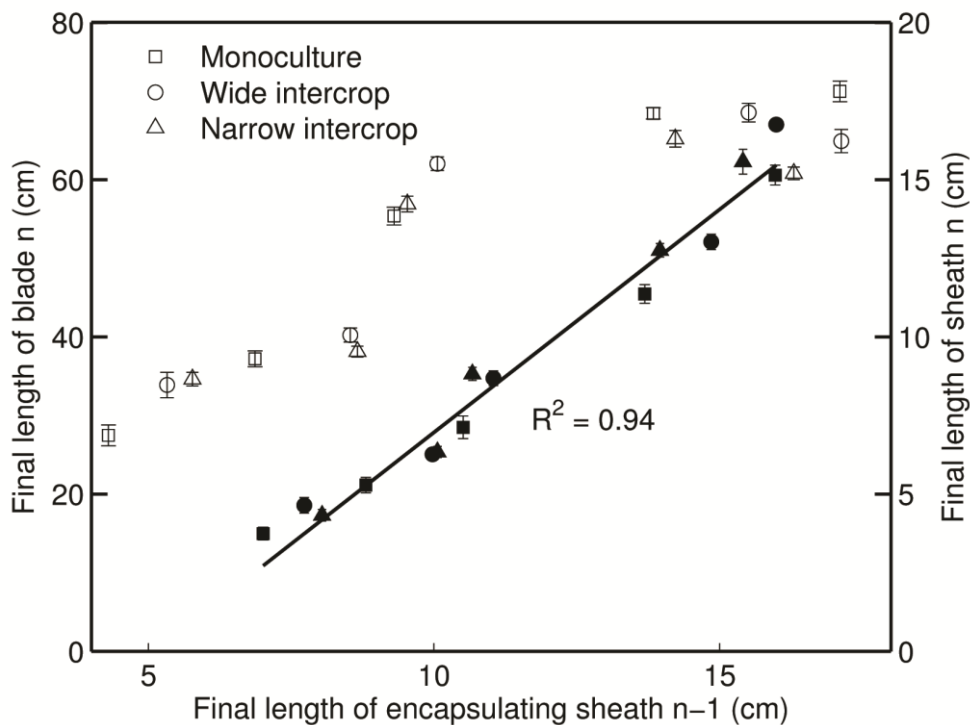


Fig. 3.4 The final length of blade (filled symbols, primary y-axis) and sheath (open symbols, secondary y-axis) plotted against final length of the encapsulating sheath (i.e. the sheath of the preceding phytomer) in monoculture (squares,  $n = 11$ ), wide intercrop (circles,  $n = 7$ ) and narrow intercrop (triangles,  $n = 7$ ) based on phytomers 3 to 7. Error bars indicate one standard error (se).

blades and sheaths length beyond rank 7. Final sheath length also increased with the length of the encapsulating sheath, but the relationship levelled off for lengths of the encapsulating sheaths above 13 cm.

#### *Blade elongation duration and rate*

The duration of the visible blade elongation from blade tip appearance to collar emergence, plotted against phytomer rank, showed a bell-shaped curve in all treatments (Fig. 3.5A). Up to the peak, monoculture had shortest blade elongation duration and lowest accumulated duration (inset in Fig. 3.5A). Beyond the peak, the trend reversed: monoculture gradually showed the

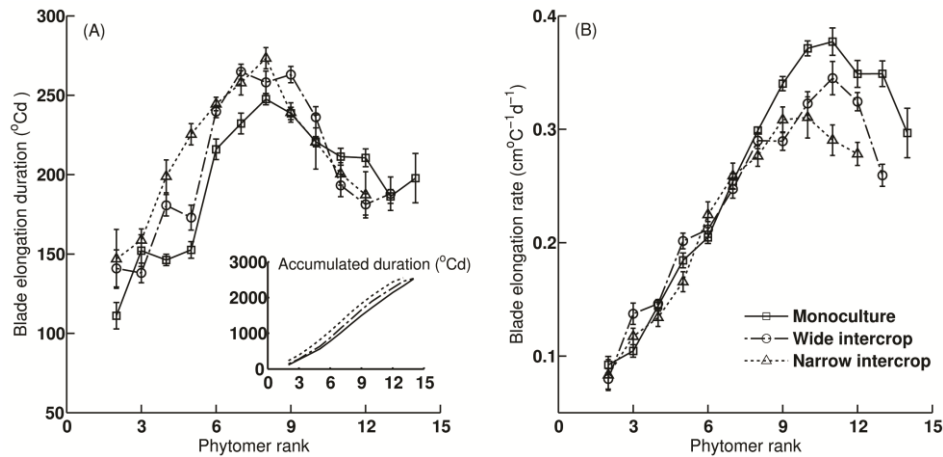


Fig. 3.5 Blade elongation duration (A) and blade elongation rate (B) versus phytomer rank in monoculture (squares,  $n = 8$ ), wide intercrop (circles,  $n = 9$ ), and narrow intercrop (triangles,  $n = 7$ ). Inset (A): Accumulated elongation duration from phytomer 2 to the last one. Error bars indicate one standard error (se).

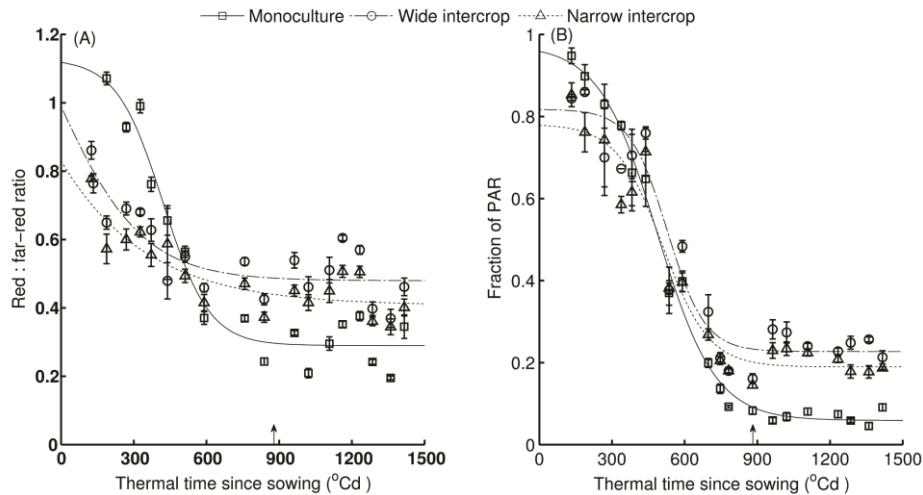


Fig. 3.6 The red : far-red ratio (A), fraction of PAR measured at soil level (B) as a function of thermal time since sowing in monoculture, wide intercrop and narrow intercrop. R:FR values represent averages of four values (sensor facing north, east, south and west) and PAR values represent averages of four or five values measured in one plot. Arrows indicate wheat harvest time (887 °Cd). Symbols represent the same treatment as in fig. 3.5. Error bars indicate standard error (se).

longest elongation duration. A similar shape was found for average blade elongation rate, with the peak at rank 10 or 11 (Fig. 3.5B). In contrast, no significant differences were found in blade elongation rate as a function of rank among treatments below rank 10. For higher ranks, the comparison was confounded with the difference in final leaf number.

#### *Red:far-red ratio and photosynthetically active radiation*

In the early stages of canopy development (before ca. 500 °Cd) the highest R:FR and fractions of PAR reaching the soil surface were found in monoculture canopies, while narrow-intercrop canopies showed the lowest values (Fig. 3.6). However, both R:FR and PAR fractions decreased faster in monoculture than that in intercrop canopies, resulting in monoculture canopies having lowest R:FR and PAR fractions in all treatments. In the end, R:FR stabilized at approx. 0.29, 0.48, 0.41 and PAR fraction at approx. 0.06, 0.23, 0.19 (Table S3.1) in monoculture, wide intercrop and narrow intercrop, respectively. The values in wide-intercrop canopies were always above those in narrow-intercrop canopies.

## **Discussion**

The aim of this study was to assess the developmental response of maize to the growth conditions in mixed cultivation with wheat. In our intercrop treatments, maize seedlings experienced strong competition for light by neighbouring wheat plants, which were about 50 cm tall at maize emergence (Fig. 3.1). Mixed cultivation lowered early R:FR in maize due to reflection of low-R:FR light by wheat, and PAR was initially lower in intercrops due to shading by adjacent wheat plants (Fig. 3.6). The real extent of R:FR and PAR reduction over the whole day must likely have been greater than presented here, since the measurements were made around noon, when shading is at the lowest point of the day. Maize development in intercrops was significantly affected, right from the start, as shown by decelerated leaf appearance and collar emergence rates, and enhanced final blade and sheath lengths of low ranks. A close relationship between blade and sheath length at low ranks was found across treatments (Fig. 3.4), explaining why intercropped plants have longer blades. Substantial

differences among treatments were found in blade elongation duration in low ranks, but blade elongation rate was not affected (Fig. 3.5).

Based on these quantitative findings and previously established rules in coordination of maize development (Skinner and Nelson, 1994; Skinner and Nelson, 1995; Fournier and Andrieu, 2000a; Fournier *et al.*, 2005; Andrieu *et al.*, 2006; Verdenal *et al.*, 2008), we infer that plasticity in leaf appearance and final length of blades and sheaths emerges as a result of coordination of developmental processes. Early modification of the light environment of maize seedlings by wheat plants in an intercrop generates local responses at the phytomer level which subsequently interact, apparently according to generic rules, to shape development of maize whole plant architecture during the remainder of the season.

#### *Enhanced sheath length during early development is a shade avoidance response*

The cross-over in R:FR ratios and fraction of PAR at soil level across treatments occurred around 500 °Cd (Fig. 3.6). This is when intercrops had 5-6 and monoculture had 7 fully expanded leaves (Fig. 3.2). Final sheath length is reached soon after collar emergence (Lafarge *et al.*, 1998; Fournier and Andrieu, 2000a). The cross over in sheath length across treatments occurred around phytomer 6 (Fig. 3.3D), and in blade length/width ratio occurred around phytomer 8 (Fig. 3.3C). Hence, it seems that some of the changes in treatment effects on organ size occurred around the same time as the cross-over in R:FR ratios and fraction of PAR at soil level, suggesting a relationship between organ size and radiation conditions. Low R:FR or low blue light intensity enhance sheath extension in grasses (Casal *et al.*, 1985), which allows plants to avoid future shading by neighbours (Corré, 1984; Ballaré, 1999). Moreover, longer sheaths were found at high population density compared to regular population density in maize (Andrieu *et al.*, 2006) which was attributed to neighbour-induced early R:FR drops. This leads us to infer that enhanced sheath length of low ranks (Fig. 3.3D) was associated with a reduction in R:FR and PAR fraction at soil surface which are intimately related (Evers *et al.*, 2006). The increase in sheath length in subsequent early phytomers supports the idea that collar emergence triggers the decline of sheath elongation rate (Fournier and Andrieu, 2000a), and is responsible for propagating differences in length

created on early phytomers because of the linear relationship between the length of successive sheath ranks and between blade length and sheath length of the preceding phytomer (Fig. 3.4) (Andrieu *et al.*, 2006).

*Leaf appearance and final leaf number are affected by sheath length at low ranks and by feedback between leaf emergence and initiation*

Leaf appearance was significantly delayed in the two intercrop treatments. For example, in comparison to monoculture maize, the appearance of leaf 10 was delayed by 67.7 °Cd in the wide intercrop and by 157.8 °Cd in the narrow intercrop. The extent of leaf appearance delay caused by intercropping was much larger than the effect of high population density in maize compared to normal density (24.2 °Cd for leaf 10) (Andrieu *et al.*, 2006). Likewise, Page *et al.* (2011) found that artificially low R:FR resulted in 1.1 fewer leaf tips at the 10-leaf tip stage of maize. Since temperature did not materially differ between treatments and leaf appearance of maize is comparatively insensitive to N supply within a wide range (Radin, 1983; Vos *et al.*, 2005), it appears plausible that early changes in light environment cause the delay in leaf appearance.

Padilla and Otegui (2005) found that there is a positive linear relationship between the number of appeared and initiated leaves in maize and that this relationship is conservative over varieties and environmental conditions. Our observation of larger phyllochron in intercropped maize as compared to monoculture maize thus indicates that plastochron is greater in intercropped maize than in monoculture maize. There was only a small effect on tassel initiation time, an event that is mainly determined by temperature and photoperiod (Muchow and Carberry, 1989; Birch *et al.*, 1998b). As a consequence the final number of leaves was lower in intercropping, which supports the positive association derived by Sadras and Villalobos (1993) that final leaf number is equal to the product of thermal time duration from emergence to tassel initiation and rate of leaf primordium initiation plus number of leaf primordium in the embryo. The comparable ratios of leaf initiation rate and leaf appearance rate between monoculture and intercrops indicate that the change in leaf initiation rate and leaf appearance rate is consistent which supports the hypothesis that leaf initiation is coordinated with leaf emergence (Padilla and Otegui, 2005).

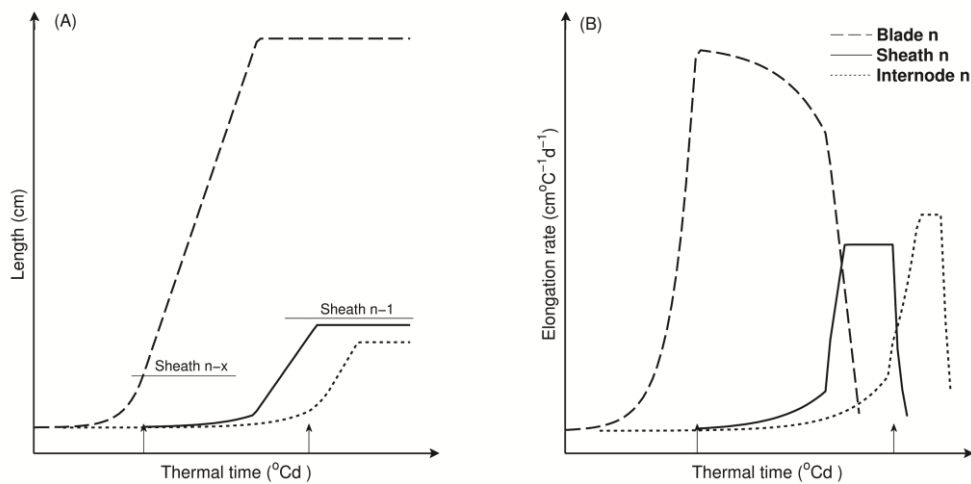


Fig. 3.7 Modelled lengths (A) and elongation rates (B) of blade, sheath and internode of a phytomer against thermal time. Arrows represent tip emergence (left arrow) and collar emergence (right arrow). Horizontal lines in (A) represent the length of the sheath with its ligule at the highest position of the plant, at tip emergence (left line) and collar emergence (right line). In this model, the rate of leaf initiation is influenced by tip emergence. The blade follows quasi-exponential growth until emergence of the tip. The associated internode is initiated about half a plastochron after the blade is initiated, and then follows exponential growth until collar emergence (Fournier and Andrieu, 2000a). Before tassel initiation, tip emergence triggers sheath initiation. After tassel initiation, sheaths are initiated according to a repetitive scheme (Andrieu *et al.*, 2006). The growth of the sheath gradually reduces the growth rate of the associated blade. Collar emergence triggers the growth shift between sheath and internode (Fournier and Andrieu, 2000a) and consequently inhibits sheath length increase.

There are two possible mechanisms for the coordination between leaf initiation and leaf emergence. First, apex growth and primordia initiation depend on carbon supply of photosynthetic leaves, especially the first leaf, and shade reduces this carbon supply (Felipe and Dale, 1973). Second, apex development is influenced by signals transferred from the emerging leaf (Bernier, 1988) or from the roots (Pons *et al.*, 2001; Wasternack, 2007). Signaling has been shown to play a role in the floral transition of maize: a transmissible signal in the leaf elicits the transformation of the shoot apex to reproductive development (Colasanti *et al.*, 1998). Thus we infer that there is a

positive feedback between leaf emergence and leaf initiation in which a delay in leaf emergence would be amplified by the delay in leaf initiation, and vice versa. This would explain why in our experiment leaf appearance continued to diverge between treatments.

We conclude that the effect of the intercrop treatments on leaf appearance can be attributed to two factors: length of the sheath whorl, and leaf initiation rate at the stem apex. For a given rate of leaf elongation, leaf emergence occurs later when the preceding sheaths are longer. Therefore, an increase in sheath length due to shade avoidance could postpone the time of leaf emergence, and this is a likely contributing factor to delayed initiation of new leaves.

### 3

#### *Final blade length distribution along the stem is driven by sheath length and tassel initiation*

A likely cause of the enhanced duration of blade elongation at low ranks in the intercropping treatments (Fig. 3.5A) was the link between elongation duration and sheath length. Due to the coordination between tip emergence and sheath initiation (Andrieu *et al.*, 2006; Parent *et al.*, 2009), longer sheaths delayed tip emergence and therefore increased duration of blade elongation (Verdenal *et al.*, 2008). In addition, extension of the sheath progressively reduces the growth rate of blade since they share the same growing zone (Fig. 3.7B) (Schnyder *et al.*, 1990; Skinner and Nelson, 1994). After tassel initiation, sheaths initiated faster, independent of leaf tip emergence. This is supported by our observation that the collar emergence diverged before rank 8 while afterwards collars emerged at similar rates across treatments (Fig. 3.2). This explained the plateau in leaf length for the middle phytomers. The reduction of final blade length in high ranks was probably due to a reduction in relative blade elongation rate and undelayed sheath initiation and fast extension (Andrieu *et al.*, 2006). This provides a mechanistic explanation how typical bell shape of the final blade length distribution along the stem was formed (Fig. 3.3A), which has been found in many studies on maize (Fournier and Andrieu, 1998; Ma *et al.*, 2007) and is generally found in cereals, e.g. wheat (Evers *et al.*, 2005); sorghum (*Sorghum bicolor*) (Lafarge *et al.*, 2002); barley (*Hordeum vulgare*) (Buck-Sorlin *et al.*, 2005) and rice (Tivet *et al.*, 2001).

*Towards a general conceptual model of maize shoot development in response to early competition*

From our results, a conceptual model of maize shoot development can be derived that captures the effects of strong competition during early development, such as in wheat-maize intercropping (Fig. 3.7). Early low R:FR and PAR in the intercrop enhance sheath length of the lower phytomers (including coleoptile) and decelerate leaf initiation. This then slows the emergence of leaf tips and collars, which is propagated to later formed phytomers by the feedback between leaf emergence and initiation. The time of switch to the reproductive phase was similar across treatments. Thus, because of the lower leaf initiation rate in intercrop, the final leaf number was lower in the intercropped maize than in the monoculture. These concepts of shoot development underlie plasticity in leaf emergence and organ size in response to environmental cues for competition, and can be scaled up to a whole-plant response.

*Relationship between maize developmental response, light interception and yield*

Crop production is closely related to the cumulative intercepted radiation (Monteith and Moss, 1977; Zhang *et al.*, 2008b). Maize and wheat grown in relay-intercrop, as in this study, where the growing seasons of the two species overlap only partly in time, have the ability to intercept more light over the season than either of the single crops would be able to do. For this to be realized, plant adaptation might be required to fill the gaps that are left in the sowing pattern for later sowing of maize. Zhang and Li (2003) reported strong overyielding in border rows of wheat in wheat-maize intercrop. Maize seedlings are competitively weaker than wheat which was already 50 cm tall at the maize seedling stage. As shown here, maize adapts by shade avoidance, which might have acted to mitigate the yield losses that could possibly have occurred, due to shading by wheat, if shade avoidance had not taken place. A simulation model that takes into account the structural adaptations and calculates light interception at the organ level (Vos *et al.*, 2010), would be helpful in evaluating the value of these adaptations in enhancing light interception and carbon assimilation. Understanding such responses can help identify intercrop designs and plant genotypes that maximize light interception and yield in a mixed stand.

Whilst such above ground responses are undoubtedly of key importance for the functioning and productivity of the crop, it should also be considered that below-ground processes could equally affect resource capture and productivity (Li *et al.*, 2007). Hence, this research has only been a first step to link intercrop productivity to crop responses at the plant and phytomer level, and the inter-phytomer regulation of plant development. In intercropping studies there needs to be special interest also in the responses of roots (de Kroon, 2007) and in coupling above-below ground plant development and architecture. We believe that further work in this domain is important and promises to contribute eventually to efficient land use, high crop productivity, and food security.

3

## **Appendix II**

Method S3.1 Calculation of weighting factor of different PAR measurement positions in intercropping

Fig. S3.1 Schematic diagrams of experimental layout

Fig. S3.2 Example of using beta function to derive blade elongation duration

Table S3.1 Fitting parameters for R:FR and PAR dynamic in three treatments

Table S3.2 Coordination between leaf initiation and leaf appearance

## **Acknowledgements**

We thank Unifarm staff and Ans Hofman for valuable help and contributions to the experiment, and Bruno Andrieu for fruitful discussion. The financial support of the China Scholarship Council (CSC) is gratefully acknowledged.

## CHAPTER 4

### Towards modelling the flexible timing of shoot development: simulation of maize organogenesis based on coordination within and between phytomers

Junqi Zhu<sup>1</sup>, Bruno Andrieu<sup>2</sup>, Jan Vos<sup>1</sup>, Wopke van der Werf<sup>1</sup>,  
Christian Fournier<sup>3,4</sup> and Jochem B. Evers<sup>1</sup>

<sup>1</sup>Centre for Crop Systems Analysis, Wageningen University, 6708 PB  
Wageningen, The Netherlands

<sup>2</sup>Institut National de la Recherche Agronomique, Unité Environnement et  
Grandes Cultures, 78850 Thiverval-Grignon, France

<sup>3</sup>INRA, UMR 759 LEPSE, F-34060 Montpellier, France

<sup>4</sup>SupAgro, UMR 759 LEPSE, F-34060 Montpellier, France

## Abstract

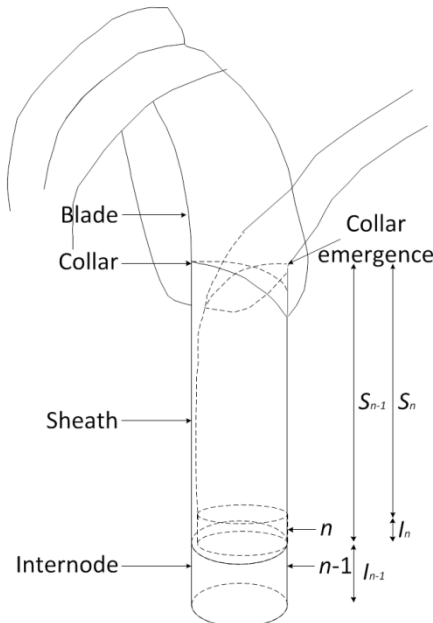
Experimental evidence challenges the approximation, central in crop models, that developmental events follow a fixed thermal time schedule, and indicates leaf emergence events play a role in the timing of development. The objective of this study is to build a structural development model of maize (*Zea mays*) based on a set of coordination rules at organ level that regulate duration of elongation, and to show how the distribution of leaf sizes emerges from this. A model of maize development was developed based on three coordination rules between leaf emergence events and dynamics of organ extension. The model was parameterized with data from maize grown at a low plant population density and tested using data from maize grown at high population density. The model gave a good account of the timing and duration of organ extension. By using initial conditions associated with high population density, the model well reproduced the increase of blade elongation duration and the delay of sheath extension in high density compared to low density. Predictions of the sizes of sheaths at high density were accurate, whereas predictions of the dynamics of blade length were accurate up to rank 9. Moderate overestimation of blade length occurred at higher ranks. A set of simple rules for coordinated growth of organs are sufficient to simulate the development of maize plant structure without taking into account any regulation by assimilates. In this model, whole plant architecture is shaped through initial conditions that feed a cascade of coordination events.

**Key words:** coordinated growth, leaf emergence events, maize, elongation duration, structural development

## Introduction

Plant development responds strongly to the environment by changing individual organ size. The relative contribution of rate and duration of elongation to the changes of organ sizes is not known. Therefore, in many plant models elongation duration of each organ is fixed while only elongation rate can be modulated by environmental factors (Fournier and Andrieu, 1998; Evers *et al.*, 2005; Guo *et al.*, 2006; Vos *et al.*, 2010). However, this fixed duration is challenged by experimental evidence that duration does vary in different environments (Sugiyama and Gotoh, 2010), and this is relevant both for understanding the distribution of organ size along a shoot (Andrieu *et al.*, 2006), as well as plant response on organ size to environmental factors such as temperature stress (Louarn *et al.*, 2010) and shading by neighbouring plants (chapter 3).

Andrieu *et al.* (2006) showed that the onset of sheath extension and duration of blade extension are major determinants of the response of blade length of maize (*Zea mays*) to plant density. Louarn *et al.* (2010) illustrated that under chilling conditions, maize leaves (blade + sheath) have a longer duration of elongation which compensates for the slower rate of growth. All these authors confirmed the positive effects of the length of the sheath tube (Fig. 4.1) on the elongation rates and durations of the blades and sheaths that grow within it (Davies *et al.*, 1983; Wilson and Laidlaw, 1985; Casey *et al.*, 1999). Thus, early growth processes appear to affect later growth processes by affecting the length of the sheath tube. Because of the positive effect of the length of a sheath  $n$  on the length of the next sheath,  $n + 1$  (Andrieu *et al.*, 2006), changes in the length of lower sheaths would continue to propagate to upper sheaths and thus also to blades. The positive effect of the length of a sheath  $n$  on the length of sheath  $n + 1$  likely acts through a coordination mechanism in which a decline of the elongation rate of a given sheath  $n$ , leading to cessation of sheath growth, is coordinated with the emergence of its collar (Fournier and Andrieu, 2000b; Fournier and Andrieu, 2000a). Such coordination rules can result in a flexible timing of organ development because the time of events is partly controlled by the architecture itself (Verdenal *et al.*, 2008). However, no structural model has been set up mainly based on



4

Fig. 4.1 Schematic diagram of two successive phytomers, showing the relationships among the time of collar emergence, the lengths of the sheaths ( $S_{n-1}$  and  $S_n$ ) and the length ( $I_n$ ) of internode  $n$ . Adapted from Fournier and Andrieu (2000a).

coordination rules, e.g. synchrony between emergence events and dynamics of organ extension. Hence, there are no tools for explaining the change of leaf elongation duration under various growth conditions. The aims of this study are to (I) set up a structural development model of maize based on a set of coordination rules at the organ level that regulate elongation duration; (II) show how the timing of organ development can be influenced by initial conditions through coordination rules.

In this study we integrated three coordination rules, in sequence of succession of leaf emergence events: (I) tip emergence of leaf  $n$  is coordinated with initiation of sheath  $n$  and stabilization of the elongation zone length of blade  $n$  (Andrieu *et al.*, 2006); (II) collar emergence of leaf  $n-1$  is coordinated with the start of linear elongation of sheath  $n$  (rule newly postulated); (III) collar emergence of leaf  $n$  is coordinated with the decline of elongation rate of sheath  $n$  and the rapid increase of the elongation rate of internode  $n$  (Fournier

and Andrieu, 2000a). These three coordination rules were implemented in a model of maize shoot development, using the principles of functional-structural plant model (FSPM, Vos *et al.*, 2010). FSPM is suited to model morphogenesis as a coordinated growth process, and allows the implementation and study of hypotheses drawn from experimental data. The model was parameterized using the parameters derived from the growth of maize plants at low density (Andrieu *et al.*, 2006) and was tested by simulating the growth of maize plants at high density by adapting only the initial conditions, but keeping model parameters the same. Thus, the model testing allows evaluation of the effect of coordination on the emergence of a modified structure of the whole plant over time, based on a change in the initial conditions only. These initial conditions were the dynamics of the length of the first three sheaths, which could therefore be used to reflect the environmental influence on the early growth of the plant. The sensitivity of time of leaf tip emergence to the changes in the relative rate of blade elongation were analysed. A scenario study was carried out to assess the effects of early competition by varying the initial conditions of the model. The model is described according to the protocol of Grimm *et al.* (2006).

## Materials and Methods

### *Model concepts*

The novel model concept developed in this study represents a holistic system view of plant development and contains coordination rules governing whole plant development during both the vegetative and reproductive phases (Fig. 4.2). Concepts taken from earlier work are (1) the synchrony between collar emergence of a leaf and the rapid increase of the elongation rate of the associated internode (Fournier and Andrieu, 2000a), (2) a model for elongation of individual grass leaf at vegetative phase (Fournier *et al.*, 2005), and (3) the synchrony between sheath initiation and leaf tip appearance before tassel initiation, and sheath initiation at a constant time interval after tassel initiation (Andrieu *et al.*, 2006). A novel element of our current model is the new coordination rule II, which was derived from the experimental observation and allows the simulation for all phytomers instead of individual phytomer. Also, our model takes into account the reproductive phase in which rules for sheath

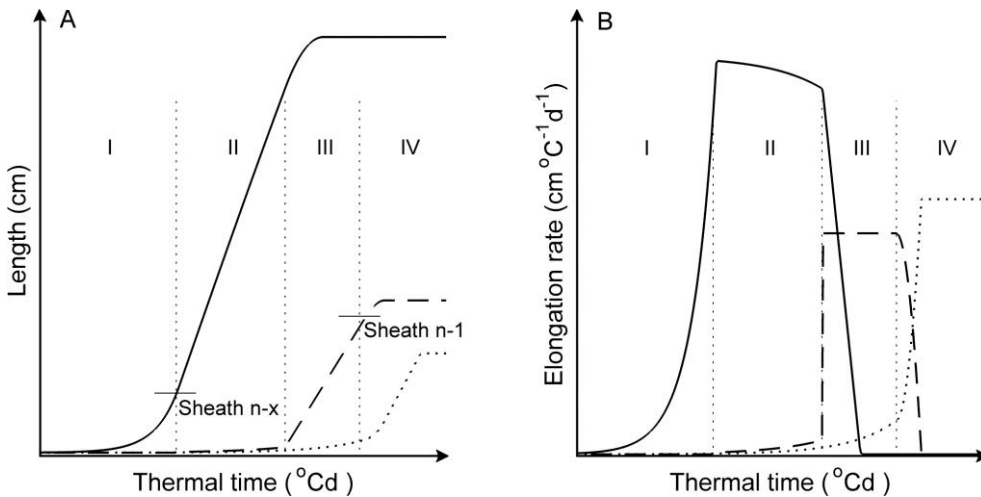


Fig. 4.2 Conceptual model of lengths (A) and elongation rates (B) of blade (solid lines), sheath (dashed lines) and internode (dotted lines) of a phytomer  $n$  with leaf tip emergence before tassel initiation, plotted against thermal time. Vertical dotted lines separate four phases of growth of the phytomer. Phase I: from blade initiation until tip emergence. Phase II: from tip emergence until collar emergence of the preceding leaf. Phase III: from collar emergence of the preceding leaf until collar emergence of the leaf itself. Phase IV: from collar emergence until completion of growth. The short horizontal line segments in (A) represent the length of the sheath which has the highest ligule on the plant at tip emergence (left line) and collar emergence (right line). The successions of leaf emergence events that linked with coordination rules were tip emergence, collar emergence of the preceding leaf and collar emergence of the leaf itself. Further explanation is given in the text. Adapted from Fig. 3.7.

initiation and start of linear elongation are different from the vegetative phase, and in which internode elongation plays an important role in the timing of events.

The model is implemented in the interactive modelling platform GroIMP (Buck-Sorlin *et al.*, 2005; Kniemeyer, 2008), and simulates growth of individual blades, sheaths and internodes (Appendix III Fig. S4.1). The state of each of these organs is characterized by their attributes (Table 4.1). Whole plant growth emerges as a result of three coordination rules.

Table 4.1: List of model attributes and parameters, their definitions, units and values

Attributes	Definition	Value/Unit
Phytomer rank	Phytomer number counting from bottom to top	
$B_n, S_n, I_n$	Length of blade, sheath and internode of phytomer $n$	cm
$E_n$	Length of the blade elongation zone of phytomer $n$	cm
$E_{n,\max}$	Maximum length of the elongation zone that was reached by blade $n$	cm
$I_n^*$	The length of internode $n$ at collar emergence	cm
hasInitiated	True when organ is initiated	true/false
hasTipEmerged	True when the sum of the length of blade, sheath and internode of rank $n$ is larger than the length of the sheath with its ligule at the highest position of the plant at that time	true/false
hasReached $E_{n,\max}$	True when $E_{n,\max}$ has been reached for blade $n$	true/false
hasCollarEmerged	True when the sum of the length of sheath and internode of rank $n$ is larger than the length of the sheath with its ligule at the highest position of the plant at that time	true/false
hasMatured	True when elongation rate of an organ is smaller than $1 \cdot 10^{-3} \text{ cm } ^\circ\text{Cd}$	true/false

In the current paper, following Andrieu *et al.* (2006), we define emergence as the event that a leaf tip or collar grows past the highest collar of the preceding sheaths (Fig. 4.1), while appearance is the event that the blade tip appears visibly out of the whorl formed by preceding growing blades. Phyllochron here was defined as the thermal time interval between emergences of successive leaf blades.

The general concepts of how the growth of blades, sheaths and internodes is coordinated are as follows (Fig. 4.2). The extension of one phytomer can be seen as four phases delineated by emergence events on the phytomer itself or on the preceding phytomer (Phase I to IV in Fig. 4.2).

During phase I (from blade initiation until tip emergence), blade and internode are present, and grow exponentially. The internode is initiated at half a plastochron after initiation of the blade at the lower half of the disc of leaf insertion (Sharman, 1942). During phase II (from tip emergence until collar emergence of the preceding leaf), blade, sheath and internode are present. The blade grows approximately linearly. The sheath and internode both grow exponentially. Tip emergence limits the further increase in the length of blade elongation zone, which has been attributed to a direct effect of light absorbed by the emerged leaf tip (Casey *et al.*, 1999). Tip emergence also triggers the initiation of the associated sheath at the base of the blade. Since blade and sheath evolve from the same elongation zone (Schnyder *et al.*, 1990), thus the extended length of the sheath is entirely subtracted from the length of blade elongation zone, which results in a gradual decrease of blade elongation rate. In phase III (from collar emergence of the preceding leaf until collar emergence of the leaf itself), collar emergence of the preceding leaf triggers the linear phase of sheath growth, which causes the rapid decrease of the length of blade elongation zone, and thus the rate of blade elongation decline rapidly to zero. During this phase, the internode still grows exponentially. In phase IV (from collar emergence until completion of growth), the blade is completely out of the sheath tube and has stopped growing. Collar emergence triggers the fading of the elongation rate of the sheath while the elongation rate of the internode increases rapidly, and the sum of them remains more or less constant. During this phase, in which the sheath is protruding from the sheath tube, the elongation rate of the internode reaches a constant rate within a short time. Subsequently, the internode grows linearly until it reaches its final length. The final length of internode  $n$  is obtained from the final length of the encapsulating sheath (rank  $n-1$ ) according to an empirical relationship (Appendix III Method S4.1 and Fig. S4.2). Thus the final internode length is not directly obtained from coordination rules.

The time of tip emergence is defined as the thermal time when the total length of blade plus sheath plus internode of rank  $n$  exceeds the length of encapsulating sheath within that time step. Collar emergence occurs when the total length of the sheath plus internode of rank  $n$  exceeds the length of encapsulating sheath which has the highest collar on the plant. Detail

justifications for the methods used for organ extension are provided in Appendix III Method S4.2. The dynamics of blade, sheath and internode extension in our model are described below.

*Blade extension was calculated according to Eq. 4.1 and Eq. 4.2:*

$$\frac{dB_n}{dt} = r_{B,n} E_n \quad (\text{Eq. 4.1})$$

$$E_n = \begin{cases} B_n & B_n < E_{n,\max} \\ E_{n,\max} - S_n & B_n \geq E_{n,\max} \end{cases} \quad (\text{Eq. 4.2})$$

Where  $B_n$  is the length of blade  $n$  (cm),  $r_{B,n}$  is the relative elongation rate of the elongation zone of blade  $n$  ( $^{\circ}\text{Cd}^{-1}$ ),  $E_n$  is the length of the elongation zone of blade  $n$ , and  $S_n$  is the length of sheath  $n$ .  $E_{n,\max}$  is the maximum length of the elongation zone that reached by blade  $n$ . After tip emergence of blade  $n$ ,  $E_{n,\max}$  is set by taking the minimum value of the length of the elongation zone at tip emergence plus 2 cm ( $\rho$ , Table 4.2) and the ratio between maximum elongation rate ( $e$ ) and relative elongation rate of blade  $n$  ( $r_{B,n}$ ). The maximum elongation rate  $e$  is a parameter, identical for all leaves. The length of elongation zone was set back to  $E_{n,\max}$  when length of blade  $n$  exceeds  $E_{n,\max}$  within one time step. A blade or sheath was mature when its elongation rate is smaller than  $1 \cdot 10^{-3}$  cm  $^{\circ}\text{Cd}^{-1}$ .

*Sheath extension was calculated according to Eq. 4.3:*

$$\frac{dS_n}{dt} = \begin{cases} r_s S_n & t < c_{n-1} \\ k_s & c_{n-1} < t \leq c_n \\ k_s - d * (I_n + S_n - S_{n-1}) & t \geq c_n \end{cases} \quad (\text{Eq. 4.3})$$

Where  $S_n$  is the length of sheath  $n$  (cm).  $t$  is the thermal time ( $^{\circ}\text{Cd}$ ).  $c_{n-1}$  and  $c_n$  are the thermal times of the collar emergence on ranks  $n-1$  and rank  $n$ , respectively.  $r_s$  is the relative elongation rate of the sheath ( $^{\circ}\text{C}^{-1} \text{d}^{-1}$ ).  $k_s$  is the linear elongation rate of the sheath (cm  $^{\circ}\text{Cd}^{-1}$ ). Since there was little variation in  $r_s$  and  $k_s$  among ranks, average values over ranks were used.  $d$  ( $^{\circ}\text{Cd}^{-1}$ ) is the decline coefficient of the elongation rate after collar emergence. The decline of the growth rate of sheath  $n$  equals the decline coefficient ( $d$ ) times the exposed length of sheath  $n$  ( $I_n + S_n - S_{n-1}$ ) which is calculated as the length of the internode

Table 4.2: List of model parameters, their definitions, units and values

Attributes	Definition	Value	Unit
Plastochron	Thermal time interval between the initiations of successive blades	19.2	°Cd
Tassel initiation	The moment when the length of apex meristem of main shoot reaches 0.5 mm length.	237	°Cd
Ear initiation	The moment when the length of axillary meristem of the top ear reaches 0.5 mm.	350	°Cd
Initial blade length	Length of a blade at initiation	$2.5 \cdot 10^{-2}$	cm
Initial sheath length	Length of a sheath at initiation	0.1	cm
Initial internode length	Length of an internode at initiation	$2.5 \cdot 10^{-3}$	cm
$r_{B,n}$	Relative elongation rate for blade $n$	$3 \cdot 10^{-2}$ $6 \cdot 10^{-2}$	°Cd $^{-1}$
$r_s$	Constant relative elongation rate of sheath	$2 \cdot 10^{-2}$	°Cd $^{-1}$
$n$	Constant relative elongation rate of internode	$2.3 \cdot 10^{-2}$	°Cd $^{-1}$
$p$	Maximum length that the elongation zone of blade can increase after tip emergence	2	cm
$e$	Maximum elongation rate that can be reached by each individual blade	0.5	cm °Cd $^{-1}$
$k_s$	Constant linear elongation rate of sheath	0.25	cm °Cd $^{-1}$
$d$	Decline coefficient of the elongation rate of sheath, per unit of exposed sheath length <sup>a</sup>	$3.0 \cdot 10^{-3}$	°Cd $^{-1}$
$\alpha_1$	The average blade age when the associated sheath is initiated for those blades who emerged after tassel initiation.	150	°Cd
$\alpha_2$	The average blade age when the associated sheath starts the linear phase of extension for those blades who emerged after tassel initiation.	300	°Cd

<sup>a</sup>The value directly get from ‘optim’ function was  $7.5 \cdot 10^{-3}$ . It was fine-tuned to  $3.0 \cdot 10^{-3}$  such that final sheath length was close to the observed values at normal density.

$n$  ( $I_n$ ) plus the length of sheath  $n$  ( $S_n$ ) minus the length of encapsulating sheath ( $S_{n-1}$ ) (Fournier and Andrieu, 2000a).  $d$  was estimated by minimizing the sum of squared residuals comparing observed and estimated exposed sheath length at normal density (Eq. S4.2, Appendix III Method S4.3) using the ‘optim’ function in the ‘stas’ package of the R programming language (R Core Team, 2014).

The equation 3 applies to sheaths that initiated after tassel initiation, but with one difference: the start of the linear phase of growth is controlled by a parameter  $a_2$  instead of  $c_{n-1}$ .  $a_2$  is defined as the average blade age when the associated sheath starts the linear phase of extension for those blades who emerged after tassel initiation.

*Internode extension was calculated according to Eq. 4.4:*

$$\frac{dI_n}{dt} = \begin{cases} r_I I_n & t < c_n \\ k_s + r_I I_n^* - \frac{dS_n}{dt} & t \geq c_n \end{cases} \quad (\text{Eq. 4.4})$$

Where  $I_n$  is the length of internode  $n$  (cm).  $r_I$  is the relative elongation rate of internodes.  $I_n^*$  is the length of internode  $n$  at collar emergence. The equation applies from ear initiation onwards. The extension of internode  $n$  stops when it reaches the final length. The length of internodes 1 through 4 was set to zero.

#### *The data set*

The model was parameterized using complete records of the dynamics of blade, sheath and internode length (typically from 1-3 mm to maturity) of all the phytomers of maize. The experiment was conducted outdoors at the INRA campus of Thiverval-Grignon, France (48°51'N, 1°58'E) on a silty loam soil. Hybrid maize *Zea mays L.* ‘Déa’ was sown on 15 May 2000, at two population densities: 9.5 and 30.5 plants  $\text{m}^{-2}$ , referred to from here on as normal density and high density. Fifteen plants in each treatment were tagged at the time at which leaf 3 was exposed. Two or three times a week, the number of visible and collared leaves, the exposed length of the two youngest visible leaves and the length of the youngest mature blades were measured for each of the tagged plants. The median values for these lengths served as references to select between two and four (usually three) plants, which were dissected to enable

measurement of the length of all blades, sheaths and internodes. Destructive measurements were performed under a binocular microscope for the early stages of development, and with a ruler once the dimension of the organ exceeded 1 cm. In both treatments, the temperature of the elongation zone was represented by soil temperature before stem extension and by the temperature behind a sheath at the height of the shoot apex which were both measured by thermocouples. Detail experimental procedures and measurements have been described in Andrieu *et al.* (2006).

The data were fitted using multi-phase regression models to derive the relative elongation rate and linear elongation rate of the extension of blades, sheaths and internodes. An exponential-linear-plateau model was used for the extension of blades and sheaths, and an exponential-exponential-linear-plateau model was used for the extension of internodes (Andrieu *et al.*, 2006). Details of the fitting procedures and choice of models were described in Hillier *et al.* (2005). Here we calculated the time of leaf tip or collar emergence by determining when the height of a leaf tip or collar equals the height of the highest collar on the plant, based on multi-phase models for the growth of each organ, as parameterized by Andrieu *et al.* (2006).

#### *Model verification and model validation*

The normal density data set was used for model parameterization and verification, and the high density data set was used for model validation. The dynamics of the length of first three sheaths at normal density and high density were input as the initial condition of the model (Appendix III Fig. S4.3). The start of model simulation was set at the time of initiation of blade 4, which was 23 °Cd since sowing. The moment of leaf tip and collar emergence and dynamics of organ extension as well as final length of blades, sheaths and internode on ranks 4 and up were output of the model. The operation of the model, and the correct estimation of its parameters were verified by comparing simulated and observed thermal times of leaf tip and collar emergence, by plotting simulated and observed final lengths of blade, sheath and internode versus rank, and by comparing simulated and observed dynamics of extension.

Model validation was done using data of maize at high density by adapting the initial conditions of the model to represent high density

(Appendix III Fig. S4.3B) while all parameters were kept at their values estimated from maize growth at normal density.

Goodness-of-fit between observed values and model output was expressed in the root mean square error (RMSE):

$$\text{RMSE} = \sqrt{\frac{1}{n} \sum_{i=1}^n (X_{\text{sim},i} - X_{\text{obs},i})^2} \quad (\text{Eq. 4.5})$$

Where  $i$  is the sample number,  $n$  the total number of measurements,  $X_{\text{sim},i}$  the simulated value, and  $X_{\text{obs},i}$  is the observed value. The units of RMSE are equal to those of the data.

### *Sensitivity analysis*

To assess sensitivity of model output to changes in relative elongation rate of blade ( $r_{B,n}$ ) at normal density, a sensitivity analysis was performed using time of tip emergence *vs* phytomer rank as test output variable. Initial conditions representing normal density maize were used. The standard values of  $r_{B,n}$  were changed at 10% intervals from -30% to +30%.

### *Effects of initial sheath length*

To assess the power of the model in predicting plant development as influenced by the effects of early competition, a scenario analysis was carried out. Typically, plants in general respond to early competition by producing longer sheaths in response to a drop in red : far red ratio, aiming at maximizing light interception (Franklin and Whitelam, 2007). Therefore, in our model the effects of early competition were represented by variations in final length of the first three sheaths, mimicking the effects of early competition on sheath length. The final sheath lengths of the first three ranks at normal density were changed jointly at 10% increments from -30% to +30%. The scenario in which initial final sheath length was increased 30% corresponded to the condition of maize plant in high density. The dynamics of blade and sheath extension on phytomers 5 and 7 were used as test output. Note that, due to the rules used for the sheaths that initiated after tassel initiation, blade development is not influenced by initial sheath length from rank 9 onwards.

Extra scenarios were simulated to explore the causes of reduction of final blade length at high ranks. The results are presented in the Appendix III Table S4.1 and Fig. S4.5. Explorations were done by replacing the  $r_{B,n}$  at normal density by

values of  $r_{B,n}$  derived from the measurements at high density for ranks beyond 8 for simulations under high density condition, and by replacing the single value of  $e$  by the linear elongation rate estimated for each rank for ranks beyond 8.

## Results

### *Experimental support for model design choices*

The time of sheath initiation was estimated separately for each rank by extrapolating the exponential growth of the sheath back to the time at which sheath length was 1 mm. The moment of sheath initiation was synchronized with the moment of tip emergence of the same phytomer for phytomers that emerged before tassel initiation (Appendix III Fig. S4). For phytomers that emerged after tassel initiation (rank 9-15 in normal density and rank 8-15 in high density), initiation of the sheath happened before tip emergence and around a constant blade age ( $a_1$ ) of 150 °Cd of the same phytomer. The difference at the initiation of sheath before and after tassel initiation has been reported by Andrieu *et al.* (2006), and is supported by the earlier findings that the initiation of the sheath are controlled by different genes before and after tassel initiation (Harper and Freeling, 1996). The start of linear sheath growth was close to the moment of collar emergence of the preceding phytomer for ranks below 9 at normal density (Fig. 4.3A) and below 8 in high density (Fig. 4.3B), the phytomers of which tip emergence occurred before tassel initiation. For upper ranks, the start of the linear phase was earlier than the moment of collar emergence of the previous phytomer. An average blade age  $a_2$  was used to control the start of the linear phase of the sheaths that initiated after tassel initiation.

### *Model verification and validation*

The model satisfactorily reproduced the change in blade, sheath and internode length over time for maize at normal density (Fig. 4.4 A, B), when using the parameter values listed in Table 4.2. The predicted major phase changes in the extension of blade, sheath and internode were all well consistent with the data, i.e. the decline of blade elongation rate, the start of the linear phase of sheath extension, and the transition from exponential phase to linear phase of the internode extension. The simulated moments of tip and collar emergence were close to the observed values (Fig. 4.5A). The model well produced the

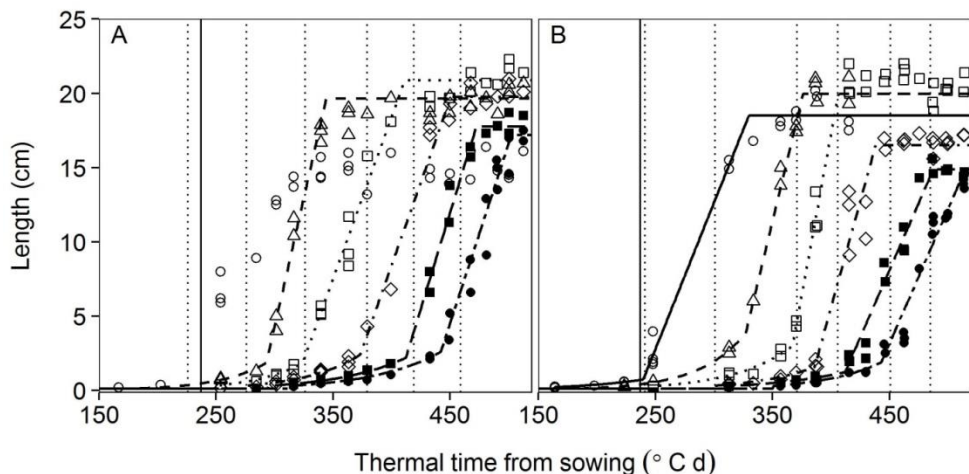


Fig. 4.3 Dynamics of sheath length against thermal time since sowing of ranks 5 (circles and solid lines), 6 (triangles and dashed lines), 7 (squares and dotted lines), 8 (diamonds and dot-dashed lines), 9 (filled squares and long-dashed lines) and 10 (filled circles and two-dashed lines) at A normal density and B high density. The vertical solid line indicates tassel initiation time. Vertical dotted lines indicate the collar emergence time of ranks 4-9. Symbols are measurements on maize 'D  a' in 2000, and lines are fitted curves. Filled symbols as well as rank 8 in panel B represents the sheaths that initiated after tassel initiation. The exponential-linear-plateau model was fitted to the data using 'gnls' function in R programming language. No line is shown for rank 5 in normal density since the fitting was not successful due to lack of data points between 200  $^{\circ}\text{Cd}$  and 250  $^{\circ}\text{Cd}$ .

acceleration of collar emergence beyond rank 8 (Fig. 4.5A). This is due to the change in the way the start of linear sheath extension was coordinated: synchronization with collar emergence of the preceding leaf before tassel initiation, and based on leaf age after tassel initiation. The coordination rule used before tassel initiation predicted a linear relationship between time of collar emergence and phytomer rank, which resulted in a delay for the time of collar emergence of ranks 9 to 15. Furthermore, the model produced final blade lengths close to experimentally observed values for phytomers 4-11 (Fig. 4.5B). Only final blade length of ranks 12 and above was overestimated.

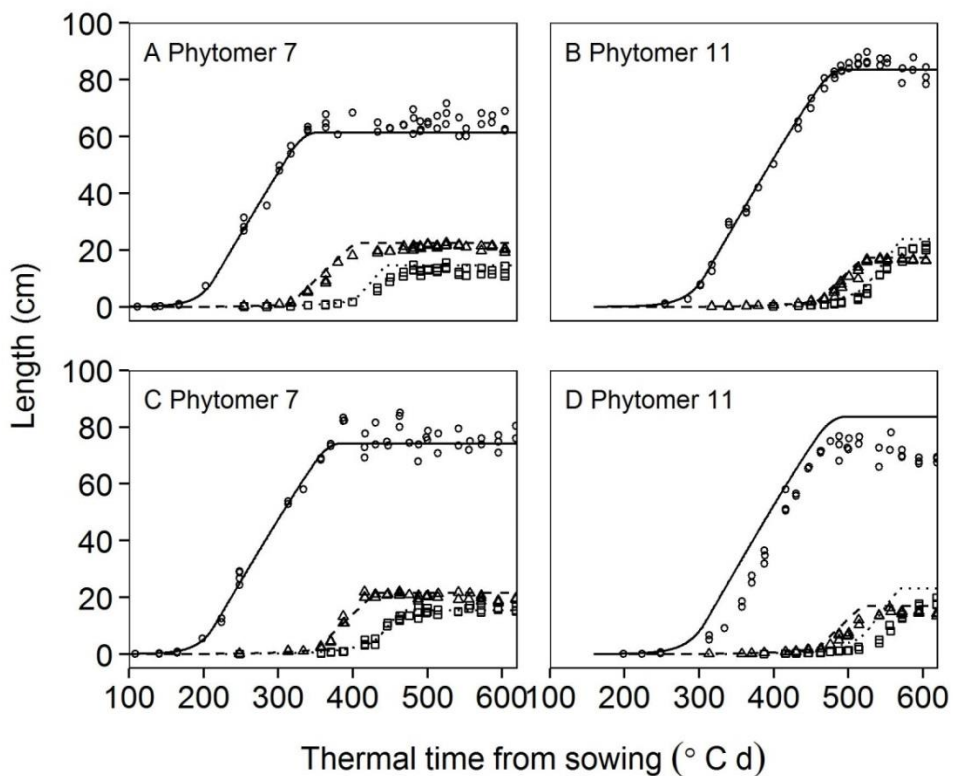


Fig. 4.4 Model verification (upper panels A and B) and model validation (lower panels C and D) of the dynamics of blade length (circles and solid line), sheath length (triangles and dashed line) and internode length (squares and dotted line) against thermal time from sowing of phytomer 7 and 11. Symbols are measurements on maize 'Déa' in 2000, and lines are simulations. RMSE values for blade, sheath and internode of phytomer 7 in panel A were 3.7 cm, 1.8 cm and 2.5 cm respectively, and phytomer 11 in panel B were 2.8 cm, 1.5 cm and 2.4 cm, respectively. RMSE values for blade, sheath and internode of phytomer 7 in panel C were 3.8 cm, 1.8 cm and 1.3 cm, respectively, and phytomer 11 in panel D were 11.2 cm, 2.5 cm and 4.8 cm for phytomer 11 in panel D, respectively.

By using initial conditions associated with high population density and parameter values listed in Table 4.2, the model well reproduced the sigmoid extension patterns of the blade, sheath and internode (Fig. 4.4 C, D). The

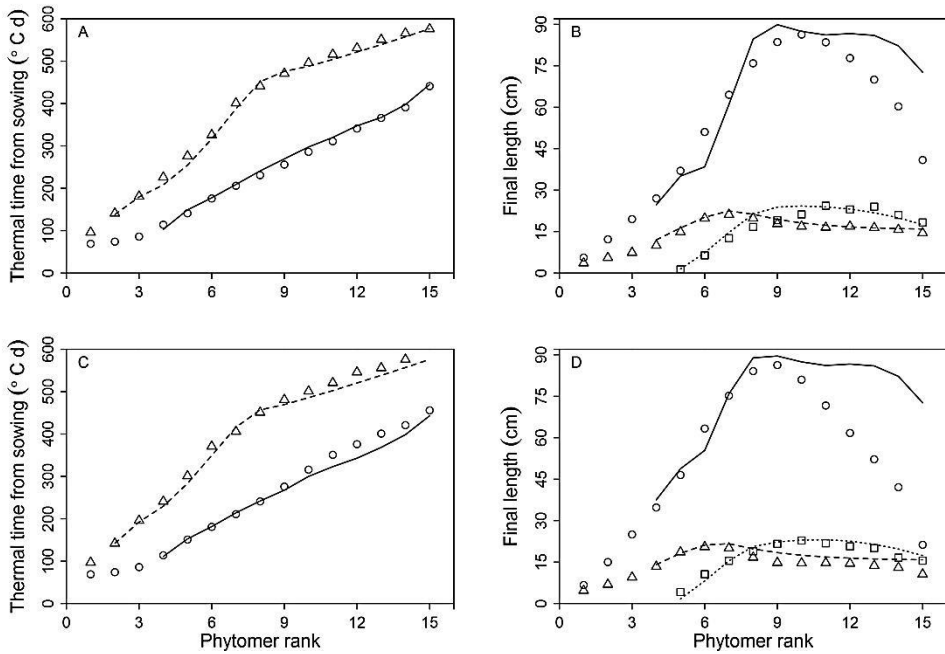


Fig. 4.5 Model verification (upper panels A and B) and model validation (lower panels C and D) of tip emergence (circles and solid line) and collar emergence (triangles and dashed line), and final length of blade (circles and solid line), sheath (triangles and dashed line) and internode (squares and dotted line) versus phytomer rank. Symbols are measurements from maize 'D  a' in 2000, and lines are simulations. RMSE values of model verification were 8.6 °Cd for tip emergence, 12.4 °Cd for collar emergence, 12.3 cm for final blade length, 1.2 cm for sheath length and 2.4 cm for internode length. RMSE values of model validation were 17.9 °Cd for tip emergence, 16.7 °Cd for collar emergence, 21.8 cm for final blade length, 2.6 cm for sheath length, 1.7 cm for internode length.

increase of blade elongation duration and delay of sheath linear extension as compared to that in normal density for rank 7 were well captured by the model (Fig. 4.4C). Also, predicted tip and collar emergence of the high density maize up to rank 9 were consistent with the data (Fig. 4.5C). Beyond rank 9, the model estimated sheath extension correctly but overestimated the elongation rate and final length of the blades, and slightly underestimated tip and collar emergence (Fig. 4.5 C, D). All blade lengths can be predicted at high accuracy when the model was run with close to real relative elongation rate and linear

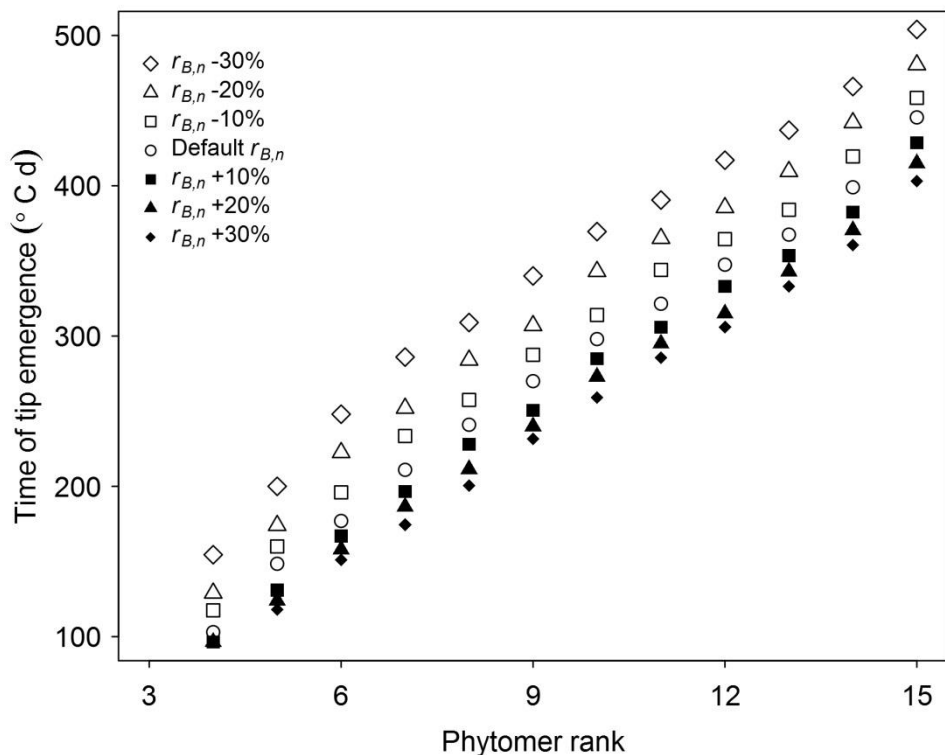


Fig. 4.6 Analysis of the sensitivity of the time of leaf tip emergence of different phytomer rank to changes in  $r_{B,n}$  at normal density.

elongation rate that were fitted for each individual blade, while elongation duration was controlled by the coordination model (Appendix III Table S4.1 and Fig. S4.5).

#### Model sensitivity

Tip emergence was delayed when  $r_{B,n}$  was decreased and *vice versa* (Fig. 4.6) for ranks beyond 4. The responses of tip emergence to changes in  $r_{B,n}$  differed between ranks 4 to 6 and ranks beyond 6. For leaf ranks above 6 a linear relationship between tip emergence and phytomer rank, with an unchanged phyllochron, was preserved at different values of  $r_{B,n}$ . Timing of tip emergence was more sensitive to a decrease in  $r_{B,n}$  than to an increase (Fig. 4.6).

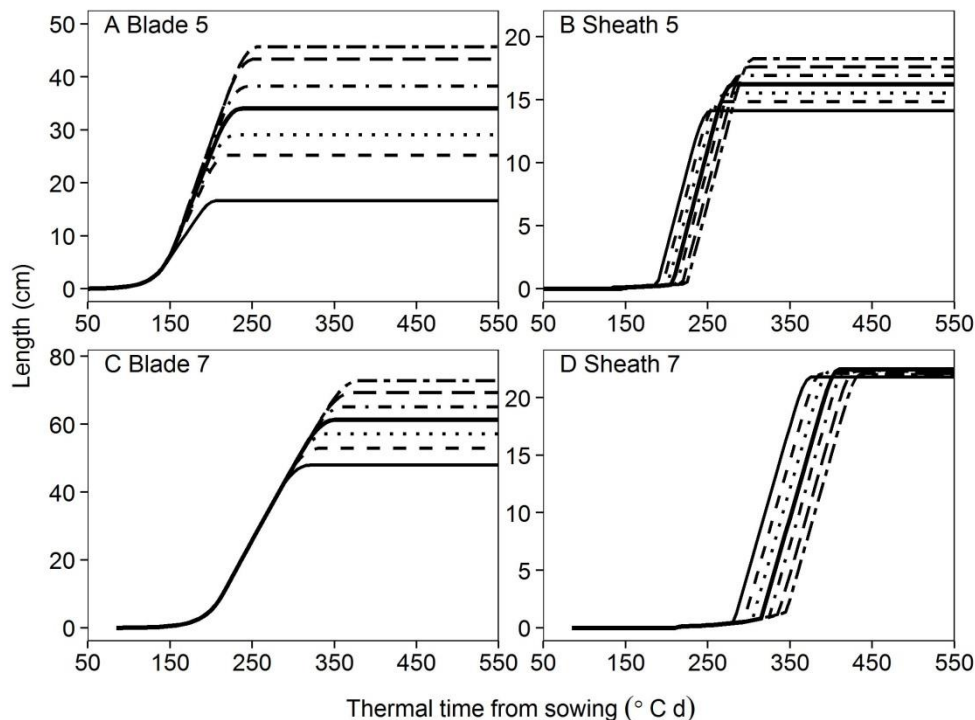


Fig. 4.7 Simulated effects of changes in final sheath length of rank 1 to 3 on dynamics of blade and sheath extension versus thermal time from sowing of phytomer 5 and 7. The final sheath length of rank 1 to 3 were changed jointly by -30% (solid lines), -20% (dashed lines), -10% (dotted lines), no change (bold solid lines), +10% (dot-dashed lines), +20% (long-dashed lines) and +30% (two-dashed lines).

#### *Effects of initial sheath length*

Final length of blades 5 and 7 were positively related to the change in final sheath length of the first three ranks, as the reduction in the value of the initial sheath length by 30% resulted in the shortest final blade lengths while setting the value 30% higher resulted in the longest lengths (Fig. 4.7 A, C). Blade elongation rates and durations at rank 5 were positively affected by changes in the sheath length at ranks 1-3, while for rank 7, only elongation durations were positively affected, elongation rates were not. The start of the phase of linear sheath extension was delayed with increasing initial sheath lengths (Fig. 4.7 B,

D). Final length of sheath 5 was increased considerably whereas final length of sheath 7 was only slightly increased.

## Discussion

The purpose of this study was to show: (I) key aspects of whole plant development such as rate of leaf emergence, dynamics of organ extension and distribution of organ size along the stem can all emerge from a set of simple coordination rules, without the need to include effects of carbon assimilation and biomass allocation; (II) a flexible time of organ development can emerge from a model based on coordination rules. The model did give a good account of the timing and duration of blade and sheath extension at both plant population densities which were different in both aspects. This supports the plausibility that phase transitions in organ extension are coordinated with leaf emergence events (Fig. 4.4). Using the coordination model we showed that events early in the life of the plant, such as increase of sheath length as a result of interplant competition at high density (Fig. 4.7), may set in motion a cascade of linked developmental events at the organ level that shape the development of the structure of the whole plant over its entire growth duration.

A novel coordination rule implemented in our model is that the start of the linear phase of sheath extension is related to collar emergence of the preceding leaf in those sheaths that were initiated before tassel initiation. This rule was derived from the observation that the linear phase of sheath growth took place later at high density than in normal density for low ranks (Fig. 4.3), and was supported by the accurate prediction of the dynamics of blade and sheath extension, and final blade length of the considered phytomers in both the normal and high density treatment. Another novel element in this model was to take into account the reproductive phase which results changes in the profile of blade length along the stem without considering the competition for assimilates among leaves, stem and ears.

### *Early competition shapes the structural plasticity at high density*

In another study, we found that the initial modification of the light environment experienced by maize seedlings in a wheat-maize intercrop in which maize was sown after wheat caused longer sheath lengths at ranks below

6 (chapter 3). Consistent with Andrieu *et al.* (2006), these longer sheaths resulted in a longer blade length for phytomers below 10 through enhancing leaf elongation duration. The scenario simulation of changes in final sheath length of ranks 1 to 3 and model validation for high density confirms the role of sheath length of low phytomers in determining the dynamics of organ extensions and final organ sizes of subsequent ranks through the three coordination rules. The rule which defines the start of the decrease of sheath elongation rate and the rapid increase of internode elongation rate is most responsible for propagating differences created on low phytomers from leaf to leaf. This rule results in a monotonous increase of final sheath length at low ranks, and a decrease at high ranks. The increase of sheath length over ranks can be seen as the length increase after collar emergence. The decrease is because (i) the slow extension of internode before collar emergence pushes up the leaf and consequently reduces the length of the sheath of the same phytomer at collar emergence (Fig. 4.1 and Fig. 4.2A); and (ii) the rapid extension of the internode after collar emergence accelerates the decline of the elongation rate of sheath and shortens the increase of sheath length after collar emergence (Fig. 4.2B). This supports the idea that early competition and differences created on low ranks influence whole plant structure, which would highlight the importance of early growth conditions and crucial role of sheath for whole plant development.

*A constant leaf emergence rate emerges from the interplay between leaf initiation, leaf elongation, sheath tube construction*

The timing of leaf emergence depends on the processes of leaf initiation and leaf elongation, and on the depth of the sheath tube (Skinner and Nelson, 1995). Despite the complexity of these dynamic processes, field experiments have often shown a linear relationship between leaf appearance and thermal time (McMaster, 2005). Consistent with this, the current modelling exercise showed that for a large range of relative blade elongation rates, the time interval between emergence of successive leaves remains stable (Fig. 4.6). The value of the phyllochron would be equal to the plastochron if all blades would emerge from a sheath tube that has a constant length. However, the depth of the sheath tube is not constant, but increases during plant development until

maturity of sheath 7 when most leaves have emerged (Appendix III Fig. S4.6). This explains why a phyllochron that is both constant and larger than the plastochron is generally observed in experiments, and also why we see it in our modelling exercise. Nevertheless, the plastochron value may vary under different light conditions because of the influence of assimilates (Sugiyama and Gotoh, 2010) or signals from leaf to the apex (Chuck and Hake, 2005; Pautler *et al.*, 2013). Our current model provides the foundation necessary to simulate the feedback of leaf emergence on leaf initiation based on ecophysiological mechanisms in the future.

#### *Strengths and weaknesses of the model*

Our model was able to satisfactorily capture the close coordination between the dynamics of blade, sheath, and internode extension and leaf emergence events within the structural development of maize plant. The model successfully predicted the rank numbers for the peak in sheath length distribution, and in blade length distribution which is usually around 2/3 of the final leaf number in field conditions (Dwyer and Stewart, 1986; Birch *et al.*, 1998a). The exercise of optimizing prediction of final blade length of high ranks indicates that assimilates is probably a limiting factor for blade size at high ranks. However, the model was not designed to consider the influence of environmental conditions and the availability of assimilates on organ extension. The aim of the modelling exercise was to provide a conceptual framework of how whole plant structural development emerges from the coordinated growth of organs.

By using coordination rules, we reduced the number of parameters needed for the timing of phase transitions in organ extension. Nevertheless, the model still needs a considerable number of parameters to specify the relative blade elongation rate for each organ. The necessity for these parameters could be eliminated by adding the effect of assimilates on organ growth: organ extension would then become dependent on assimilate supply.

The model requires the input of the dynamics of first three sheaths as initial conditions. When this was reduced to only the first sheath, the model overestimated the final sheath length of the subsequent ranks and thus run with less accuracy (Appendix III Fig. S4.7). This is because the linear

elongation rate of the first three sheaths is lower than the subsequent ranks due to a short elongation zone of the leaf in question.

## **Conclusions**

The current model presents a framework for the structural development of a maize plant and shows the plausibility of coordination rules underlying the structural development. Based on three coordinating rules, whole-plant structural development in terms of leaf tip and collar emergence, dynamics of organ extension and distribution of organ size along the stem emerged as model output, without considering any process related to biomass formation. The model gave a good account of the timing and duration of the extension of blade and sheath, but not the changes of elongation rate at high ranks. To further improve model predictions, a next step could be to include the effect of assimilates on organ and whole-plant growth, and take into account the possible effects of resource capture and assimilate supply on relative growth rates of the leaves. Nevertheless, we show that many aspects of maize plant development can be captured using relatively simple rules, which illustrates the relative resource independency of several developmental events. Also, models based on such rules can be used to study plant plasticity like shade avoidance, as such responses are typically triggered by cues that precede any drop in light capture (Pierik and de Wit, 2013) and therefore do not depend on changes in carbon assimilation to happen.

## **Appendix III**

Method S4.1. Estimation of the ratio between the final length of internode  $n$  and sheath  $n-1$

Method S4.2. Justification of coordination rules used in the model

Method S4.3. Calculation of the decline coefficient ( $d$ ) of the elongation rate of sheath

Table S4.1. Simulation scenarios for exploring the cause of reduction of final length of blade at high ranks

Fig. S4.1. Model visualization of blade, sheath and internode on separated phytomers 1 to 15

Fig. S4.2. The ratio between the final length of internode  $n$  and sheath  $n-1$  versus the phytomer rank

Fig. S4.3. Dynamics of length growth of sheath 1 to 3 in normal density and high density

Fig. S4. Relationship between blade age at sheath initiation and blade age at tip emergence

Fig. S4.5. Final blade length of ranks 4-15 under different simulation scenarios

Fig. S4.6. The dynamics of the depth of sheath tube over time

Fig. S4.7. Simulation results of the time of tip and collar emergence and organ sizes when only input the length dynamics of the first sheath

### **Acknowledgements**

We thank Michael Henke for valuable comments in optimizing the programming code. The financial support of the China Scholarship Council (CSC) and the Key Sino-Dutch Joint Research Project of NSFC (grant number: 31210103906) are gratefully acknowledged.

## CHAPTER 5

# The contribution of plastic architectural traits to complementary light capture in plant mixtures

Junqi Zhu, Wopke van der Werf, Niels P. R. Anten,  
Jan Vos, Jochem B. Evers

Centre for Crop Systems Analysis, Wageningen University, PO Box 430, 6700  
AK, Wageningen, the Netherlands

## **Abstract**

Little is known about the consequence of phenotypic plasticity in complementary resource capture in mixed vegetation. Here, we present a novel approach to quantify the role of architectural trait plasticity in light capture in a wheat-maize intercrop, as an elementary example of mixed vegetation. Whole-vegetation light capture was simulated for scenarios with and without plasticity based on empirical plant traits data. The plasticity effect was estimated as the difference in light capture between simulations with and without plasticity. Light capture was 23% higher in intercrop with plasticity than the expected value from monocultures, of which 36% was due to intercrop configuration alone and 64% was due to plasticity. For wheat, plasticity in tillering was the main reason for increased light capture, whereas for maize it was due to intercrop configuration. These results show the potential of plasticity for enhancing resource acquisition in intercropping and for mixed stands in general.

**Keywords:** Phenotypic plasticity, complementarity effect, plasticity effect, configuration effect, architectural traits, light capture, wheat-maize intercrop

## Introduction

A number of studies in experimental ecosystems, such as grasslands (Tilman *et al.*, 1996; Tilman *et al.*, 2001) and forests (Lovelock and Ewel, 2005) as well as a meta-analysis of both aquatic and terrestrial ecosystems (Cardinale *et al.*, 2006) show that primary production increases with species richness. Complementary strategies for resource capture are regarded as a key factor driving the yield advantage of species-diverse plant communities (Tilman *et al.*, 2001; Cardinale *et al.*, 2007; Yachi and Loreau, 2007). The complementarity hypothesis states that, because of niche differentiation and resource partitioning in space and time, e.g. difference in rooting depths or phenology, individuals in a mixture experience, on average, less niche overlap in resource use than in the corresponding monocultures, resulting in an increase in biomass production of the system as a whole. The reduced niche overlap changes the competition intensity in a mixture as compared to monoculture due to the difference in the competitiveness of each species. It could create two opposite effects: competitive relaxation due to a less competitive neighbour species, but also competitive intensification due to a more competitive neighbour species (Yachi and Loreau, 2007). The change in competition intensity in turn will induce or force plants to respond in a coordinated manner, resulting in phenotypic plasticity which is crucial for reaching the realized niche in mixed vegetation. Although plastic responses of plant phenotypes to a wide range abiotic and biotic environments have been extensively documented (Valladares *et al.*, 2000; Huber *et al.*, 2012), very little is known about the consequences of such phenotypic plasticity for performance of plant communities and the contribution of plasticity to complementarity effect (Callaway *et al.*, 2003; Werner and Peacor, 2003).

Plasticity is defined as the production of multiple phenotypes from a single genotype, depending on environmental conditions (Bradshaw *et al.*, 1965; Sultan, 2000). It enables plants to alter morphological, physiological and developmental traits to match their phenotypes to the composition of the communities and abiotic environments they are growing in (Ballaré *et al.*, 1994; Price *et al.*, 2003). Therefore, plasticity can enable plants to buffer the potentially negative effects of environmental variation on growth and

reproduction, and take advantage of opportunities, i.e. incompletely occupied niches (Silvertown and Gordon, 1989; Pearcy, 2007). Remarkable levels of phenotypic plasticity have been found in recent grassland experiments between different levels of species richness (Gubsch *et al.*, 2011; Roscher *et al.*, 2013). However, the effects of such phenotypic plasticity on community performance were immersed in the overall complementarity effect (Loreau and Hector, 2001; Tilman *et al.*, 2001), and were thus not explicitly considered. Analysing and quantifying the role of plasticity in complementarity effects will be crucial in unveiling the relationship between biodiversity and overyielding.

This study aims at developing a method for quantifying the respective role of ‘configuration effect’ and ‘plasticity effect’ in complementarity effect using light capture as an example. The configuration effect strictly quantifies the effect of diversity-induced variation in the structure of the community caused by the component species being inherently different in phenology, root and shoot architecture, nutrient requirement, etc. We quantify the pure configuration effect, by calculating light capture of the mixture if plants in the mixture exhibit a monoculture phenotype. The plasticity effect quantifies to which extent plastic responses of each species enhance resource capture beyond the level expected from monoculture phenotypes. To this end we use wheat-maize relay strip intercropping as an elementary example of a mixed vegetation (Fig. 1.1). Wheat-maize is a common intercropping system in Northern China, e.g. it is cultivated on 275,000 ha in Gansu province and Ningxia autonomous region (Li *et al.*, 2001). This system was chosen because: (i) it has a clear yield advantage characterized by a land equivalent ratio of  $\sim 1.2$  (Li *et al.*, 2001; Li *et al.*, 2007). That is, one would need 20% more land to achieve the same combined yield if these crops were to be grown as monocrops than when grown as a mixture; (ii) it can be well-managed, e.g. fertilization, irrigation, etc., thus enhanced light capture would be the most plausible reason for the yield advantage; (iii) it is a relatively simple system (two species) with a clearly defined configuration in terms of timing and positioning of the species relative to each other, (ii) the two species have distinct physiologies (wheat has the C3 and maize has the C4 photosynthetic pathway) and with differences in phenology and stature of the plants. This is similar to many grassland ecosystems where there is a gradual replacement of C3 species

by C4 species (Turner and Knapp, 1996; Anten and Hirose, 1999). The light conditions in wheat-maize intercropping system are highly dynamic and heterogeneous. Wheat experiences a favourable light environment during the early stages of this intercrop because maize is sown later. However, during wheat grain filling, maize achieves competitive dominance for light. Maize seedlings are initially suppressed by the taller wheat plants, but gradually outgrow the wheat until ultimately the wheat is harvested and removed from the system. It has been shown that wheat and maize display great plasticity in architectural development in reaction to the changed light environment in this system (chapter 3). However, the contribution of these plastic responses to total light capture has not been quantified. For quantifying this, an architectural modelling approach was used which can simulate the light capture of a plant phenotype in relation to the structure of the surrounding vegetation in a 3D realistic manner (Vos *et al.*, 2010).

Our objectives are: (1) to introduce a new method for estimating configuration and plasticity effects in resource capture in multi-species plant communities, (2) to apply this method to an elementary mixed vegetation of wheat and maize, and quantify the contribution of configuration and plant plasticity to light capture in this system; and (3) to analyse the relative contribution of individual plant traits to the estimated plasticity effect.

## Materials and Methods

### *Components of a complementarity effect*

The complementarity effect on yield of a species  $i$  measures the difference between the observed yield of species  $i$  in a mixture and the expected yield in the mixture, calculated as the product of its yield in monoculture and the relative density of the species in the mixture in comparison to the monoculture (Loreau and Hector, 2001):

$$\Delta Y_i = Y_{o,i} - Y_{e,i} = Y_{o,i} - RD_i \times M_{o,i} \quad (\text{Eq. 5.1})$$

where  $Y_{o,i}$  is the observed yield of species  $i$  in mixture,  $Y_{e,i}$  is the expected yield of species  $i$  in mixture,  $RD_i$  is the relative density of species  $i$  in mixture (density in mixture divided by density in pure stand) and  $M_{o,i}$  is the monoculture yield of species  $i$ . The same formula may also be used here to calculate resource capture, e.g. light. The overall complementarity effect on

total yield or resource capture is simply the sum over all species of the terms  $\Delta Y_i$ :

$$\Delta Y = \sum_i \Delta Y_i \quad (\text{Eq. 5.2})$$

The complementarity effect can be positive resulting from resource partitioning or facilitation, or negative resulting from physical or chemical interference. In this study we use light capture as the indicator for plant performance.

We consider that the complementarity effect can be divided into two components: a configuration effect ( $\Delta Y_{\text{configuration}}$ ) and a plasticity effect ( $\Delta Y_{\text{plasticity}}$ ):

$$\Delta Y_i = \Delta Y_{\text{configuration},i} + \Delta Y_{\text{plasticity},i} \quad (\text{Eq. 5.3})$$

The configuration effect and plasticity effect can be separately identified in a mechanistic modelling framework. The configuration effect is obtained by calculating light capture by plants with a monoculture phenotype (no plastic responses to the mixture) in a mixture configuration ( $Y_{\text{monoculture phenotype},i}$ ), and subtracting the expected light capture in mixture under the hypothesis that each plant in mixture captured per individual of species  $i$  the same quantity of light as in monoculture ( $M_{o,i}$ ). This yields an equation similar to Eq. 5.1:

$$\Delta Y_{\text{configuration},i} = Y_{\text{monoculture phenotype},i} - RD_i \times M_{o,i} \quad (\text{Eq. 5.4})$$

5

The plasticity effect is obtained by allowing for trait plasticity, and calculating light capture by plants with mixture phenotype in a mixture configuration ( $Y_{\text{mixture phenotype},i}$ ), and subtracting the light capture by plants with monoculture phenotype in mixture configuration.

$$\Delta Y_{\text{plasticity},i} = Y_{\text{mixture phenotype},i} - Y_{\text{monoculture phenotype},i} \quad (\text{Eq. 5.5})$$

This equation captures the pure effect of plasticity on resource capture. For the system as a whole, the complementarity effect is calculated by summing over species (Eq. 5.2). Likewise, the overall configuration and plasticity effect are calculated with:

$$\Delta Y_{\text{configuration}} = \sum_i \Delta Y_{\text{configuration},i} \quad (\text{Eq. 5.6})$$

$$\Delta Y_{\text{plasticity}} = \sum_i \Delta Y_{\text{plasticity},i} \quad (\text{Eq. 5.7})$$

In this paper, the effects of plant configuration in time and space and plasticity in shoot architectural development on light capture were analysed using an architectural model through four steps: plant architectural measurement, model development, model verification, scenario simulations.

#### *Plant architectural measurement*

For characterizing the development of wheat and maize architecture, a field experiment was conducted at the experimental farm of Wageningen University, the Netherlands ( $51^{\circ}59'20''\text{N}$ ,  $5^{\circ}39'16''\text{E}$ ), from March to October 2011 (Fig. 1.1). The following data on the architectural development of wheat and maize were gathered: (1) time of leaf appearance; (2) time of collar appearance, (3) time of leaf senescence, (4) final leaf number, (5) final sizes of blade, sheath and internode, (6) leaf azimuth and (7) leaf declination angle (all data shown in Fig. S5.3-S5.10; observation methods are given in chapter 3 ). Leaf azimuth was defined as the clockwise angle between the vertical projection of the leaf on a horizontal plane and true south. Leaf declination angle was defined as the declination angle between the stem and the blade midrib. In addition, the appearance and senescence time and probability of each wheat tiller were quantified (see Table S5.1). The experiment included three contrasting treatments with three replications each: sole wheat, sole maize, and wheat-maize strip intercropping with alternating six wheat rows (the ‘wheat strip’) with two maize rows (the ‘maize strip’). Within the intercrop wheat, we distinguished the growth and development of the border rows (row 1 and row 6, called ‘border rows’) from that of the first inner rows (row 2 and row 5, called ‘inner rows I’) and second inner rows (row 3 and row 4, called ‘inner rows II’). Within the two rows of intercrop maize, we distinguish row 1 and row 2 for leaf azimuth while consider them as the same for other traits.

Wheat cultivar Tybalt was sown on 9 March 2011 at a row distance of 12.5 cm and a density of approximately 250 plants  $\text{m}^{-2}$ , and was harvested on 10 August 2011. Maize cultivar LG30208 was sown at a row distance of 75 cm and a plant distance of 13.5 cm (9.87 plants  $\text{m}^{-2}$ ) on 11 May and harvested on 14 October. Sowing and harvesting dates of each species were the same in the intercrop as in the monocrop. Plant distances in intercrop wheat and maize strip were the same as in respective sole crops. Distance between adjacent

wheat and maize rows was set at half the row distance of wheat plus half the row distance of maize ( $6.25\text{ cm} + 37.5\text{ cm} = 43.75\text{ cm}$ ). Therefore, width of a wheat strip was 75 cm and width of a maize strip was 150 cm, which resulted in a relative density of 1/3 for wheat and 2/3 for maize. Details on the experimental set-up and the measurements on plant development can be found in chapter 3.

#### *Model development: general features*

A new wheat-maize strip intercropping model was developed based on the concepts of the 'ADELwheat' model for spring wheat development (Fournier *et al.*, 2003; Evers *et al.*, 2005). ADELwheat accurately describes the three-dimensional development of wheat canopy structure (Evers *et al.*, 2010; Barillot *et al.*, 2014), and its concepts on plant development were used to simulate both wheat and maize architecture. The model was written using the GroIMP platform (Hemmerling *et al.*, 2008; Kniemeyer, 2008). The model presented here includes two major parts: (1) the architectural development of wheat and maize plants in any spatial configuration; (2) a radiation model (Fig. 5.1 and Appendix IV Fig. S5.1-S5.2).

#### *Plant architectural development*

The model considers the phytomer (internode, sheath, blade, and a lateral bud) as the basic unit of plant architecture. The model simulates three major aspect of architectural development: (i) the (relative) timing of developmental events, i.e. rates and duration of organ initiation, appearance and elongation; (ii) (final) organ dimensions; and (iii) organ geometric properties, e.g. leaf azimuth, leaf declination angle, curvature of leaves in space (see Method S5.1 and Fig. S5.11). The main differences between the current model and ADELwheat were:

*Final trait values.* Geometric properties and final organ sizes of each rank were randomly drawn from a dataset collected in the field (chapter 3), instead of summarized using empirical relationships.

*Organ appearance and elongation.* Phyllochron (thermal time between appearances of successive leaf blades) was set at  $90.8\text{ }^{\circ}\text{Cd}$  for wheat,  $44.2\text{ }^{\circ}\text{Cd}$  for sole maize and  $54.2\text{ }^{\circ}\text{Cd}$  for intercrop maize. The start of blade and sheath elongation was set when the physiological age of a plant (number of appeared

main stem leaves) was larger than the rank number in question, while an internode started to elongate when the associated sheath was mature. Physiological age was calculated based on thermal time from sowing. Daily thermal time was input separately for wheat and maize according to measurements in the field. A base temperature of 0°C used for wheat and 8°C for maize. The dynamic of organ elongation was described with a sigmoid beta function (Eq. 5.8) (Yin *et al.*, 2003):

$$L(t) = L_{\max} \left( 1 + \frac{t_e - t}{0.5t_e} \right) \left( \frac{t}{t_e} \right)^2 \quad (\text{Eq. 5.8})$$

Where  $L(t)$  is length of an organ at thermal time  $t$  (°Cd).  $L_{\max}$  is the measured final organ length (cm).  $t_e$  is the time when final organ length is reached (°Cd) corresponding to the elongation duration. The elongation duration of blade and sheath was calculated as the thermal time duration from leaf tip appearance to collar appearance, while the elongation duration of the internode was 2.116 times the phyllochron (Fournier *et al.*, 2003).

#### *Radiation model and light absorption*

The radiation model of GroIMP was used to simulate light distribution and local light absorption based on the optical properties of the objects, and was invoked once per simulation step, computing the local photosynthetic active radiation (PAR) absorption by all plant objects in the 3D scene (Hemmerling *et al.*, 2008; Kniemeyer, 2008). Two light sources, illuminating the scene, were simulated: direct sunlight and diffuse sky light. The direct sunlight was simulated using an array of 24 directional lights sources (see Fig. S5.12A), equally spread over the day time, representing the course of the sun, see a similar arrangement in Evers *et al.* (2010) and Buck-Sorlin *et al.* (2011). The position of each direct light point is modified by the day length, azimuth and solar elevation angle which were calculated from Goudriaan and Van Laar (1994), using latitude and day of year as input. The instantaneous light intensity at the perpendicular plane of each direct light source was calculated according to Spitters (1986). Diffuse sky light was simulated using an array of 72



Fig. 5.1 Comparison of an intercrop plot with wheat and maize (top panel) with an simulated plot (bottom panel) at wheat flowering stage on 16 June (day of year 169). The colour gradient in the bottom panel represents the proportion absorbed photosynthetic active radiation (PAR) (from black to light green for plant organs, and from black to light yellow for soil surface). More comparisons are shown in Appendix IV Fig. S5.1-S5.2.

5

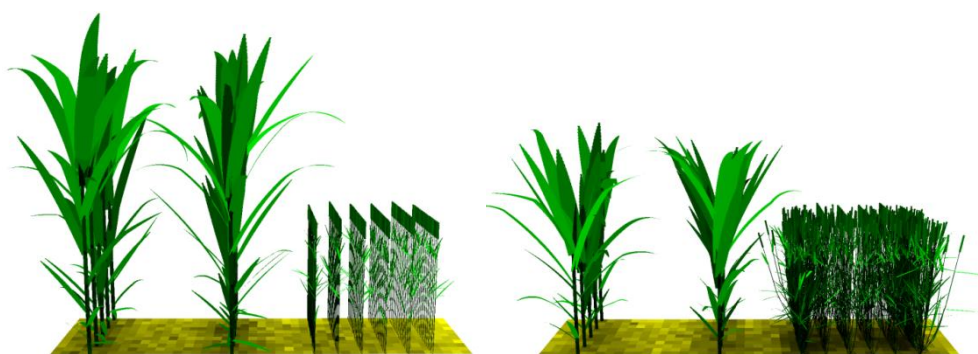


Fig. 5.2 Comparison of the architecture of different phenotypes of wheat and maize at wheat flowering stage on 17 July (day of year 198) when assuming no plasticity (left panel) and when assuming plastic responses to the intercrop situation (right). Thus, the left panel depicts the empirically non-observable situation of plants with monoculture phenotype in a mixture setting.

directional lights positioned regularly in a hemisphere in six circles with 12 lights each (see Fig. S5.12B), with emitted power densities being a fixed function of elevation angle (Evers *et al.*, 2007; Buck-Sorlin *et al.*, 2011). The diffuse light hemisphere was randomly rotated in each time step to minimize the variation in light distribution due to the approximation of diffuse sky light by individual sources.

A mean atmospheric transmissivity ( $\tau$ ) of 0.43 was used for calculating the daily global radiation during the whole growing season based on the global radiation data between March to October from 2000 to 2010 measured at weather station Deelen ( $52^{\circ}3'39''\text{N}$ ,  $5^{\circ}53'17''\text{E}$ , see Fig. S5.13). The fraction of diffuse light in daily radiation was set to 0.70 based on the mean transmissivity (Spitters, 1986). Absorption, reflection, and transmission of light at the level of an organ were calculated by summing the contributions of all the segments that constitute the organ. The transmittance and reflectance of the blade for PAR for both wheat and maize were set to 0.0127 and 0.0923, respectively, based on the measurement in Evers *et al.* (2010). Sheaths and internodes were defined as opaque objects, i.e. objects not transmitting any light, and their reflectance was set as the sum of the transmittance and reflectance of the blade.

#### *Simulations and model verification*

Simulations of plots were done using the same plant population densities as in the field experiment for both wheat and maize. Monoculture plot sizes were 972 plants (12 rows by 81 plants per row) for wheat and 240 plants (12 by 20) for maize. For intercrop each simulation comprised 972 wheat plants distributed into two wheat strips of six rows each, and 120 maize plants distributed into three maize strips of two rows each (Fig. 5.1 bottom panel). Within each simulated plot, 30 wheat plants and seven maize plants at the south side, and ten wheat plants and three maize plants at the north side were considered as border plants and were omitted from the calculation of light capture. Wheat rows 4, 5 and 6 in the first wheat strip (Fig. 1 bottom panel, counting from the left), and the middle maize strip were further used for light capture calculation. Simulation started at the first day after wheat sowing (day of year 69) and ended on the date of maize harvest (day of year 288) except for sole wheat which ended on the date of wheat harvest (day of year 222). Since

the model included variation in organ geometry and size, three replicate simulations were run per species scenario (sole-wheat, sole-maize or intercropping). Model time step was one day

To evaluate the model performance in terms of light distribution, the simulated fraction of PAR above the canopy that reaches the soil around solar noon was compared with measurements of relative PAR at soil-level taken in the field measurement at the same time of the day (see Fig. S5.14 and measurement description in Zhu *et al.* (2014b) ). The model was further tested for the dynamics of leaf area (See Fig. S5.15).

#### *Contribution of plasticity in architectural traits to light capture*

The contribution of configuration and plasticity to light capture by each species were quantified by using simulations scenarios with combination of different wheat phenotypes (Fig. 5.2, sole wheat (SW) and intercrop wheat phenotypes (IntW)), and maize phenotypes (Fig. 5.2 sole maize (SM) and intercrop maize phenotypes (IntM)), see Eqs 5.1-5.7.

To assess which trait contributed most to the plasticity effect, simulations were run with and without certain plastic trait values. The contribution of plasticity in individual trait of wheat was assessed both at the wheat strip and at the border rows of the wheat strip where the main yield advantage of wheat in intercrop were come from (Li *et al.*, 2001; Zhang *et al.*, 2007). In these simulations maize was set to the intercrop phenotype as the objective was here to analyse the contribution of wheat plasticity to its performance in a realistic intercrop setting. A full factorial design of all plastic traits was run, see list of simulation scenarios in Table 5.1. The contribution of plasticity in each individual trait to light capture (by the whole wheat strip as well as by the border rows only) over the whole growing season in intercrop was calculated as the difference of light capture between the full model and the model without this trait divided by difference of light capture between the full model and monoculture (Eq. 5.9). In other words, this quantifies how much light interception would have been affected if wheat would not have plastic in a given trait.

$$C_i = 100 * \frac{L_{\text{Full}} - L_{\text{Full}-i}}{L_{\text{Full}} - L_{\text{SW}}} \quad (\text{Eq. 5.9})$$

Table 5.1 List of simulation scenarios for assessing the contribution of individual plasticity trait

Plasticity	S	T	L	A	D	TL	TA	TD	LA	LD	AD	TLA	TLD	TAD	LAD	Full
Leaf size	✗	✗	✓	✗	✗	✓	✗	✗	✓	✓	✗	✓	✓	✗	✓	✓
Tiller dynamic	✗	✓	✗	✗	✗	✓	✓	✓	✗	✗	✗	✓	✓	✓	✗	✓
Leaf azimuth	✗	✗	✗	✓	✗	✗	✓	✗	✓	✓	✓	✓	✗	✓	✓	✓
Declination angle	✗	✗	✗	✗	✓	✗	✗	✓	✓	✓	✗	✓	✓	✓	✓	✓

✗ the plasticity is turned off, and thus the value in sole wheat phenotype is used.

✓ the plasticity is turned on, and thus the value in intercrop wheat phenotype is used specified for border row, inner row I and inner row II.

Sole wheat phenotype represents a combination of tiller dynamics of sole wheat, plus leaf size, leaf azimuth and declination angle of inner row II, plus mean leaf life (leaf appearance, maturity and senescence) across treatments. Intercrop wheat phenotype represents a combination of tiller dynamics, leaf size, leaf azimuth and declination angle specified for each row of intercrop wheat, plus mean leaf life (leaf appearance, maturity and senescence) across treatments.

$C_i$  represents the contribution of trait  $i$ , i.e. tillering, leaf size, leaf azimuth and declination angle, to the increase of light capture of wheat in intercrop as compared to monoculture.  $L_{\text{Full}}$  represents the light capture of wheat in intercrop with all plastic traits turned on.  $L_{\text{Full-}i}$  represents the light capture of wheat in intercrop setting all traits to their intercrop value except one (indicated by  $i$ ) which is set to the mono-crop value.  $L_{\text{SW}}$  represents the light capture of sole wheat. The light capture for a wheat strip or wheat row was converted into energy per square meter, counting a meter row length as an area of  $0.125 \text{ m}^2$ , based on the row distance of sowing.

## Results

### Contribution of configuration effect and plasticity effect to light capture

The seasonal accumulated light capture was  $437.9 \pm 1.2 \text{ MJ m}^{-2}$  in sole wheat, and  $589.0 \pm 4.2 \text{ MJ m}^{-2}$  in sole maize (Fig. 5.3), resulting in an expected light capture of  $146.0 \text{ MJ m}^{-2}$  for wheat (i.e.,  $437.9*1/3$  being that wheat occupies 1/3 of

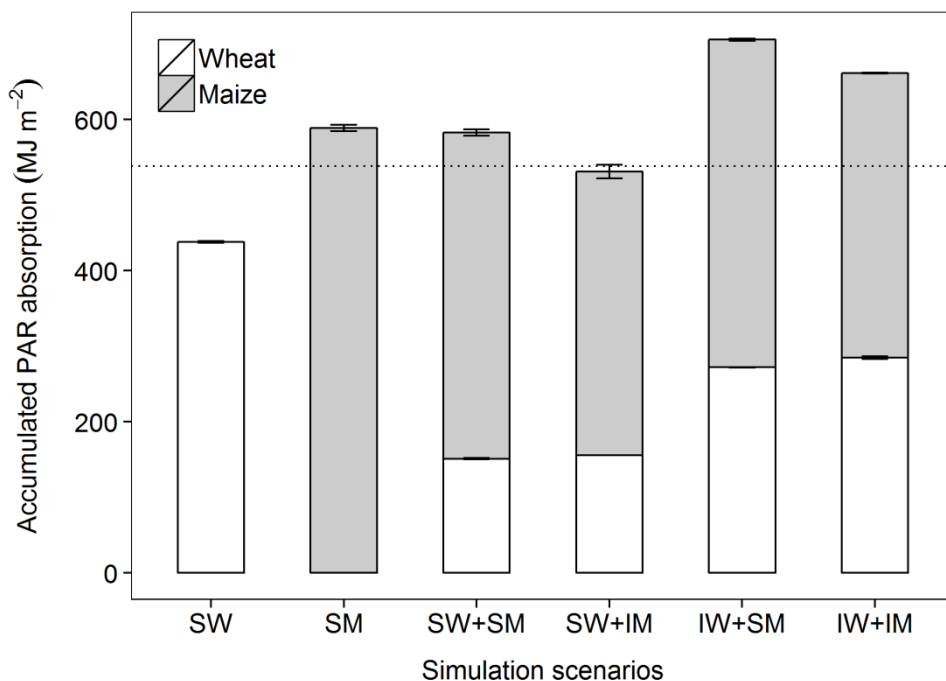


Fig. 5.3 Seasonal accumulated PAR capture in different systems. SW represents sole wheat, SM represents sole maize, IntW represents intercrop wheat phenotype. IntM represents intercrop maize phenotype. SW + SM represents a relay strip wheat-maize intercrop with phenotype of sole wheat and sole maize. The remaining bars depict SW + IntM, IntW + SM, IntW + IntM. The light capture for crops in intercrops was expressed per unit of whole intercrop area, in which 1/3 was sown with wheat and 2/3 with maize. Horizontal dotted line represent the expected light capture in intercrop. Errors bars represent the standard error of the mean of three simulations. Per each simulation, 246 plants in sole wheat, 60 plants in sole maize, and 123 wheat plants plus 20 maize plants in intercrop were included in the calculation of light capture.

the area in the intercrop), 392.7 MJ m<sup>-2</sup> for maize (i.e., 589.0\*2/3), and thus 538.6 MJ m<sup>-2</sup> for the whole wheat-maize intercropping system. Simulated light capture was  $661.6 \pm 1.5$  MJ m<sup>-2</sup> in the intercrop system with both species set to intercrop phenotypes where wheat captured  $284.7 \pm 1.8$  MJ m<sup>-2</sup> and maize

captured  $376.8 \pm 0.5 \text{ MJ m}^{-2}$ . Simulated light capture was  $582.7 \pm 3.4 \text{ MJ m}^{-2}$  in the intercrop system with monoculture phenotypes where wheat captured  $151.1 \pm 0.6 \text{ MJ m}^{-2}$  and maize captured  $431.6 \pm 4.0 \text{ MJ m}^{-2}$ . Therefore overall, complementarity effect increased the light capture of the whole system by  $123.0 \text{ MJ m}^{-2}$  (i.e.,  $661.6 - 538.6$  with Eq. 5.2 being 23% higher than the expected light capture). Thirty six percent ( $44.1 \text{ MJ m}^{-2}$ ; i.e.,  $582.7 - 538.6$  with Eq. 5.6) of this benefit was attributable to configuration effect and 64% ( $78.9 \text{ MJ m}^{-2}$ ; i.e.,  $661.6 - 582.7$  with Eq. 5.7) to plasticity effect. Dividing into species, the configuration effect of wheat increased the light capture by  $5.1 \text{ MJ m}^{-2}$  (i.e.,  $151.1 - 146.0$  with Eq. 5.4 being 3% of the expected value of wheat), and the configuration effect of maize increased the light capture by  $38.9 \text{ MJ m}^{-2}$  (i.e.,  $431.6 - 392.6$  with Eq. 5.4 being 10% of the expected value of maize). The plasticity of wheat added additional  $133.6 \text{ MJ m}^{-2}$  (i.e.,  $284.7 - 151.1$  with Eq. 5.5 being 91% of the expected value of wheat), while the plasticity of maize reduced the light capture by  $54.8 \text{ MJ m}^{-2}$  (i.e.,  $376.8 - 431.6$  with Eq. 5.5 being -14% of the expected value of maize).

#### *Dynamics of light capture over the whole growing season*

The sign and relative magnitude of the configuration and plasticity effects depended on the growth stage. Before wheat flowering (day of year 167), the configuration effect was positive for wheat and negative for maize due to the difference in plant size (Fig. 5.4). Gradually the situation was reversed when the maize grew taller and exceeded the wheat in height. The configuration effect reached a maximum slightly before wheat flowering for wheat and after wheat harvest for maize. Overall, the plasticity effect of wheat was substantially larger than the configuration effect. Conversely, the plasticity effect was negative for maize because of a slow early development caused by the shading from wheat and a small final leaf area index due to negative repercussions of reduced early development on later development (Fig. S5.15), see details at chapter 3.

#### *Light capture of whole wheat strip and border-row wheat under different scenarios*

A set of full factorial designed simulations was done to assess the contribution of four individual traits of wheat (Fig. 5.5). Among all scenarios, scenarios with

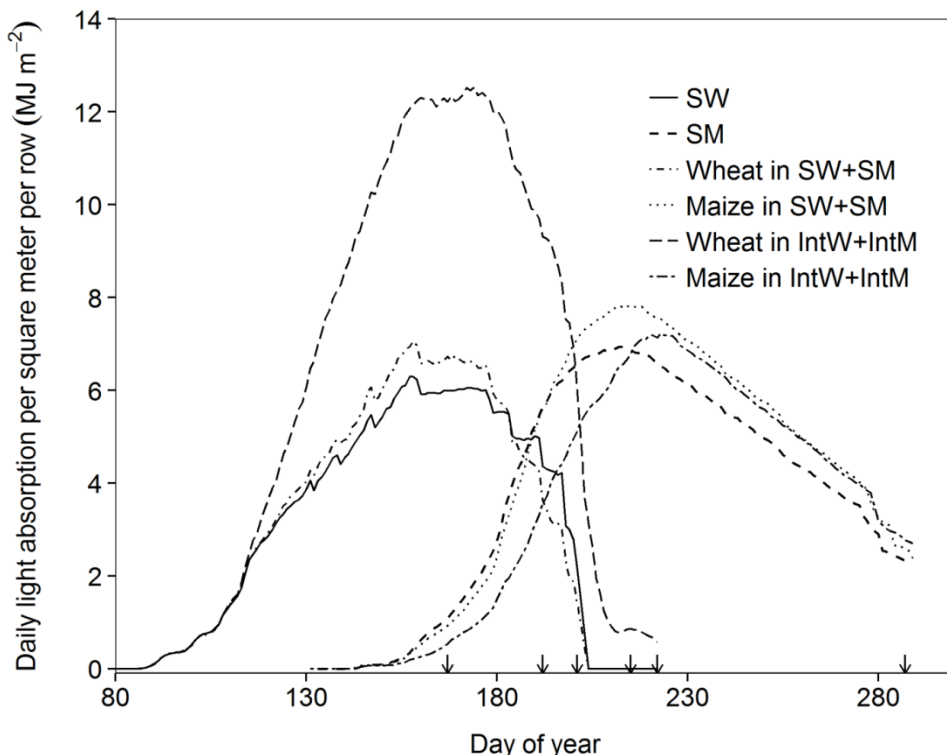


Fig. 5.4 Contribution of configuration effect and plasticity effect to seasonal patterns of light capture by wheat and maize in sole and mixed crops. SW represents sole wheat. SM represents sole maize. SW + SM represents a relay strip wheat-maize intercrop with phenotype of sole wheat and sole maize. IntW + IntM represents a relay strip wheat-maize intercrop with phenotype of intercrop wheat and intercrop maize. Arrows from left to right represent the time of wheat flowering (day of year 167), the time when sole maize overgrew intercrop wheat in height (192), the time when intercrop maize overgrew intercrop wheat in height (201), maize flowering (215), wheat harvest (222), and maize harvest (287). In order to facilitate comparison, the light capture for a wheat or maize strip here was converted into energy per square meter, counting a meter row length as an area of  $0.125\text{ m}^2$  or  $0.75\text{ m}^2$ , based on the row distance of sowing. Error bars were not shown since they were within one percentage of the simulated values.

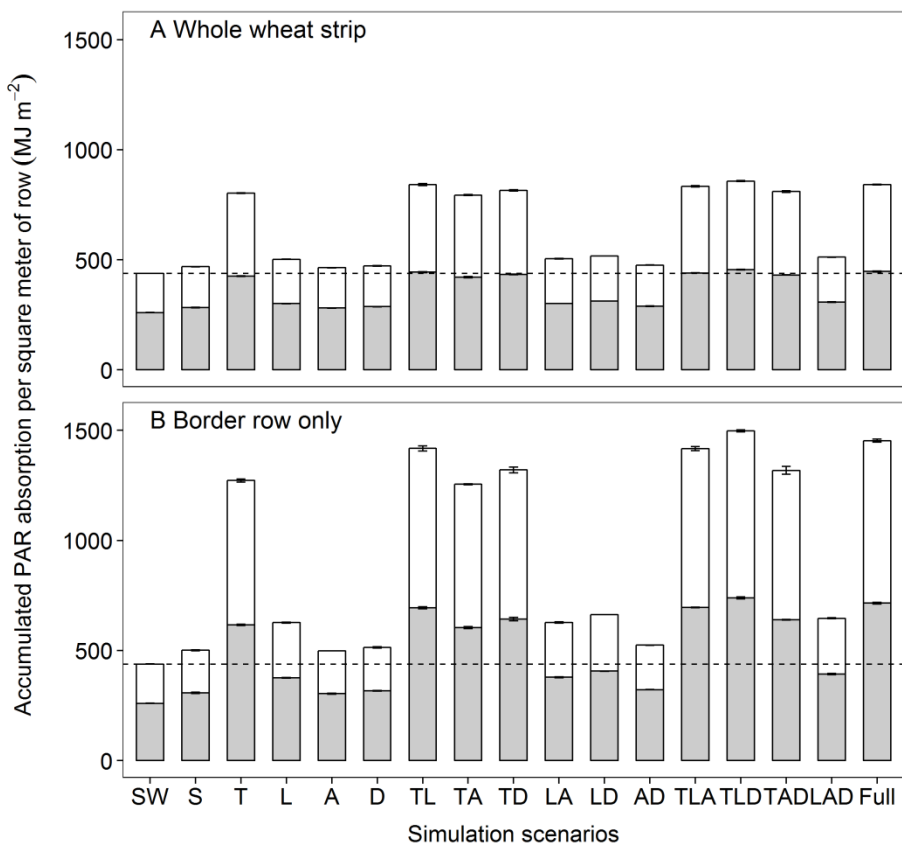


Fig. 5.5 Accumulated seasonal light capture at whole wheat strip (A) and at border row only. Shaded bars represent the accumulated light capture before wheat flowering and white bars represent accumulated light capture after wheat flowering. SW represents sole wheat. S represents using sole wheat phenotype in intercrop. T represents sole wheat phenotype with updated intercrop tiller dynamics. L represents sole wheat phenotype with updated intercrop leaf sizes. A represents sole wheat phenotype with updated intercrop leaf azimuth. D represents sole wheat phenotype with updated intercrop leaf declination angle. The combination of different symbols means update all those traits, see Table 1. Errors bars denote one standard error of the mean of three simulations. In order to facilitate comparison, the light capture for a wheat strip and for a wheat border row here were converted into per square meter, counting a meter row length as an area of  $0.125 \text{ m}^2$ , based on the row distance of sowing.

plasticity of tillering stand out with average light capture being 58% higher than in the remaining scenarios (Fig. 5.5A). Overall, average light capture in the wheat strip was 93% higher in the full plasticity scenario than in sole wheat. Eighty two percent of this increase was due to plasticity in tillering. Plasticity in the leaf size, declination angle and azimuth angle of leaves contributed respectively 8%, 2% and -4%. The remainder 12% resulted from the interactions between traits and the configuration effect for wheat.

The light capture of a fully plastic border-row wheat was 2.3 times higher than that of sole wheat (Fig. 5.5B). However, the light capture of scenario 'S' with sole wheat phenotype in wheat-maize intercrop was only 14% higher than sole wheat, showing the large contribution of plasticity to light capture in the border row. The results were also compared to a clear sky day where the atmospheric transmissivity was equal to 0.75 and the fraction of diffuse light in total radiation was 0.23 (Spitters *et al.*, 1986). A clear sky condition only increased the total absolute light capture compared to the default radiation set up in the model (transmissivity 0.43, fraction of diffuse light 0.7), while the effect of different plasticity traits on light capture remained the same.

## Discussion

5

Using an architectural model, we quantified the respective contributions of configuration effect and plasticity effect to complementary in light capture in a wheat-maize intercrop. Overall the complementarity effect increased the light capture by 23%, similar to the reported yield advantage in this system (Li *et al.*, 2010). The plasticity effect contributed considerably more to this benefit in light capture than the configuration effect (64% vs 36%). To our knowledge this is the first study that explicitly separated the complementarity effect in a mixed species plant stand into two components: one due to plant configuration in time and space and the other due to plasticity in shoot development. Based on these quantitative findings in a simple two-species system, we argue that in general, plasticity can have a large contribution in driving the potential benefits of niche differentiation in diversified plant systems.

### *Potential ecological implications*

Quantifying the role of phenotypic plasticity in complementary effect helps to disentangle the biodiversity effects on ecosystem functioning. The current challenge for biodiversity research is no longer whether biodiversity matters, but how it matters and how diversity research can result in quantitative predictions (Loreau *et al.*, 2001; Loreau *et al.*, 2002; Rosenfeld, 2002). Insight in the mechanisms of enhanced resource capture in diverse vegetation is a prerequisite for making such predictions. This makes it important to separate the biodiversity effects into components and to analyse these components. Many studies (Loreau and Hector, 2001; Tilman *et al.*, 2001; Cardinale *et al.*, 2007) consider niche or trait complementarity effect as a whole, and do not consider the required plasticity for achieving the realized niche differentiation. In fact, most treatments of complementarity in current ecological textbooks do not even mention the role of plasticity (Smith and Smith, 2014). The current study shows that it is important to distinguish the separate effects of configuration and plasticity on complementary resource capture, and provides a methodology to do so.

In diversity experiments the strongest over-yielding responses are typically observed in the range of 5-10 species, showing saturation for species-richer systems (Hector *et al.*, 1999; Loreau and Hector, 2001; Niklaus *et al.*, 2001; Hooper *et al.*, 2005). Extending our approach to experiments conducted at this level of diversity could represent an important next step in analysing the contribution of plasticity to complementarity effects in more complex natural systems than the one studied by us. Furthermore, there is an increasing consensus that a minimum subset of complementarity species is sufficient to explain diversity effects (Loreau *et al.*, 2001), e.g. four out of 18 species explained most of the biomass response in Tilman *et al.* (2001). Our approach could help identify the crucial traits of those dominant species in enhancing productivity of a certain ecosystem, and recognize the importance of belowground processes, e.g. nitrogen fixation by leguminous, when complementarity in shoot development cannot explain the increase in biomass production.

### *Limitations of this study*

We found a strong contribution of plasticity to complementarity effects in our relatively simple intercrop system. This raises the question whether it would be similarly important in more complex natural systems, as natural systems are generally more complex and diverse than our intercrop system. In our system the difference in environment between the mono and mixed stand was relatively uniform for all individuals within a species (or at least for those within a row). This could explain the dominant effect of plasticity in a single trait (i.e. tillering in wheat) in driving the complementarity in our system. In a natural system, all species are mixed up with various plant-to-plant distances, each plant experiences a complex pattern of environment signals. Thus, for individuals of a given species the contribution of plasticity in different traits will vary with the species identity, size and proximity of its neighbours.

Furthermore, the current model was designed to evaluate the consequence of plasticity in architectural traits on light capture without considering the (physiological) causes of such plastic responses. Plasticity in this study is defined as the ability of individual genotypes to produce different phenotypes under different environmental conditions (Pigliucci *et al.*, 2006). However, for obtaining a complete understanding of plasticity, it is important to distinguish between passive plasticity and ontogenetic (or true) plasticity (Sultan, 1995; Pigliucci and Hayden, 2001; Wright and Mcconnaughay, 2002). The former refers to an inevitable change in phenotype due to resource limitation whereas the latter refers to an active developmental response. The contribution of plasticity in maize was negative to light capture in this study. This is partly because the early development of maize was constrained by wheat, and partly because the light signal for maize was unsTable ince maize experienced a strong shading at early stage but good light condition at late stage. Furthermore, the criterion of total light capture that used in this study would fail in assessing the goodness of a certain passive response since we did not consider resource limitations in the model. Model like ours potentially could analyse this through incorporating the carbon balance, growth dependence on assimilates supply and carbon costs of plastic response.

In addition, due to plasticity in wheat tillering contributed considerably to the light capture of the wheat strip, the simulation results were very sensitive to the number of tillers simulated. A uncertainty analysis was done for quantifying the effect of variations in tillering pattern on the respective contribution of configuration and plasticity to the complementary light capture in intercropping, *see general discussion*.

### **Conclusions**

A new concept was developed for separating the complementarity effect on resource capture into the effects of community structure ('configuration effect') and plasticity in architectural development. Using a detailed 3D plant canopy architectural model, we quantified the contributions of spatial-temporal configuration and plant plasticity to the overall complementarity, and showed that plasticity effect contributed more than configuration effect in the system studied. The results indicated that predicting the performance of a mixture system based on plant traits in monoculture, e.g. phenology and plant height, without considering plastic responses would result in considerable deviations, and thus points out the importance of including plasticity in the study of species-diverse plant communities. Understanding and quantifying the plant plastic development in response to biotic and abiotic environment and the their interactions in mixture will help us disentangling the effects of biodiversity on ecosystem functioning.

### **Acknowledgements**

We thank Unifarm staff, Mr Peter van der Putten, and Mrs Ans Hofman for valuable help and contributions to the experiment, and Dr. Peter Vermeulen for valuable comments. The financial support of the China Scholarship Council (CSC) and the Key Sino-Dutch Joint Research Project of NSFC (grant number: 31210103906) are gratefully acknowledged.



# CHAPTER 6

## General discussion

In this thesis I described the plastic responses of wheat and maize plants to an intercrop environment, and provided a conceptual model for explaining the emergence of maize phenotype in intercrop as well as in monoculture. Furthermore I calculated the contribution of the plastic responses of wheat and maize to the light capture in intercrop using an architectural model. To my knowledge, this is the first study that has documented plant development in intercropping in detail and assessed the effect of above-ground plastic responses on the performance of a mixed vegetation.

The first three sections of this chapter address the research questions raised in the *general introduction*. Each of those three sections includes four elements: main findings, innovations, strengths and weaknesses of the methods, and future directions. Based on these findings, two additional planting patterns are tested using the wheat-maize intercropping model towards improving the total light capture of this system. After this, I compare the similarities and differences between agricultural and basic ecological studies based on my experience in studying intercropping. I also discuss a number of examples of where cross-fertilization between agricultural- and basic ecological research contributes to developing new insights.

#### *Description: how do plants growth in intercrops differ from that in monocrops?*

The temporal and spatial distribution of light and other environmental factors differ strongly between inter- and monocrops. In the current study wheat and maize were grown in strip intercrop with alternating six rows of wheat with two rows of maize. For clarity I briefly review the dynamics of these systems and the plastic responses of the two species before discussing their potential implications. Strips of spring wheat were sown on 9 March, with a strip of bare soil between the wheat strips. Maize was sown in these bare strips on 11 May. After wheat harvest on 10 August, maize continued to grow as a sole crop until its harvest on 14 October (Fig. 1.1). The light conditions in this system were highly heterogeneous, both in time and space. Wheat experienced a favourable light environment at early stages of development because of the absence of maize which was sown later, but it was shaded by the much taller maize plants during its grain filling stage. Maize seedlings were initially suppressed by the

taller wheat plants, but gradually outgrew the wheat until ultimately the wheat was harvested and removed from the system.

A wide range of plastic responses of wheat and maize plants to these environmental differences between inter- and monocrops were documented in chapter 2 and 3. Those plastic responses involved changes in the tiller dynamics of wheat, rate of leaf initiation and appearance of maize, as well as leaf length and width of both species. For instance, intercropped wheat plants acclimated to the favourable light environment at early growth stage (due to initial absence of maize) by producing more tillers both in border rows (rows adjacent to the maize strip) and inner rows of a wheat strip, compared to sole wheat. The light environment of inner-row wheat deteriorated as the shade cast from border-row wheat increased. Thus, inner-row wheat exhibited a strong degree of tiller senescence (Fig. 2.4, chapter 2). Conversely, border-row wheat plants continuously experienced a favourable light environment and maintained almost all of their tillers. Border-row wheat plants further acclimated to the favourable conditions by increasing the size of their upper leaves and the number of grains per ear. However, the favourable light environment for the border rows did not last until the end. The neighbouring maize plants gradually outgrew the wheat and achieved competitive dominance for light capture during the grain filling stage of wheat. Thus, border-row wheat suffered from the shade and showed a decreased thousand grain weight, compared to inner-row and sole wheat (Fig. 2.2).

Intercropped maize experienced strong shading right from emergence for approximately two months. Maize plants tried to escape from the shading by increasing the length of the sheaths and blades of low ranks (chapter 3). However due to the size difference between maize and wheat plants, the shade avoidance of maize was not successful. Therefore, maize had a phenotype characterized by decelerated leaf appearance rates, lower leaf number, smaller leaf area, and shorter internodes for upper ranks compared to sole maize. Such an intercrop maize phenotype could be expected to be more advantageous for a shaded environment than a high light environment because of smaller leaves and plant height compared to sole maize phenotype (see results manipulative experiments e.g. Dudley & Schmitt 1996). However, the maize plants were exposed to gradually improving light conditions as it was overgrowing wheat.

Maize acclimated to this high light environment by adapting its blade length : width ratio (Fig. 3.3). Yet, the improved light conditions were too late for maize to adapt its overall architecture to the new conditions. This was partly because the changes in light environment came after tassel initiation when maize could not change its final leaf number anymore, and partly because the effects of the low-light environment on early growth propagated throughout maize development, e.g. the effects of sheath length on the subsequent sheath length and blade length as discussed in chapter 3 and 4.

Plasticity in traits such as internode length and specific leaf area could contribute to niche segregation in a community and increase the performance of the community as a whole. However, most research on plant plasticity focuses exclusively on either individual plants or stands composed of one genotype (Schmitt *et al.*, 1999; Andrieu *et al.*, 2006). Few studies determined the plant plastic responses in species-diversified vegetation and assessed the role of plasticity in the functioning of the community. For instance, Roscher *et al.* (2011) and Gubsch *et al.* (2011) assessed the plastic responses of twelve legume and twelve grass species, respectively, to environmental differences caused by growing them in experimental gardens with different background species, which differed in number of species and functional groups. The legume and grass species displayed various plastic responses to these changes in background species. The variations in functional traits between different plots for each of those 24 species generally indicated strategies to optimize light and nutrient capture. For instance, both legume and grass species with shorter statures showed increased shoot and leaf length, reduced branching, higher specific leaf areas. However, even closely related species, e.g. grasses, displayed different responses. These studies therefore concluded that analyses of the plastic development of individual plant species is essential to get a deeper insight into the mechanisms behind biodiversity-ecosystem functioning relationships.

The current study provided insight in the plastic responses of individual wheat and maize plants in intercropping compared to monocrop throughout their developmental cycle, and quantified effects of these responses on the performance of the whole community. As noted above, wheat exhibited strong changes in tiller dynamics and both wheat and maize showed changes in

the size and dimensions of different organs which were consistent with former findings in density treatments (Andrieu *et al.*, 2006; Evers *et al.*, 2006; Dornbusch *et al.*, 2011), indicating the generality of those plastic responses. Furthermore it was observed that plants display multiple plastic responses, e.g. leaf length and leaf appearance rate, to a single environment condition at the same time. As those plastic responses occurred at the same time, it is likely that they were part of a coordinated response.

In this study, I limited myself mainly to the plasticity in shoot development and morphological traits, e.g. leaf appearance rates and organ sizes. Functional traits such as photosynthesis rate were beyond the scope of the thesis, since my key hypothesis was that the yield advantage of wheat-maize intercropping can largely be explained by the increase in light capture, not by the increase in light use efficiency. This hypothesis was based on work by Zhang *et al.* (2008) who found that the high performance of different wheat and cotton intercropping planting patterns, compared to monocultures, can be fully explained by an increase in accumulated light interception per unit cultivated land area, while no difference in light-use efficiency was detected. In addition, it was shown for the wheat-maize system studied here that approximately two thirds of the yield advantage of this system comes from complementarity in light capture (Zhang *et al.*, 2001). Furthermore, belowground interactions, e.g. root distribution, may also play an important role in determining the performance of the intercropping system. For instance, the roots of intercropped wheat spread under maize plants and had much greater root length density, length of roots per unit volume of soil, in all soil layers than sole wheat (Li *et al.*, 2006). Li *et al.* (2007) further showed that maize roots avoided those of wheat in intercrop, but grew near roots of faba bean due to better phosphorus availability near faba bean roots. The method that we demonstrated in chapter 5 for exchanging phenotypes between systems in architectural model, could in principle also be used for quantifying the contribution of plasticity in root development. Further work can be made on integrating the plasticity of belowground and aboveground growth and development to make a systematic view of how plants grow in intercrop. Such work can help us to identify the importance of different processes under a

given environment, and thus shed light on the solutions and options for improvement.

To summarize, a wide range of effects on wheat and maize shoot development were found when intercrop them together. However, little is known how those plastic responses are related with each other which is important for understanding how a whole plant phenotype emerges in a certain environment. Further work can be done on examining and modelling the formation of those plasticity pattern. Such modelling exercises are useful for evaluating and exploring the optimal plant traits for a certain crop system, and thus can be used as an assistant for plant breeding.

#### *Induction: how are different plastic traits correlated and regulated?*

In chapter 4, a structural development model of maize was constructed based on three coordination rules between leaf emergence events and the dynamics of organ (blade, sheath and internode) extension. Those coordination rules defined the sequence of organ development, the time of organ formation and elongation duration, and the dynamics of organ elongation rate. The model was parameterized using data of maize development at low population density and was tested by simulating development of maize plants at high density by adapting only the initial conditions (the dynamics of first three sheath length), but keeping model parameters the same. It was found that by using initial conditions associated with high population density, the model well reproduced the increase in blade elongation duration and the delay in sheath extension in high-density populations compared with low-density populations. Predictions of the sizes of sheaths at high density were accurate, whereas predictions of the dynamics of blade length were accurate up to rank 9; moderate overestimation of blade length occurred at higher ranks.

The model gave a good account of the timing and duration of blade and sheath extension at both plant population density, and thus supports the plausibility of phase transitions in organ extension being synchronized and coordinated with leaf emergence events. This is consistent with early experimental results (Davies *et al.*, 1983; Wilson and Laidlaw, 1985; Casey *et al.*, 1999; Fournier and Andrieu, 2000b; Fournier and Andrieu, 2000a; Andrieu *et al.*, 2006; Parent *et al.*, 2009) and modelling excises (Fournier *et al.*, 2003;

Fournier *et al.*, 2005; Verdenal *et al.*, 2008). Fournier and Andrieu (2000a) found that collar emergence was synchronized with the onset of internode elongation of the same phytomer, and later applied this synchrony in their ADEL-wheat model which resulted in good model performance (Fournier *et al.*, 2003). Fournier *et al.* (2005) analysed the association between the ontogeny of the growth zone of leaves with the time of leaf tip emergence using a dynamic model of leaf elongation based on the functioning of the growth zone in wheat and tall fescue, *Festuca arundinacea*. Their simulation results showed that tip emergence was synchronized with the end of the exponential growth phase of the blade. Within this study, I integrated these former findings, and proposed a new coordination rule between collar emergence and extension of the following sheath, and included the effects of reproductive phase on organ development. Thus, the innovation of this part of the study is that I present a holistic system view of plant development and coordination rules that govern whole-plant development during both the vegetative and reproductive phases.

This coordination framework of plant development may be the result of communication among organs through the hormonal system. For instance, the exposure of the leaf tip to light could result in changes in auxin synthesis in the leaf. Those auxins would transport out of the leaf towards the apical meristem, and thus influence leaf initiation and expansion (Covington and Harmer, 2007; Roig-Villanova *et al.*, 2007; Keuskamp *et al.*, 2010). Also, ultrastructural and cytochemical studies of the membranous ligules of several taxa, particularly *Lolium* species, found that ligules produce many chemical compounds that can affect the growth of leaves (Chaffey, 2000). This suggests that ligules play a rather active role in the life of the grass plant as a secretory tissue than simply being passive organs that protect the leaf from the entry of water, dust and harmful spores. However, until now no definitive evidence at the genetic and molecular level has been found that supported that the emergence of leaf tips or collars influences the dynamics of organs. Most of the coordination rules are induced from experimental results. Nevertheless, as long as the patterns of plant development predicted by the coordination rules is correct, the underlying mechanisms being unknown may not necessarily hamper the usage of such model in predicting phenotype and study the effect of early conditions on plant development.

Fifty years ago, De Wit and Penning-de Vries published a paper titled 'Crop growth models without hormones' (De Wit and Penning de Vries, 1983). They argued that models that aim to simulate growth (or other processes) acting at the plant- or community-level (e.g. crop stands) can take the existing intra-plant system for granted and do not need to explicitly model communication within the plant. The argument for this was that a plant growth model should not simulate relatively fast processes such as hormone balances as it will make the model include more than two or three hierarchical organization levels which will increase the uncertainty of the model. The application of root-shoot functional-balance theory in plant growth models provides a clear example of using the results of a communication system without considering hormones as intermediates. For example, the participation of carbon and nitrogen between root and shoot can be calculated based on the functional balance concept of Brouwer (1962) by assuming that plants would allocate resources to roots and shoots in such a way that the net carbon gain of the plant is maximized (Ågren and Ingestad, 1987; Yin and van Laar, 2005). However, the coordination in structural development presented in chapter 4, represent another type of internal communication beyond the concept of functional balance. Structural development coordination can be seen as the balance among the sizes and development timing of different organs, while functional balance can be seen as the efforts for maintaining the stoichiometric ratio of carbon, nitrogen, phosphorous etc. within the plant.

Introducing developmental coordination into structural models could bring several advantages in simulating plant development. For instance, models based on developmental coordination rules can provide a flexible time of organ elongation which are fixed in most current models (Fournier and Andrieu, 1998; Evers *et al.*, 2005; Guo *et al.*, 2006). Such models are especially suitable to be applied in cases where variation in elongation time plays an important role in determining changes in blade and sheath length, e.g. at high plant density (Andrieu *et al.*, 2006) and under cold stress (Louarn *et al.*, 2008). Furthermore, since plant development patterns like leaf appearance rate and distribution of organ size would emerge from the developmental coordination, the use of such rules can reduce the number of parameters related to the characterization of those traits. Finally, models based on developmental coordination rules will

provide more insights into the way plants functions, and such models can simulate plant development for a wide range of environmental conditions as they are based on fundamental mechanisms. Therefore, it is promising to include developmental coordination as well as functional balance concepts in models as well as in plant development theory and education in future.

Models featuring developmental coordination are especially useful for studying the effects of early plant plastic responses on later development. The findings that early structural changes in low rank leaves under competition influence whole plant structure in chapter 3, highlights the importance of early growth conditions for whole plant development. In addition to the structural changes, internal resource status, e.g. sugar, affected by early growth conditions would also change the plastic responses to environmental cues at later developmental stages. Huber *et al.* (2012) found that the responses of leaf elongation to submergence in *Rumex palustris*, a common terrestrial plant species inhabiting river floodplains, depends on light and nutrient availability in its early life stage. Therefore, further work could be done to include the effect of assimilate supply on organ and whole-plant growth, and to take into account the possible effects of assimilate supply on relative growth rates of the leaves. Such improvement could eliminate the need for having the relative elongation rates for each leaf as input (chapter 4), as elongation rates will then emerge as a function of assimilate availability and carbon source-sink relationships. In combination with experimental testing, models including both developmental coordination and carbon balance would greatly improving the efficiency in understanding complex plant developmental processes and how they in concert determine the structure and functioning of plants.

*Upscaling and synthesis: what are the consequences of plasticity for resource capture and productivity?*

Using an architectural model, we quantified the respective contributions of field configuration and plant plasticity to the complementary light capture in a wheat-maize intercrop (chapter 5). The field configuration effect is the contribution to complementarity caused by the spatial and temporal arrangement of the component species (i.e., in crops this arrangement is strongly controlled) as well as by the inherent differences in traits between

species. The plasticity effect is the contribution of plastic adjustments in traits to the complementary light capture. Overall the complementarity effect increased light capture by 23% as compared to the expected value from sole crops under the null hypothesis that each individual plant in intercrop performs the same as in sole crops (661.6 vs 538.6 MJ m<sup>-2</sup>). We showed that plasticity in shoot development contributes substantially to the performance of the wheat-maize intercropping system. However, the effect of configuration and plasticity on the light capture of wheat and maize differed from each other. For wheat the greater light capture in the intercrop was mostly attributable to plasticity in tillering and to a lesser extent to plasticity in leaf size and leaf angle distribution, while the configuration effect was almost negligible. Conversely, in maize the increased light capture in the intercrop was entirely due to configuration effect and plasticity even contributed negatively.

Architectural models like the one used in this study have been used to quantify the light partitioning within contrasting canopies in several studies: agroforestry (Lamanda *et al.*, 2008), a legume-weed system (Cici *et al.*, 2008) and grass-legume mixtures involving perennial and annual species (Sonohat *et al.*, 2002; Barillot *et al.*, 2011). Furthermore, Barillot *et al.* (2014) analysed the sensitivity of light partitioning within virtual wheat-pea mixtures to the variations in architectural traits of wheat and pea, and found that number of branches/tillers and length of internodes determined the partitioning of light within mixtures. However, the system that they analysed was a fully mixed system (pea and wheat in the same row), not a strip design. To my knowledge, our study is the first study that explicitly separated the complementarity effect in mixed cultivation into two components (plant configuration in time and space and plasticity in shoot development), and quantified the respective contribution of each component. Furthermore, I quantified to what extent plasticity in individual traits contributed to performance (i.e., light capture) of the whole system through a sensitivity analysis of the model. The sensitivity analysis was done by virtually transplanting the sole-crop plants into the intercrop configuration. Subsequently, one by one I replaced individual trait values for these virtual plants (e.g., leaf size or tiller number) by the values that had been measured on intercrop plants. In this manner I could show that plasticity in traits such as tiller dynamics and leaf size in wheat contributed

positively to light capture. However, decelerated leaf appearance rate and smaller leaf area per plant in intercropped maize actually contributed negatively, i.e. changing the sole-crop trait value for the intercrop trait value lowered light capture. This suggests that, at least in terms of light capture, some plastic responses were maladaptive.

The adaptiveness in plastic responses to a given environmental cue largely depends on the link between the cue and the environment in which a plant will grow (Dudley and Schmitt, 1996). Neighbour plants produce light cues (e.g. neutral shading and shifts in the red to far red ratio of light). Those light cues could be associated with neighbouring plants of similar size growing simultaneously with the target individual in which case a shade avoidance response would be adaptive. But such light cues can also be produced by much larger plants, e.g. trees, and in such a case strong SAS is actually maladaptive (Dudley and Schmitt, 1995). In the case of the intercropping system in this study, the plasticity shown by wheat can be seen as adaptive. Although intercropped wheat was shaded by maize at its grain filling stage, its architecture was already determined, and only moderate reduction in thousand grain weight was caused by this shade (chapter 2). The light cues experienced by intercropped maize were produced by wheat plants that were larger during early maize growth, smaller during later maize growth and then suddenly removed when they were harvested. Thus intercropped maize first experienced a progressively improving light environment and then a sudden shift to an ever better light climate. The adaptiveness of plastic responses caused by such changing light environments is similar to what was found in experiments in which phenotypes are exchanged between contrasting conditions. For instance, Dudley and Schmitt (1996) tested the adaptive value of plastic stem elongation in *Impatiens capensis*, common jewelweed, by manipulating the light cue (red to far-red ratio), to produce elongated and non-elongated plants. These plants were then transplanted into high and low densities in a natural population. They found that both the elongated plants in lower density and the non-elongated plants in high density show a lower fitness, indicating that a certain phenotype is only advantageous in the environment in which it had been induced. Thus, for increasing the light capture of maize in intercrop, it could

be wise to consider selecting varieties that show less or even no shade avoidance responses.

The advantage of plastic responses in enhancing performance in heterogeneous environments has long been known (Grime, 1994), but it was surprising to observe that plant plasticity contributed significantly more to the complementarity effect than the field configuration in wheat-maize intercropping system. One of the main reasons was the considerable contribution of plasticity in wheat tillering to the light capture of the wheat strip (chapter 5). Yet, this also makes the simulation results very sensitive to variation in the number of tillers simulated.

An uncertainty analysis was done on the simulation results to the number of tillers simulated in sole wheat. As shown in chapter 4, 40% more ears per square meter, total number of reproductive tillers plus main stem, were found in the block used for yield assessment compared to the plants that we observed in the morphology block (348 vs 250). This difference may have been due to a block effect (soil quality, soil compaction etc.), or to sampling effects as we only monitored four plants per plot, compared to the four square meter of plants used for the yield determination. The uncertainty analysis was done by decreasing the senescence probability of each tiller type of the plants we observed in sole wheat by 20% (Table S5.1 chapter 5). This resulted in approximately 0.5 tillers per plant on average in sole wheat at harvest which is comparable to the data we found in yield block. Under this reduced tiller senescence, the light capture of sole wheat was increased to 521.6 MJ m<sup>-2</sup> (vs 437 MJ m<sup>-2</sup> in the calculation in chapter 5), resulting in an expected light capture of 566.5 MJ m<sup>-2</sup> (vs 538.6 MJ m<sup>-2</sup>) for the whole wheat-maize intercropping system. This somewhat changed the simulated effect of intercropping on light capture as compared to chapter 5. That is, intercropping now increased the light capture of the whole system by 95.1 MJ m<sup>-2</sup> (instead of 123 MJ m<sup>-2</sup>), where 56.0 MJ m<sup>-2</sup> (59%, instead of 36%) comes from configuration effect and 39.1 MJ m<sup>-2</sup> (41%, instead of 64%) comes from plasticity effect. Thus, the contributions of configuration and plasticity to the complementary light capture vary with the tillering pattern of the corresponding monoculture. However, this does not contradict our

conclusions on the importance of plasticity for the performance of an intercropping system as it was demonstrated in both scenarios.

Further work can be done in evaluating the optimal plant traits for wheat-maize intercropping with help of the model. One particularly interesting case study could be a comparison between the performance of wheat-maize intercropping with different varieties of wheat and maize along the breeding history. This would be very helpful in demonstrating the differences between old and new varieties. In the past intercropping was much more prevalent than it is now, e.g. intercropping maize with other species was the dominant form of agriculture in the Pre-Columbian America's (Lewandowski, 1987). It is possible that by focussing on optimizing sole-crops, modern crop selection has unwittingly resulted in a loss of traits that would facilitate high performance in intercrops. Due to the importance of plasticity in improving the performance of the wheat-maize system documented here, e.g. tillering in wheat, differential selection for plasticity traits could partly have driven this hypothetical pattern. In addition, it would be interesting to set these trait differences against changes in management, that is, modern intercrops are managed in a different than say the intercrops grown by pre-Columbian Americans. A strong integration between breeding of crop cultivars for intercropping and the management of the intercrops in which these cultivars are most likely used, would provide a useful practice package for the farmers (Costanzo and Barberi, 2014). Answering such questions is highly complex as it entails an interplay between cropping patterns, management and variation in trait plasticity. A combination of experiments and FSPM could contribute to addressing them.

#### *Towards optimizing the planting pattern of wheat-maize intercropping*

Regarding optimizing the system based on the findings of this work, I tested additional planting patterns using the wheat-maize intercropping model. The exploration had two objectives: increase the percentage of border rows of wheat and reduce the radiation lost at the empty strip before maize emergence and after wheat harvest. A planting pattern with two rows of wheat and one row of maize was tested as it maximizes the percentage of wheat border rows to 100%, and has a relative small distance between wheat strips before maize emergence and can potentially close the field after wheat harvest. Two planting

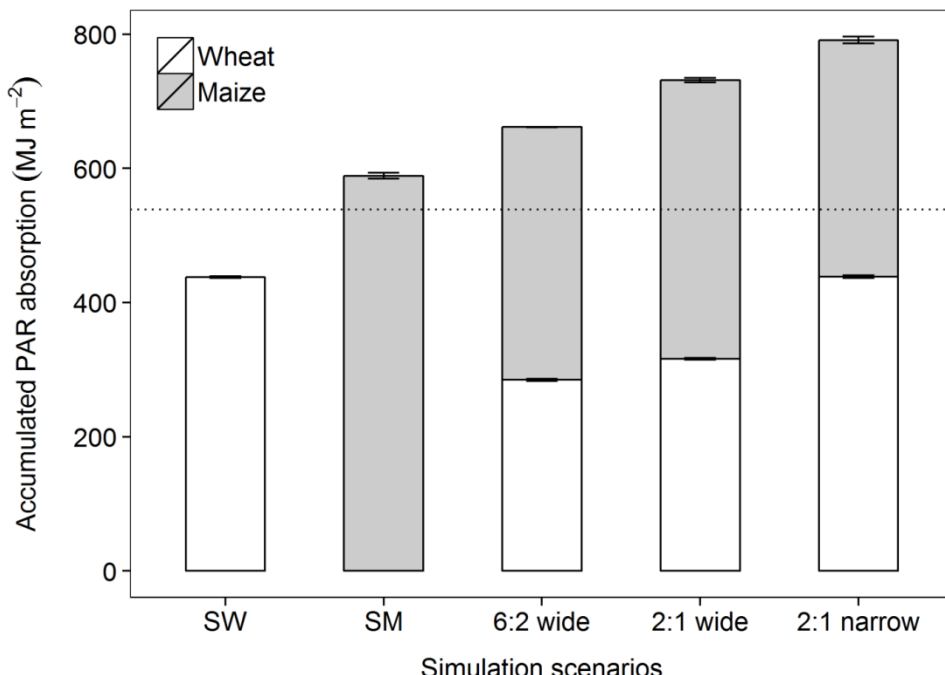


Fig. 6.1 Seasonal accumulated PAR capture in different systems. SW represents sole wheat, SM represents sole maize. 6:2 represents a wheat-maize intercrop with six rows of wheat and two rows of maize. 2:1 represents a wheat-maize intercrop with two rows of wheat and one row of maize. Wide represents a row distance of maize of 75 cm, narrow represents a row distance of maize of 50 cm. The horizontal dotted line represent the expected light capture in intercrop based on light capture in sole crops under the null hypothesis that each individual plant in intercrop perform the same as in sole crops. Errors bars represent the standard error of the mean of three simulations. For each simulation, 246 plants in sole wheat, 60 plants in sole maize, and 123 wheat plants plus 20 maize plants in intercrop were included in the calculation of light capture.

patterns both with two rows of wheat and one row of maize but with different row distance of maize were compared: one with a large width (75 cm, hereafter 2:1 wide intercropping system), one with a small width (50 cm, hereafter 2:1 narrow intercropping system). I did not further reduce the distance between wheat and maize as it would probably cause excessive competition (as shown in chapter 3) and result in plant phenotypes beyond the scope that our data can

represent. The relative density (i.e., density of species  $i$  in intercrop divided by its density in monoculture) was one fourth for wheat, and three fourths for maize in the 2:1 wide intercropping system, while the relative density was one third for wheat and two thirds for maize in the 2:1 narrow intercropping system. Two maize phenotypes were used, referred as wide-intercrop maize and narrow-intercrop maize; i.e., these phenotypes as measured in chapter 3 were virtually placed in the above-mentioned cropping configurations and light capture was calculated using the same FSPM as in chapter 5. Light capture was  $731.5 \text{ MJ m}^{-2}$  in the 2:1 wide intercropping system resulting in a LER of 1.4, and  $791.3 \text{ MJ m}^{-2}$  in the 2:1 narrow intercropping system resulting in a LER of 1.6 (Fig. 6.1). This clearly shows the advantage of the planting patterns with two rows of wheat and one row of maize in increasing the light capture of the whole system. However, the extent to which this increased light capture results in similarly increased yields still needs to be investigated.

#### *Exchange findings at agricultural system and natural system for mutual benefit*

This study lies at the intersection of agricultural sciences and basic ecology as it is aimed at understanding how plants grow in intercrop and how plasticity in plant traits contribute to the performance of an intercropping system. Agricultural and basic ecological studies are similar in a way that they are both dealing with ecosystems defined as the community of organisms and their interactions with each other and with the abiotic environment (Smith and Smith, 2014). Thus, they both study plant responses to light, nutrient, water, and neighbouring plants, and the population dynamics, energy flow and nutrient cycle of the system. An agroecosystem differs from a natural ecosystem in that at least one plant or animal population is of agricultural value and that humans play an important management role. Traditionally agricultural research tends to focus on problems associated with specific systems, e.g. a particular crop or cropping system. Conversely basic ecology tends to be driven more by an urge to understand how nature works. Thus to some extent, agricultural research is more objective based, while ecological studies are performed more out of curiosity. For instance, the study of plasticity in ecology is more focusing on how plasticity increases plant fitness and results in bigger survival rate in a community and how phenotypic plasticity interacts

with the evolution of species (Price *et al.*, 2003; Pigliucci, 2005). Agricultural studies mainly focus on selecting varieties that can produce phenotypes that perform best under a given environment, and thus view plastic responses to variation in external inputs like light, nutrients and water availability in the light of their contribution to yields or other agro-ecological functions.

Due to those similarities and differences, agricultural and ecological studies can benefit and learn from each other. For instance, ecological research has been very important for studies on sustainable agriculture. Thirty years ago, agricultural research was largely focusing on maximizing production and economic benefit and less concerned about environmental impacts. The application of ecological concepts and principles, e.g. closing nutrient cycles and biological pest management, resulted in the study of agroecology, which has shifted the objective of agriculture to a perspective that also values the ability to sustain productivity over the long term. Furthermore, it makes agricultural study focus more on the whole system rather than a single variable in the system, e.g. the recent raised study of water and nitrogen footprint of agriculture products allows the analysis of resource flow at the regional and global level (Aldaya *et al.*, 2012; Ma, 2014).

On the other hand, agricultural studies can also help address ecological questions. For example, an important question in ecology is how plasticity in traits increases plant fitness under certain environments and survival rate under natural selection. However, the selection pressure under a natural system is often unknown and varies in time, thus it is hard to answer this question. Fortunately, within crops there tends to be a rich palette of varieties developed under known selection forces due to the directional selection of crops, e.g. maximization of yield under high input condition, which can help in addressing this question. Furthermore agricultural systems such as intercropping can demonstrate plant-plant interaction and facilitation processes which are much harder to measure in more complex natural systems. For example, Zuo *et al.* (2000) showed that maize improved the iron nutrition of peanut on a calcareous soil when intercropped together. Li *et al.* (2007) demonstrated that faba-bean facilitates the phosphorus uptake of maize through acidification of rhizosphere on phosphorus-deficient soils in maize-faba bean intercropping. In this thesis, I showed that plasticity contributes significantly to the performance

of a mixed community using wheat-maize intercrop as a case study. While similar experiments can be set up with wild species, e.g. growing species mixtures in gardens (e.g. Hector *et al.*, 2002), the degree to which the setup is representative for the conditions under which they normally grow and under which they evolved remains questionable.

Moreover, the long history of agricultural practice has resulted in a vast knowledge base on plant development, the performance of different plant phenotypes in different regions, effective crop combinations in enhancing productivity and reducing diseases, e.g. squash-maize-climbing beans. This knowledge on crops and crop systems can serve as a start, a trigger, or a library for exploring the mechanisms behind plant development and the performance of a certain system which is within the scopes of ecological study. For example, the effect of crop rotation on enhancing crop performance and controlling plant diseases, e.g. potato cyst nematodes (Mai and Spears, 1954; Dropkin, 1955), has been known by farmers probably since early days of agriculture (Curl, 1963). Recently ecological studies have shown that the growth of a certain plant species would lead to accumulation of species-specific soil pathogens which cause negative feedback on plant growth even on the next few successions through changes in the soil community (vanderPutten, 1997). All in all, the combined force of ecological and agricultural research can result in fruitful results for the whole society. Agriculture is originally developed and will ultimately depend on a strong ecological foundation. Applying ecological principles and concepts in agriculture will result in a more sustainable production system. Ecology can also benefit from the fast developed agricultural science, and use its tools to answer ecological questions.

#### *Concluding remark*

The relationship between diversity and overyielding is studied at one of the frontiers of agricultural and ecological research. However, relatively little has been done in quantifying the role of phenotypic plasticity in the positive relationship between productivity and plant diversity. This thesis documented detailed plastic responses of wheat and maize in a wheat-maize intercrop, and highlighted the importance of phenotypic plasticity for reaching high performance in a plant mixture. Furthermore, I derived a model for explaining

how an intercrop maize phenotype was shaped by early plastic responses to the neighbouring wheat plants through developmental coordination, and thus emphasized the role of early growth condition in shaping the whole plant phenotype. How does a plant phenotype emerge under a given environment? How does phenotypic plasticity contribute to the productivity of a more diversified natural system? What are respective roles of belowground and aboveground processes in driving overyielding in diversified plant communities? These are the important questions that remain to be answered in the future.

## References

### A

**Agren GI, Ingestad T.** 1987. Root: Shoot ratio as a balance between nitrogen productivity and photosynthesis. *Plant, Cell & Environment* **10**(7): 579-586.

**Aldaya MM, Chapagain AK, Hoekstra AY, Mekonnen MM.** 2012. *The water footprint assessment manual: Setting the global standard*: Routledge.

**Alexandratos N, Bruinsma J** 2012. World agriculture towards 2030/2050: The 2012 revision. In: ESA Working paper Rome, FAO.

**Altieri MA.** 2009. Agroecology, small farms, and food sovereignty. *Monthly Review* **61**(3): 102-113.

**Andrieu B, Hillier J, Birch C.** 2006. Onset of sheath extension and duration of lamina extension are major determinants of the response of maize lamina length to plant density. *Annals of Botany* **98**(5): 1005-1016.

**Anten NP, Hirose T.** 1999. Interspecific differences in above-ground growth patterns result in spatial and temporal partitioning of light among species in a tall-grass meadow. *Journal of Ecology* **87**(4): 583-597.

### B

**Ballaré CL.** 1999. Keeping up with the neighbours: Phytochrome sensing and other signalling mechanisms. *Trends in Plant Science* **4**(3): 97-102.

**Ballaré CL, Scopel AL, Jordan ET, Vierstra RD.** 1994. Signaling among neighboring plants and the development of size inequalities in plant populations. *Proceedings of the National Academy of Sciences* **91**(21): 10094-10098.

**Barillot R, Escobar-Gutiérrez AJ, Fournier C, Huynh P, Combes D.** 2014. Assessing the effects of architectural variations on light partitioning within virtual wheat-pea mixtures. *Annals of Botany* **114**(4): 725-737.

**Barillot R, Louarn G, Escobar-Gutiérrez AJ, Huynh P, Combes D.** 2011. How good is the turbid medium-based approach for accounting for light partitioning in contrasted grass-legume intercropping systems? *Annals of Botany* **108**(6): 1013-1024.

**Beemster GTS, Fiorani F, Inzé D.** 2003. Cell cycle: The key to plant growth control? *Trends in Plant Science* **8**(4): 154-158.

**Begg JE, Wright MJ.** 1962. Growth and development of leaves from intercalary meristems in *phalaris arundinacea* l. *Nature* **194**(4833): 1097-1098.

**Bernier G.** 1988. The control of floral evocation and morphogenesis. *Annual Review of Plant Physiology and Plant Molecular Biology* **39**(1): 175-219.

**Birch CJ, Hammer GL, Rickert KG.** 1998a. Improved methods for predicting individual leaf area and leaf senescence in maize (*zea mays*). *Australian Journal of Agricultural Research* **49**(2): 249-262.

## References

**Birch CJ, Hammer GL, Rickert KG.** 1998b. Temperature and photoperiod sensitivity of development in five cultivars of maize (*zea mays l.*) from emergence to tassel initiation. *Field Crops Research* **55**(1-2): 93-107.

**Birch CJ, Vos J, Kiniry J, Bos HJ, Elings A.** 1998c. Phyllochron responds to acclimation to temperature and irradiance in maize. *Field Crops Research* **59**(3): 187-200.

**Bradshaw AD, Caspary EW, Thoday JM** 1965. Evolutionary significance of phenotypic plasticity in plants. *Advances in genetics*: Academic Press, 115-155.

**Briggs WR, Christie JM.** 2002. Phototropins 1 and 2: Versatile plant blue-light receptors. *Trends in Plant Science* **7**(5): 204-210.

**Brouwer R.** 1962. Nutritive influences on the distribution of dry matter in the plant. *Netherlands Journal of Agricultural Science* **10**(5): 399-408.

**Buck-Sorlin G, de Visser PHB, Henke M, Sarlikioti V, van der Heijden GWAM, Marcelis LFM, Vos J.** 2011. Towards a functional-structural plant model of cut-rose: Simulation of light environment, light absorption, photosynthesis and interference with the plant structure. *Annals of Botany* **108**(6): 1121-1134.

**Buck-Sorlin GH, Kniemeyer O, Kurth W.** 2005. Barley morphology, genetics and hormonal regulation of internode elongation modelled by a relational growth grammar. *New Phytologist* **166**(3): 859-867.

## C

**Callaway RM, Pennings SC, Richards CL.** 2003. Phenotypic plasticity and interactions among plants. *Ecology* **84**(5): 1115-1128.

**Cardinale BJ, Srivastava DS, Duffy JE, Wright JP, Downing AL, Sankaran M, Jouseau C.** 2006. Effects of biodiversity on the functioning of trophic groups and ecosystems. *Nature* **443**(7114): 989-992.

**Cardinale BJ, Wright JP, Cadotte MW, Carroll IT, Hector A, Srivastava DS, Loreau M, Weis JJ.** 2007. Impacts of plant diversity on biomass production increase through time because of species complementarity. *Proceedings of the National Academy of Sciences* **104**(46): 18123-18128.

**Casal JJ, Deregibus VA, Sanchez RA.** 1985. Variations in tiller dynamics and morphology in *loliium multiflorum lam.* Vegetative and reproductive plants as affected by differences in red/far-red irradiation. *Annals of Botany* **56**(4): 553-559.

**Casey IA, Brereton AJ, Laidlaw AS, McGilloway DA.** 1999. Effects of sheath tube length on leaf development in perennial ryegrass (*loliium perenne l.*). *Annals of Applied Biology* **134**(2): 251-257.

**Chaffey N.** 2000. Physiological anatomy and function of the membranous grass ligule. *New Phytologist* **146**(1): 5-21.

**Chappell MJ, Wittman H, Bacon CM, et al.** 2013. Food sovereignty: An alternative paradigm for poverty reduction and biodiversity conservation in latin america. *F1000Research* **2**.

**Chen BJW, During HJ, Anten NPR.** 2012. Detect thy neighbor: Identity recognition at the root level in plants. *Plant Science* **195**(0): 157-167.

**Chuck G, Hake S.** 2005. Regulation of developmental transitions. *Current Opinion in Plant Biology* **8**(1): 67-70.

**Cici S-Z-H, Adkins S, Hanan J.** 2008. A canopy architectural model to study the competitive ability of chickpea with sowthistle. *Annals of Botany* **101**(9): 1311-1318.

**Colasanti J, Yuan Z, Sundaresan V.** 1998. The indeterminate gene encodes a zinc finger protein and regulates a leaf-generated signal required for the transition to flowering in maize. *Cell* **93**(4): 593-603.

**Cong W-F, Hoffland E, Li L, Six J, Sun J-H, Bao X-G, Zhang F-s, Van derwerf W.** 2014. Intercropping enhances soil carbon and nitrogen. *Global Change Biology*: n/a-n/a.

**Connolly J, Goma HC, Rahim K.** 2001. The information content of indicators in intercropping research. *Agriculture, Ecosystems & Environment* **87**(2): 191-207.

**Corré WJ.** 1984. *Growth and morphogenesis of sun and shade plants*. Phd thesis thesis, van de Landbouwhogeschool te Wageningen Wageningen.

**Costanzo A, Barberi P.** 2014. Functional agrobiodiversity and agroecosystem services in sustainable wheat production. A review. *Agronomy for Sustainable Development* **34**(2): 327-348.

**Covington MF, Harmer SL.** 2007. The circadian clock regulates auxin signaling and responses in *arabidopsis*. *PLoS Biol* **5**(8): e222.

**Curl EA.** 1963. Control of plant diseases by crop rotation. *Botanical Review* **29**(4): 413-479.

## D

**Davidson J, Milthorpe F.** 1966. Leaf growth in dactylis glomerata following defoliation. *Annals of Botany* **30**(2): 173-184.

**Davies A, Evans ME, Exley JK.** 1983. Regrowth of perennial ryegrass as affected by simulated leaf sheaths. *The Journal of Agricultural Science* **101**(01): 131-137.

**de Kroon H.** 2007. How do roots interact? *Science* **318**(5856): 1562-1563.

**de Kroon H, Huber H, Stuefer JF, Van Groenendaal JM.** 2005. A modular concept of phenotypic plasticity in plants. *New Phytologist* **166**(1): 73-82.

**de Kroon H, Visser EJW, Huber H, Mommer L, Hutchings MJ.** 2009. A modular concept of plant foraging behaviour: The interplay between local responses and systemic control. *Plant, Cell & Environment* **32**(6): 704-712.

**De Wit C, Penning De Vries FWT.** 1983. Crop growth models without hormones. *Netherlands Journal of Agricultural Science* **31**: 313-323.

**de Wit M, Kegge W, Evers JB, Vergeer-van Eijk MH, Gankema P, Voesenek LACJ, Pierik R.** 2012. Plant neighbor detection through touching leaf tips

precedes phytochrome signals. *Proceedings of the National Academy of Sciences* **109**(36): 14705-14710.

**Dornbusch T, Baccar R, Watt J, Hillier J, Bertheloot J, Fournier C, Andrieu B. 2011.** Plasticity of winter wheat modulated by sowing date, plant population density and nitrogen fertilisation: Dimensions and size of leaf blades, sheaths and internodes in relation to their position on a stem. *Field Crops Research* **121**(1): 116-124.

**Dropkin VH. 1955.** The relations between nematodes and plants. *Experimental parasitology* **4**(3): 282-322.

**Drouet JL, Bonhomme R. 1999.** Do variations in local leaf irradiance explain changes to leaf nitrogen within row maize canopies? *Annals of Botany* **84**(1): 61-69.

**Dudley SA, Schmitt J. 1995.** Genetic differentiation in morphological responses to simulated foliage shade between populations of *impatiens capensis* from open and woodland sites. *Functional Ecology* **9**(4): 655-666.

**Dudley SA, Schmitt J. 1996.** Testing the adaptive plasticity hypothesis: Density-dependent selection on manipulated stem length in *impatiens capensis*. *American Naturalist*: 445-465.

**Durand JL, Onillon B, Schnyder H, Rademacher I. 1995.** Drought effects on cellular and spatial parameters of leaf growth in tall fescue. *Journal of Experimental Botany* **46**(9): 1147-1155.

**Dwyer LM, Stewart DW. 1986.** Leaf area development in field-grown maize1. *Agronomy Journal* **78**(2): 334-343.

**Dybzinski R, Tilman D. 2009.** Competition and coexistence in plant communities. *The Princeton guide to ecology*: 186-195.

**E**

**Eichhorn M, PParis P, Herzog F, et al. 2006.** Silvoarable systems in europe – past, present and future prospects. *Agroforestry Systems* **67**(1): 29-50.

**Evers JB, Vos J, Andrieu B, Struik PC. 2006.** Cessation of tillering in spring wheat in relation to light interception and red : Far-red ratio. *Annals of Botany* **97**(4): 649-658.

**Evers JB, Vos J, Chelle M, Andrieu B, Fournier C, Struik PC. 2007.** Simulating the effects of localized red:Far-red ratio on tillering in spring wheat (*triticum aestivum*) using a three-dimensional virtual plant model. *New Phytologist* **176**(2): 325-336.

**Evers JB, Vos J, Fournier C, Andrieu B, Chelle M, Struik PC. 2005.** Towards a generic architectural model of tillering in gramineae, as exemplified by spring wheat (*triticum aestivum*). *New Phytologist* **166**(3): 801-812.

**Evers JB, Vos J, Yin X, Romero P, van der Putten PEL, Struik PC. 2010.** Simulation of wheat growth and development based on organ-level

photosynthesis and assimilate allocation. *Journal of Experimental Botany* **61**(8): 2203-2216.

**F**

**FAO.** 2011. *The state of the world's land and water resources for food and agriculture (solaw)*: The Food and Agriculture Organization of the United Nations and Earthscan.

**Felippe GM, Dale JE.** 1973. Effects of shading the first leaf of barley plants on growth and carbon nutrition of the stem apex. *Annals of Botany* **37**(1): 45-56.

**Fischer R.** 1985. Number of kernels in wheat crops and the influence of solar radiation and temperature. *Journal of Agricultural Science* **105**(2): 447-461.

**Fischer R, Stockman Y.** 1986. Increased kernel number in norin 10-derived dwarf wheat: Evaluation of the cause. *Functional Plant Biology* **13**(6): 767-784.

**Fischer RA.** 1975. Yield potential in a dwarf spring wheat and the effect of shading. *Crop Science* **15**(5): 607-613.

**Fischer RA, Byerlee D, Edmeades GO, No AM** 2014. Crop yields and global food security: Will yield increase continue to feed the world? In. Canberra: Australian Centre for International Agricultural Research.

**Foley JA, Ramankutty N, Brauman KA, et al.** 2011. Solutions for a cultivated planet. *Nature* **478**(7369): 337-342.

**Forster BP, Franckowiak JD, Lundqvist U, Lyon J, Pitkethly I, Thomas WTB.** 2007. The barley phytomer. *Annals of Botany* **100**(4): 725-733.

**Fournier C, Andrieu B.** 1998. A 3d architectural and process-based model of maize development. *Annals of Botany* **81**(2): 233-250.

**Fournier C, Andrieu B.** 2000a. Dynamics of the elongation of internodes in maize (*zea mays l.*): Analysis of phases of elongation and their relationships to phytomer development. *Annals of Botany* **86**(3): 551-563.

**Fournier C, Andrieu B.** 2000b. Dynamics of the elongation of internodes in maize (*zea mays l.*): Effects of shade treatment on elongation patterns. *Annals of Botany* **86**(6): 1127-1134.

**Fournier C, Andrieu B, Ljutovac S, Saint-Jean S, eds.** 2003. *Adel-wheat: A 3d architectural model of wheat development*. International symposium on plant growth modeling, simulation, visualization, and their applications. Beijing, China PR: Tsinghua University Press / Springer.

**Fournier C, Durand JL, Ljutovac S, Schaufele R, Gastal F, Andrieu B.** 2005. A functional-structural model of elongation of the grass leaf and its relationships with the phyllochron. *New Phytologist* **166**(3): 881-894.

**Franca JB, Jochem BE, Niels PRA, Ronald P.** 2014. From shade avoidance responses to plant performance at vegetation level: Using virtual plant modelling as a tool. *New Phytologist* **204**(2): 268-272.

**Franklin KA, Whitelam GC** 2007. Red:Far-red ratio perception and shade avoidance. In: Whitelam GC, Halliday KJ eds. *Light and plant development*. Oxford: Blackwell Publishing Ltd, 211-234.

**Fujita K, Ofosu-Budu K, Ogata S 1992.** Biological nitrogen fixation in mixed legume-cereal cropping systems. *Biological nitrogen fixation for sustainable agriculture*: Springer, 155-175.

## G

**Gelang J, Pleijel H, Sild E, Danielsson H, Younis S, Selldén G. 2000.** Rate and duration of grain filling in relation to flag leaf senescence and grain yield in spring wheat (*triticum aestivum*) exposed to different concentrations of ozone. *Physiologia plantarum* **110**(3): 366-375.

**Ghosh P, Mohanty M, Bandyopadhyay K, Painuli D, Misra A. 2006.** Growth, competition, yield advantage and economics in soybean/pigeonpea intercropping system in semi-arid tropics of india: I. Effect of subsoiling. *Field Crops Research* **96**(1): 80-89.

**Giller K, Cadisch G 1995.** Future benefits from biological nitrogen fixation: An ecological approach to agriculture. *Management of biological nitrogen fixation for the development of more productive and sustainable agricultural systems*: Springer, 255-277.

**Gommers CMM, Visser EJW, Onge KRS, Voesenek LACJ, Pierik R. 2013.** Shade tolerance: When growing tall is not an option. *Trends in Plant Science* **18**(2): 65-71.

**Goudriaan J, Van Laar H. 1994.** *Modelling potential crop growth processes: Textbook with exercises*: Springer.

**Grime J 1994.** The role of plasticity in exploiting environmental heterogeneity. In: M.Caldwell. M, Pearcy RW eds. *Exploitation of environmental heterogeneity by plants: Ecophysiological processes above-and belowground*. California: Academic Press, Inc, 19.

**Grimm VB, Berger UB, Bastiansen F, et al. 2006.** A standard protocol for describing individual-based and agent-based models. *Ecological Modelling* **198**(1-2): 115-126.

**Gubsch M, Buchmann N, Schmid B, Schulze E-D, Lipowsky A, Roscher C. 2011.** Differential effects of plant diversity on functional trait variation of grass species. *Annals of Botany* **107**(1): 157-169.

**Guo Y, Ma Y, Zhan Z, Li B, Dingkuhn M, Luquet D, De Reffye P. 2006.** Parameter optimization and field validation of the functional-structural model greenlab for maize. *Annals of Botany* **97**(2): 217-230.

## H

**Hanway J. 1963.** Growth stages of corn (*zea mays*, l.). *Agronomy Journal* **55**(5): 487-492.

**Harper L, Freeling M. 1996.** Interactions of liguleless1 and liguleless2 function during ligule induction in maize. *Genetics* **144**(4): 1871-1882.

**Hector A, Bazeley-White E, Loreau M, Otway S, Schmid B. 2002.** Overyielding in grassland communities: Testing the sampling effect hypothesis with replicated biodiversity experiments. *Ecology Letters* **5**(4): 502-511.

**Hector A, Schmid B, Beierkuhnlein C, et al. 1999.** Plant diversity and productivity experiments in european grasslands. *Science* **286**(5442): 1123-1127.

**Hemmerling R, Kniemeyer O, Lanwert D, Kurth W, Buck-Sorlin G. 2008.** The rule-based language xl and the modelling environment groimp illustrated with simulated tree competition. *Functional Plant Biology* **35**(10): 739-750.

**Hillier J, Makowski D, Andrieu B. 2005.** Maximum likelihood inference and bootstrap methods for plant organ growth via multi-phase kinetic models and their application to maize. *Annals of Botany* **96**(1): 137-148.

**Hooper DU, Chapin I.F, Ewel J, et al. 2005.** Effects of biodiversity on ecosystem functioning: A consensus of current knowledge. *Ecological Monographs* **75**(1): 3-35.

**Horwith B. 1985.** A role for intercropping in modern agriculture. *BioScience* **35**(5): 286-291.

**Huber H, Chen X, Hendriks M, Keijsers D, Voesenek LA, Pierik R, Poorter H, de Kroon H, Visser EJ. 2012.** Plasticity as a plastic response: How submergence-induced leaf elongation in rumex palustris depends on light and nutrient availability in its early life stage. *New Phytologist* **194**(2): 572-582.

**J**

**Jose P, Douglas B, Saikat D, Deepayan S, Team tRDC. 2013.** Nlme: Linear and nonlinear mixed effects models. *R package version 3.1-113.*

**K**

**Kasperbauer MJK, D.L. USDA, ARS. 1986.** Light-mediated bioregulation of tillering and photosynthate partitioning in wheat. *Physiologia plantarum* **66**(1): 159-163.

**Keuskamp DH, Pollmann S, Voesenek LA, Peeters AJ, Pierik R. 2010.** Auxin transport through pin-formed 3 (pin3) controls shade avoidance and fitness during competition. *Proceedings of the National Academy of Sciences* **107**(52): 22740-22744.

**Kiesselbach TA. 1999.** *The structure and reproduction of corn*: Cold spring harbor laboratory press.

**Kimani SM, Chhabra SC, Lwande W, Khan Z, Hassanali A, Pickett JA. 2000.** Airborne volatiles from melinis minutiflora p. Beauv., a non-host plant of the spotted stem borer. *Journal of Essential Oil Research* **12**(2): 221-224.

**Kiniry JR, Ritchie JT, Musser RL. 1983.** Dynamic nature of the photoperiod response in maize1. *Agronomy Journal* **75**(4): 700-703.

**Kirby E, Riggs T. 1978.** Developmental consequences of two-row and six-row ear type in spring barley: 2. Shoot apex, leaf and tiller development. *The Journal of Agricultural Science* **91**(01): 207-216.

**Kirby EJM. 1990.** Co-ordination of leaf emergence and leaf and spikelet primordium initiation in wheat. *Field Crops Research* **25**(3-4): 253-264.

**Kniemeyer O.** 2008. *Design and implementation of a graph grammar based language for functional-structural plant modelling*. University of Technology at Cottbus.

**Knörzer H, Graeff-Hönninger S, Guo B, Wang P, Claupein W.** 2009. The rediscovery of intercropping in china: A traditional cropping system for future chinese agriculture – a review. In *Climate Change, Intercropping, Pest Control and Beneficial Microorganisms*, Springer, Netherlands, 13-44.

**L**

**Lafarge T, de Raïssac M, Tardieu F.** 1998. Elongation rate of sorghum leaves has a common response to meristem temperature in diverse african and european environmental conditions. *Field Crops Research* **58**(1): 69-79.

**Lafarge TA, Broad IJ, Hammer GL.** 2002. Tillering in grain sorghum over a wide range of population densities: Identification of a common hierarchy for tiller emergence, leaf area development and fertility. *Annals of Botany* **90**(1): 87-98.

**Lamanda N, Dauzat J, Jourdan C, Martin P, Malézieux E.** 2008. Using 3d architectural models to assess light availability and root bulkiness in coconut agroforestry systems. *Agroforestry Systems* **72**(1): 63-74.

**Lauer JG, Simmons SR.** 1988. Photoassimilate partitioning by tillers and individual tiller leaves in field-grown spring barley. *Crop Science* **28**(2): 279-282.

**Lauer JG, Simmons SR.** 1989. Canopy light and tiller mortality in spring barley. *Crop Science* **29**(2): 420-424.

**Lewandowski S.** 1987. Diohe'ko, the three sisters in seneca life: Implications for a native agriculture in the finger lakes region of new york state. *4*(2-3): 76-93.

**Li L, Li SM, Sun JH, Zhou LL, Bao XG, Zhang HG, Zhang FS.** 2007. Diversity enhances agricultural productivity via rhizosphere phosphorus facilitation on phosphorus-deficient soils. *Proceedings of the National Academy of Sciences* **104**(27): 11192-11196.

**Li L, Sun JH, Zhang FS, Guo TW, Bao XG, Smith FA, Smith SE.** 2006. Root distribution and interactions between intercropped species. *Oecologia* **147**(2): 280-290.

**Li L, Sun JH, Zhang FS, Li XL, Yang SC, Rengel Z.** 2001. Wheat/maize or wheat/soybean strip intercropping i. Yield advantage and interspecific interactions on nutrients. *Field Crops Research* **71**(2): 123-137.

**Li L, Tilman D, Lambers H, Zhang F-S.** 2014. Plant diversity and overyielding: Insights from belowground facilitation of intercropping in agriculture. *New Phytologist* **203**(1): 63-69.

**Li L, Zhang L, Zhang F** 2013. Crop mixtures and the mechanisms of overyielding. In: Levin SA ed. *Encyclopedia of biodiversity (second edition)*. Waltham: Academic Press, 382-395.

**Li Q-Z, Sun J-H, Wei X-J, Christie P, Zhang F-S, Li L.** 2010. Overyielding and interspecific interactions mediated by nitrogen fertilization in strip

intercropping of maize with faba bean, wheat and barley. *Plant and Soil* **339**(1-2): 147-161.

**Lichtfouse ENavarrete MDebaeke P, et al. 2009.** Mixing plant species in cropping systems: Concepts, tools and models: A review. *Sustainable agriculture*: Springer Netherlands, 329-353.

**Lithourgidis AS, Dordas CA, Damalas CA, Vlachostergios DN. 2011.** Annual intercrops: An alternative pathway for sustainable agriculture. *Australian Journal of Crop Science* **5**(4): 396-410.

**Loreau M, Hector A. 2001.** Partitioning selection and complementarity in biodiversity experiments. *Nature* **412**(6842): 72-76.

**Loreau M, Naeem S, Inchausti P. 2002.** *Biodiversity and ecosystem functioning: Synthesis and perspectives*: Oxford University Press.

**Loreau M, Naeem S, Inchausti P, et al. 2001.** Biodiversity and ecosystem functioning: Current knowledge and future challenges. *Science* **294**(5543): 804-808.

**Louarn G, Andrieu B, Giauffret C. 2010.** A size-mediated effect can compensate for transient chilling stress affecting maize (*zea mays*) leaf extension. *New Phytologist* **187**(1): 106-118.

**Louarn G, Chenu K, Fournier C, Andrieu B, Giauffret C. 2008.** Relative contributions of light interception and radiation use efficiency to the reduction of maize productivity under cold temperatures. *Functional Plant Biology* **35**(10): 885-899.

**Lovelock CE, Ewel JJ. 2005.** Links between tree species, symbiotic fungal diversity and ecosystem functioning in simplified tropical ecosystems. *New Phytologist* **167**(1): 219-228.

**M**

**Ma L. 2014.** *Nutrient use efficiency in the food chain of china*. Proefschrift Wageningen University ter verkrijging van de graad van doctor in het jaar 2014 Met literatuuropgave. - Met samenvatting in het Engels en Nederlands thesis, Wageningen University Wageningen.

**Ma YT, Li BG, Zhan ZG, Guo Y, Luquet D, De Reffye P, Dingkuhn M. 2007.** Parameter stability of the functional-structural plant model greenlab as affected by variation within populations, among seasons and among growth stages. *Annals of Botany* **99**(1): 61-73.

**MacAdam JW, Volenec JJ, Nelson CJ. 1989.** Effects of nitrogen on mesophyll cell division and epidermal cell elongation in tall fescue leaf blades. *Plant Physiology* **89**(2): 549-556.

**Machado S. 2009.** Does intercropping have a role in modern agriculture? *Journal of Soil and Water Conservation* **64**(2): 55A-57A.

**Maddonni GA, Otegui ME, Andrieu B, Chelle M, Casal JJ. 2002.** Maize leaves turn away from neighbors. *Plant Physiology* **130**(3): 1181-1189.

**Mai WF, Spears JF.** 1954. The golden nematode in the united states. *American Journal of Potato Research* **31**(12): 387-396.

**Makumba W, Akinnifesi FK, Janssen B, Oenema O.** 2007. Long-term impact of a gliricidia-maize intercropping system on carbon sequestration in southern malawi. *Agriculture, Ecosystems & Environment* **118**(1-4): 237-243.

**Makumba W, Janssen B, Oenema O, Akinnifesi FK, Mweta D, Kwasiga F.** 2006. The long-term effects of a gliricidia-maize intercropping system in southern malawi, on gliricidia and maize yields, and soil properties. *Agriculture, Ecosystems & Environment* **116**(1-2): 85-92.

**McDonald BA, Linde C.** 2002. Pathogen population genetics, evolutionary potential, and durable resistance. *Annual Review of Phytopathology* **40**: 349-+.

**McMaster G, LeCain D, Morgan J, Aiguo L, Hendrix D.** 1999. Elevated co<sub>2</sub> increases wheat cer, leaf and tiller development, and shoot and root growth. *Journal of Agronomy and Crop Science* **183**(2): 119-128.

**McMaster GS.** 2005. Phytomers, phyllochrons, phenology and temperate cereal development. *The Journal of Agricultural Science* **143**(2-3): 137-150.

**Mohr H.** 1964. The control of plant growth and development by light. *Biological Reviews* **39**(1): 87-112.

**Monteith JL, Moss CJ.** 1977. Climate and the efficiency of crop production in britain [and discussion]. *Philosophical Transactions of the Royal Society of London. B, Biological Sciences* **281**(980): 277-294.

**Morris RA, Garrity DP.** 1993a. Resource capture and utilization in intercropping: Water. *Field Crops Research* **34**(3-4): 303-317.

**Morris RA, Garrity DP.** 1993b. Resource capture and utilization in intercropping; non-nitrogen nutrients. *Field Crops Research* **34**(3-4): 319-334.

**Muchow RC, Carberry PS.** 1989. Environmental control of phenology and leaf growth in a tropically adapted maize. *Field Crops Research* **20**(3): 221-236.

**Mulugeta G.** 2014. Evergreen agriculture: Agroforestry for food security and climate change resilience. *Journal of Natural Sciences Research* **4**(11): 80-90.

## N

**Nelson C.** 1988. Genetic associations between photosynthetic characteristics and yield: Review of the evidence. *Plant physiology and biochemistry* **26**(4): 543-554.

**Nelson CJ** 2000. Shoot morphological plasticity of grasses: Leaf growth vs. Tillering.In Lemaire G, Hodgson, J., De Moraes, A., C. Nabinger, P.C. de F. Carvalho. *Grassland ecophysiology and grazing ecology*. Wallingford: CABI. 101-126.

**Nemoto K, Morita S, Baba T.** 1995. Shoot and root development in rice related to the phyllochron. *Crop Science* **35**(1): 24-29.

**Niklaus PA, Kandeler E, Leadley P, Schmid B, Tscherko D, Körner C.** 2001. A link between plant diversity, elevated co<sub>2</sub> and soil nitrate. *Oecologia* **127**(4): 540-548.

**Novoplansky A, Cohen D, Sachs T. 1994.** Responses of an annual plant to temporal changes in light environment: An interplay between plasticity and determination. *Oikos* **69**(3): 437-446.

**Novozamsky I, Houba VJG, van Eck R, van Vark W. 1983.** A novel digestion technique for multi-element plant analysis. *Communications in Soil Science and Plant Analysis* **14**(3): 239-248.

## O

**Ong C, Marshall C. 1979.** The growth and survival of severely-shaded tillers in lolium perenne l. *Annals of Botany* **43**(2): 147-155.

**Ong C, Marshall C, Saoar G. 1978.** The physiology of tiller death in grasses. 2. Causes of tiller death in a grass sward. *Grass and Forage Science* **33**(3): 205-211.

## P

**Padilla JM, Otegui ME. 2005.** Co-ordination between leaf initiation and leaf appearance in field-grown maize (zea mays): Genotypic differences in response of rates to temperature. *Annals of Botany* **96**(6): 997-1007.

**Page ER, Liu W, Cerrudo D, Lee EA, Swanton CJ. 2011.** Shade avoidance influences stress tolerance in maize. *Weed Science* **59**(3): 326-334.

**Parent B, Conejero G, Tardieu F. 2009.** Spatial and temporal analysis of non-steady elongation of rice leaves. *Plant, Cell & Environment* **32**(11): 1561-1572.

**Pautler M, Tanaka W, Hirano H-Y, Jackson D. 2013.** Grass meristems i: Shoot apical meristem maintenance, axillary meristem determinacy and the floral transition. *Plant and Cell Physiology* **54**(3): 302-312.

**Paysant-Leroux C. 1998.** *Mise en place de la longueur et de la largeur des feuilles de maïs. Etablissement d'un modèle de développement à l'échelle de la plante pour deux génotypes.*, Université de Pau et des Pays de l'Adour Pau, France.

**Pearcy RW. 2007.** Responses of plants to heterogeneous light environments. *Handbook of functional plant ecology*: 213-257.

**Pelzer EBazot MMakowski D, et al. 2012.** Pea-wheat intercrops in low-input conditions combine high economic performances and low environmental impacts. *European Journal of Agronomy* **40**(0): 39-53.

**Pierik R, de Wit M. 2013.** Shade avoidance: Phytochrome signalling and other aboveground neighbour detection cues. *Journal of Experimental Botany*: ert389.

**Pigliucci M. 2005.** Evolution of phenotypic plasticity: Where are we going now? *Trends in Ecology & Evolution* **20**(9): 481-486.

**Pigliucci M, Hayden K. 2001.** Phenotypic plasticity is the major determinant of changes in phenotypic integration in arabidopsis. *New Phytologist* **152**(3): 419-430.

**Pigliucci M, Murren CJ, Schlichting CD. 2006.** Phenotypic plasticity and evolution by genetic assimilation. *Journal of Experimental Biology* **209**(12): 2362-2367.

**Pons TL, Jordi W, Kuiper D. 2001.** Acclimation of plants to light gradients in leaf canopies: Evidence for a possible role for cytokinins transported in the transpiration stream. *Journal of Experimental Botany* **52**(360): 1563-1574.

**Poorter H, Lambers H. 1986.** Growth and competitive ability of a highly plastic and a marginally plastic genotype of *plantago major* in a fluctuating environment. *Physiologia plantarum* **67**(2): 217-222.

**Pretty JS, Sutherland WJ, Ashby J, et al. 2010.** The top 100 questions of importance to the future of global agriculture. *International Journal of Agricultural Sustainability* **8**(4): 219-236.

**Prévet L, Aries F, Monestiez P. 1991.** Modélisation de la structure géométrique du maïs. *Agronomie* **11**(6): 491-503.

**Price TD, Qvarnström A, Irwin DE. 2003.** The role of phenotypic plasticity in driving genetic evolution. *Proceedings of the Royal Society of London. Series B: Biological Sciences* **270**(1523): 1433-1440.

**R**

**R Core Team 2014.** R: A language and environment for statistical computing. In. Vienna, Austria: R Foundation for Statistical Computing.

**Radin JW. 1983.** Control of plant growth by nitrogen: Differences between cereals and broadleaf species. *Plant, Cell & Environment* **6**(1): 65-68.

**Rao MR, Singh M. 1990.** Productivity and risk evaluation in contrasting intercropping systems. *Field Crops Research* **23**(3-4): 279-293.

**Ratnadass A, Fernandes P, Avelino J, Habib R. 2012.** Plant species diversity for sustainable management of crop pests and diseases in agroecosystems: A review. *32*(1): 273-303.

**Roig-villanova I, Bou-Torrent J, Galstyan A, Carretero-Paulet L, Portolés S, Rodríguez-Concepción M, Martínez-García JF. 2007.** Interaction of shade avoidance and auxin responses: A role for two novel atypical bhlh proteins. *The EMBO journal* **26**(22): 4756-4767.

**Roscher C, Schmid B, Buchmann N, Weigelt A, Schulze E-D. 2011.** Legume species differ in the responses of their functional traits to plant diversity. *Oecologia* **165**(2): 437-452.

**Roscher C, Schumacher J, Lipowsky A, et al. 2013.** A functional trait-based approach to understand community assembly and diversity-productivity relationships over 7 years in experimental grasslands. *Perspectives in Plant Ecology, Evolution and Systematics* **15**(3): 139-149.

**Rosenfeld JS. 2002.** Logical fallacies in the assessment of functional redundancy. *Conservation Biology*: 837-839.

**Rusinamhodzi L, Corbeels M, Nyamangara J, Giller KE. 2012.** Maize-grain legume intercropping is an attractive option for ecological intensification that reduces climatic risk for smallholder farmers in central mozambique. *Field Crops Research* **136**(0): 12-22.

## S

**Sadras VO, Villalobos FJ.** 1993. Floral initiation, leaf initiation and leaf appearance in sunflower. *Field Crops Research* **33**(4): 449-457.

**Schlüchting CD.** 1986. The evolution of phenotypic plasticity in plants. *Annual Review of Ecology and Systematics* **17**: 667-693.

**Schnyder H, Seo S, Rademacher IF, Kühbauch W.** 1990. Spatial distribution of growth rates and of epidermal cell lengths in the elongation zone during leaf development in *lolium perenne* l. *Planta* **181**(3): 423-431.

**Sharman BC.** 1942. Developmental anatomy of the shoot of *zea mays* l. *Annals of Botany* **6**(2): 245-282.

**Siemer EG, Leng ER, Bonnett OT.** 1969. Timing and correlation of major developmental events in maize, *Zea mays* L. *Agronomy Journal* **61**(1): 14-17.

**Silvertown J, Gordon DM.** 1989. A framework for plant behavior. *Annual Review of Ecology and Systematics*: 349-366.

**Simpson GM.** 1968. Association between grain yield per plant and photosynthetic area above the flag-leaf node in wheat. *Canadian Journal of Plant Science* **48**(3): 253-260.

**Skinner RH, Nelson CJ.** 1994. Epidermal cell division and the coordination of leaf and tiller development. *Annals of Botany* **74**(1): 9-16.

**Skinner RH, Nelson CJ.** 1995. Elongation of the grass leaf and its relationship to the phyllochron. *Crop Science* **35**(1): 4-10.

**Smith H.** 2000. Phytochromes and light signal perception by plants—an emerging synthesis. *Nature* **47**: 581-591.

**Smith TM, Smith RL.** 2014. *Elements of ecology*. Harlow: Pearson Education Limited.

**Sofield I, Evans L, Cook M, Wardlaw I.** 1977. Factors influencing the rate and duration of grain filling in wheat. *Functional Plant Biology* **4**(5): 785-797.

**Sonohat G, Sinoquet H, Varlet-Grancher C, Rakocevic M, Jacquet A, Simon JC, Adam B.** 2002. Leaf dispersion and light partitioning in three-dimensionally digitized tall fescue-white clover mixtures. *Plant Cell and Environment* **25**(4): 529-538.

**Sparkes DL, Holme SJ, Gaju O.** 2006. Does light quality initiate tiller death in wheat? *European Journal of Agronomy* **24**(3): 212-217.

**Spitters CJT.** 1986. Separating the diffuse and direct component of global radiation and its implications for modeling canopy photosynthesis part ii. Calculation of canopy photosynthesis. *Agricultural and Forest Meteorology* **38**(1-3): 231-242.

**Spitters CJT, Toussaint HAJM, Goudriaan J.** 1986. Separating the diffuse and direct component of global radiation and its implications for modeling canopy photosynthesis part i. Components of incoming radiation. *Agricultural and Forest Meteorology* **38**(1-3): 217-229.

**Stamm P, Kumar PP.** 2010. The phytohormone signal network regulating elongation growth during shade avoidance. *Journal of Experimental Botany* **61**(11): 2889-2903.

**Stuefer JF, During HJ, Kroon Hd.** 1994. High benefits of clonal integration in two stoloniferous species, in response to heterogeneous light environments. *Journal of Ecology* **82**(3): 511-518.

**Sugiyama S-i, Gotoh M.** 2010. How meristem plasticity in response to soil nutrients and light affects plant growth in four *festuca* grass species. *New Phytologist* **185**(3): 747-758.

**Sultan S.** 1995. Phenotypic plasticity and plant adaptation\*. *Acta botanica Neerlandica* **44**(4): 363-383.

**Sultan SE.** 2000. Phenotypic plasticity for plant development, function and life history. *Trends in Plant Science* **5**(12): 537-542.

**Sultan SE.** 2010. Plant developmental responses to the environment: Eco-devo insights. *Current Opinion in Plant Biology* **13**(1): 96-101.

## T

**Tilman D, Reich PB, Knops J, Wedin D, Mielke T, Lehman C.** 2001. Diversity and productivity in a long-term grassland experiment. *Science* **294**(5543): 843-845.

**Tilman D, Wedin D, Knops J.** 1996. Productivity and sustainability influenced by biodiversity in grassland ecosystems. *Nature* **379**(6567): 718-720.

**Tivet F, DA Silveira Pinheiro B, DE Raïssac M, Dingkuhn M.** 2001. Leaf blade dimensions of rice (*oryza sativa* l. And *oryza glaberrima* steud.). Relationships between tillers and the main stem. *Annals of Botany* **88**(3): 507-511.

**Trenbath BR.** 1993. Intercropping for the management of pests and diseases. *Field Crops Research* **34**(3-4): 381-405.

**Turner C, Knapp A.** 1996. Responses of a c4 grass and three c3 forbs to variation in nitrogen and light in tallgrass prairie. *Ecology*: 1738-1749.

## V

**Valladares F, Wright SJ, Lasso E, Kitajima K, Pearcy RW.** 2000. Plastic phenotypic response to light of 16 congeneric shrubs from a panamanian rainforest. *Ecology* **81**(7): 1925-1936.

**Vandermeer J.** 1989. *The ecology of intercropping*. Cambridge: Cambridge University Press.

**Vandermeer JH.** 2011. *The ecology of agroecosystems*. Boston, MA [etc.]: Jones and Bartlett Publishers.

**vanderPutten WH.** 1997. Plant-soil feedback as a selective force. *Trends in Ecology & Evolution* **12**(5): 169-170.

**Verdenal A, Combes D, Escobar-Gutiérrez AJ.** 2008. A study of ryegrass architecture as a self-regulated system, using functional-structural plant modelling. *Functional Plant Biology* **35**(10): 911-924.

**Verma V, Foulkes MJ, Worland AJ, Sylvester-Bradley R, Caligari PDS, Snape JW.** 2004. Mapping quantitative trait loci for flag leaf senescence as a yield

determinant in winter wheat under optimal and drought-stressed environments. *Euphytica* **135**(3): 255-263.

**Vos J, Evers JB, Buck-Sorlin GH, Andrieu B, Chelle M, de Visser PHB. 2010.** Functional-structural plant modelling: A new versatile tool in crop science. *Journal of Experimental Botany* **61**(8): 2101-2115.

**Vos J, Putten PELvd, Birch CJ. 2005.** Effect of nitrogen supply on leaf appearance, leaf growth, leaf nitrogen economy and photosynthetic capacity in maize (*zea mays* l.). *Field Crops Research* **93**(1): 64-73.

**W**

**Wasternack C. 2007.** Jasmonates: An update on biosynthesis, signal transduction and action in plant stress response, growth and development. *Annals of Botany* **100**(4): 681-697.

**Weiner J. 1990.** Asymmetric competition in plant populations. *Trends in Ecology & Evolution* **5**(11): 360-364.

**Werner EE, Peacor SD. 2003.** A review of trait-mediated indirect interactions in ecological communities. *Ecology* **84**(5): 1083-1100.

**Wilson RE, Laidlaw AS. 1985.** The role of the sheath tube in the development of expanding leaves in perennial ryegrass. *Annals of Applied Biology* **106**(2): 385-391.

**Wolfe MS. 2000.** Crop strength through diversity. *Nature* **406**(6797): 681-682.

**Wright SD, Mcconnaughay KD. 2002.** Interpreting phenotypic plasticity: The importance of ontogeny. *Plant Species Biology* **17**(2-3): 119-131.

**X**

**Xu L, Huber H, During HJ, Dong M, Anten NPR. 2013.** Intraspecific variation of a desert shrub species in phenotypic plasticity in response to sand burial. *New Phytologist* **199**(4): 991-1000.

**Y**

**Yachi S, Loreau M. 2007.** Does complementary resource use enhance ecosystem functioning? A model of light competition in plant communities. *Ecology Letters* **10**(1): 54-62.

**Yin X, Goudriaan J, Lantinga EA, Vos Jan S, Huub J. 2003.** A flexible sigmoid function of determinate growth. *Annals of Botany* **91**(3): 361-371.

**Yin X, van Laar HH. 2005.** *Crop systems dynamics : An ecophysiological simulation model for genotype-by-environment interactions.* Wageningen: Wageningen Academic.

**Z**

**Zhang F, Li L. 2003.** Using competitive and facilitative interactions in intercropping systems enhances crop productivity and nutrient-use efficiency. *Plant and Soil* **248**(1-2): 305-312.

## References

**Zhang F, Li L, Sun J 2001.** Contribution of above-and below-ground interactions to intercropping. In: Horst WJ, Schenk MK, Bürkert Aet al eds. *Plant nutrition*: Springer, 978-979.

**Zhang FS, Li L. 2003.** Using competitive and facilitative interactions in intercropping systems enhances crop productivity and nutrient-use efficiency. *Plant and Soil* **248**(1-2): 305-312.

**Zhang L. 2007.** *Productivity and resource use in cotton and wheat relay intercropping*. Proefschrift Wageningen University ter verkrijging van de graad van doctor in het jaar 2007 thesis, Wageningen university Wageningen.

**Zhang L, Spiertz JHJ, Zhang S, Li B, Werf W. 2008a.** Nitrogen economy in relay intercropping systems of wheat and cotton. *303*(1-2): 55-68.

**Zhang L, van der Werf W, Bastiaans L, Zhang S, Li B, Spiertz JHJ. 2008b.** Light interception and utilization in relay intercrops of wheat and cotton. *Field Crops Research* **107**(1): 29-42.

**Zhang L, van der Werf W, Zhang S, Li B, Spiertz JHJ. 2007.** Growth, yield and quality of wheat and cotton in relay strip intercropping systems. *Field Crops Research* **103**(3): 178-188.

**Zhu Y-Y, Fang H, Wang Y-Y, Fan JX, Yang S-S, Mew TW, Mundt CC. 2005.** Panicle blast and canopy moisture in rice cultivar mixtures. *Phytopathology* **95**(4): 433-438.

**Zhu YChen HFan J, et al. 2000.** Genetic diversity and disease control in rice. *Nature* **406**(6797): 718-722.

**Zuo YM, Zhang FS, Li XL, Cao YP. 2000.** Studies on the improvement in iron nutrition of peanut by intercropping with maize on a calcareous soil. *Plant and Soil* **220**(1-2): 13-25.

## Appendix I

### Overyielding of wheat in intercrops is associated with plant architectural responses that enhance light capture

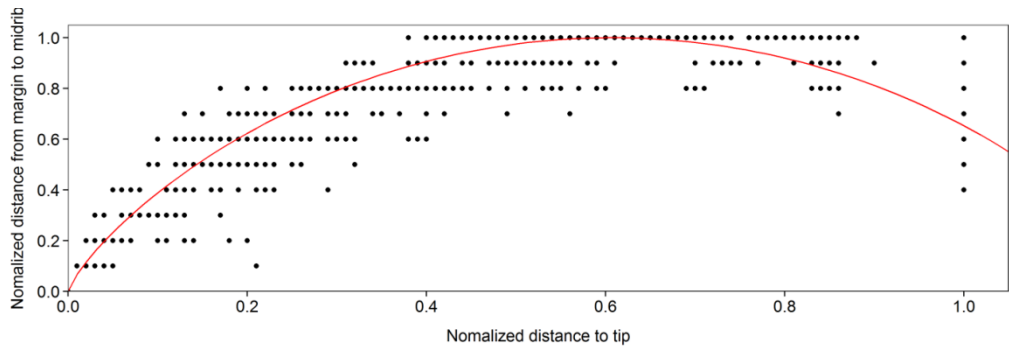


Fig. S2.1 The shape of a full-grown wheat leaf by plotting normalized margin to midrib distance ( $0.5 * \text{the width measured}$ ) versus normalized distance to leaf tip. Points are measurements, line is the shape function with fitted parameters (Eq. 2.1 in main text). For the spring wheat cultivar used in this study, coefficient values were  $L_m = 0.713$  and  $C = 0.760$ .

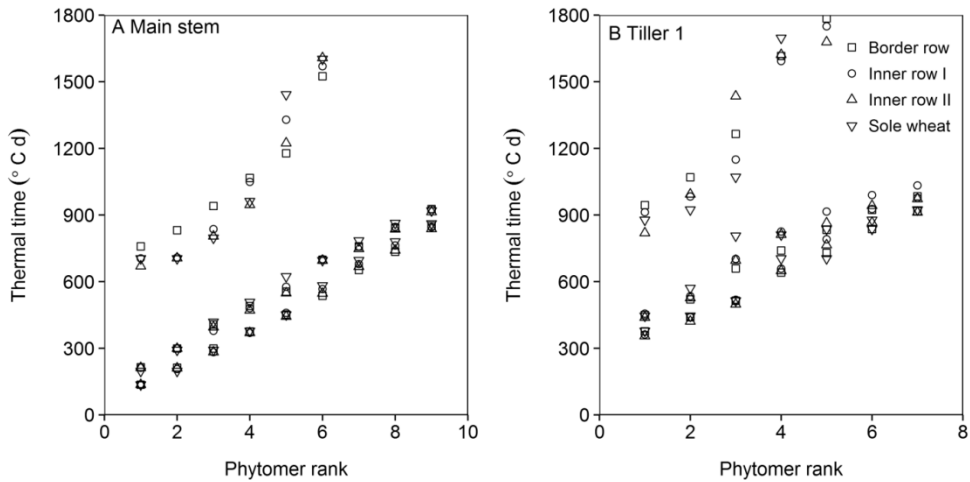


Fig. S2.2 Moment of leaf tip and collar appearance on main stem (A) and tiller 1 (B) of wheat in row 1 (border row, squares), row 2 (circles) and row 3 (triangles) in wheat-maize relay strip intercropping and in sole wheat (transverse triangles) versus phytomer rank. The top series of symbols represent leaf senescence time, middle series of symbols represent leaf mature time, and bottom series of symbols represent appearance time. Error bar representing SE are not shown since they would be smaller than the symbols.

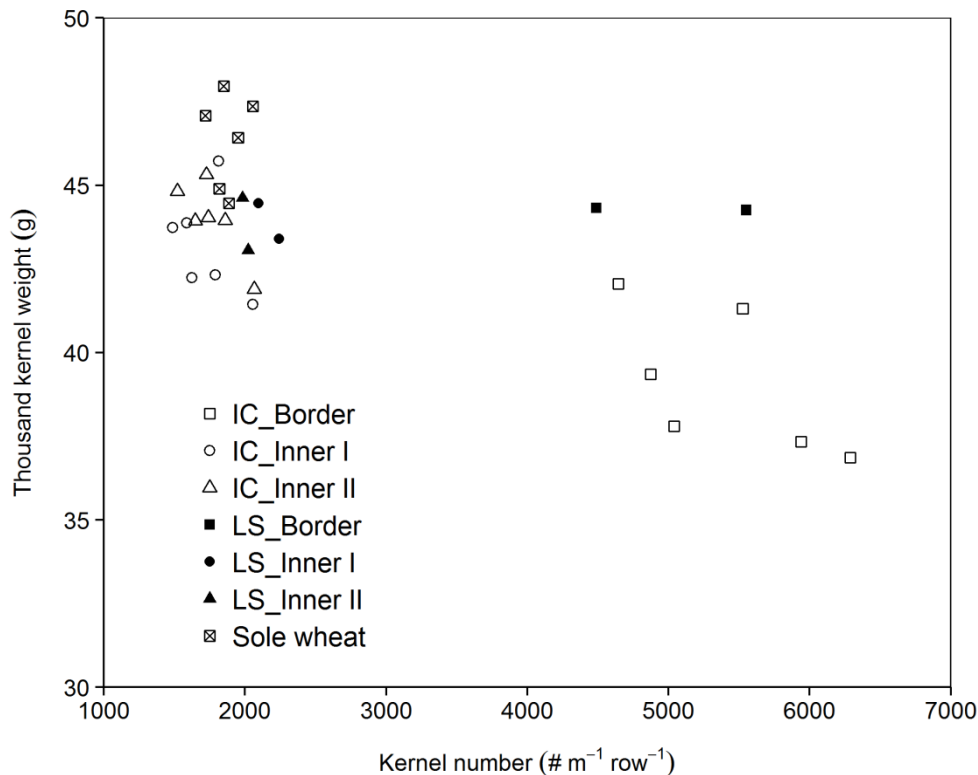


Fig. S2.3 Thousand kernel weight versus number of kernels per meter row length. LS represent the intercrop treatment with maize been sowed two weeks later compared to the default IC. Number of kernels per meter row length can be seen as the sink capacity. A big sink capacity would require a big source. This figure indicates that the low value of thousand kernel weight could be result from the interfere of maize plant which cast shade on the neighbouring wheat plants.

Table S2.1 Yield components in different rows of intercrop with late sown maize1.

Treatment	Grain (g m <sup>-1</sup> row <sup>-1</sup> )	Chaff (g m <sup>-1</sup> row <sup>-1</sup> )	Stem (g m <sup>-1</sup> row <sup>-1</sup> )	Number of ears (# m <sup>-1</sup> row <sup>-1</sup> )	Weight per ear (g)	Grain number per ear (#)	Thousand grain weight (g)
LS border rows	2222.3 ±23.4	52.6 ±11.9	116.9 ±18.7	118.2 ±1.2	1.9 ±0.2	42.4 ±4.0	44.3 ± 0.0
LS inner rows I	95.2 ± 2.0	17.1 ± 1.5	45.6 ± 1.0	51.2 ±1.7	1.9 ±0.0	42.3 ± 0.0	43.9 ±0.5
LS inner rows II	87.8 ± 0.7	15.0 ± 0.9	39.6 ± 1.2	49.5 ±3.0	1.8 ±0.1	40.6 ± 2.9	43.8 ± 0.8

1In this pilot intercrop treatment, maize was sown two weeks later than that in the intercrop maize. The treatment was conducted adjacent to the yield trial for assessing the effect of sowing time of maize on the wheat yield. The pilot treatment had two plots which had the same plot size and row settings as the plot in the yield trial.

## Appendix II

### Early competition shapes maize whole plant development in mixed stands

Method S3.1 Calculation of weighting factors of different PAR measurement positions in intercropping.

Because the distance between different measurement locations was not equal (see PAR measurement position one to five in Fig.1 counting from left to right), we calculated the representative length of each measurement and its weight relative to the width of maize strip based on several assumptions.

Before wheat harvest (taking wide intercrop as an example):

- a) Assume the space occupied by the wheat border row is 12.5cm (same for narrow intercrop) and the remaining 31.5 cm (12.5 cm for narrow intercrop) between wheat and maize row is occupied by maize, so the width of maize strip is  $75 + 31.5*2 = 138$  cm (100 cm for narrow intercrop)
- b) The mean PAR values of positions one and two represent the 31.5 cm (12.5 cm) between wheat and maize row; same for positions four and five. Mean values of position two and three represent the space from the maize row to the middle of two maize rows (37.5 cm), same for mean of position three and four.
- c) Subsequently, the weighting factors based on the representative length and maize strip width are 0.114, 0.250, 0.272, 0.250, 0.114 (wide intercrop) and 0.063, 0.250, 0.375, 0.250, 0.063 (narrow intercrop) before wheat harvest for position one to five

After wheat harvest:

The width of maize strip is 150 cm (width in monoculture maize) and mean value of position one and two represent 37.5cm. Therefore, the weighting factors are 0.125, 0.25, 0.25, 0.25, 0.125 for positions one to five, respectively, for both wide intercrop and narrow intercrop.

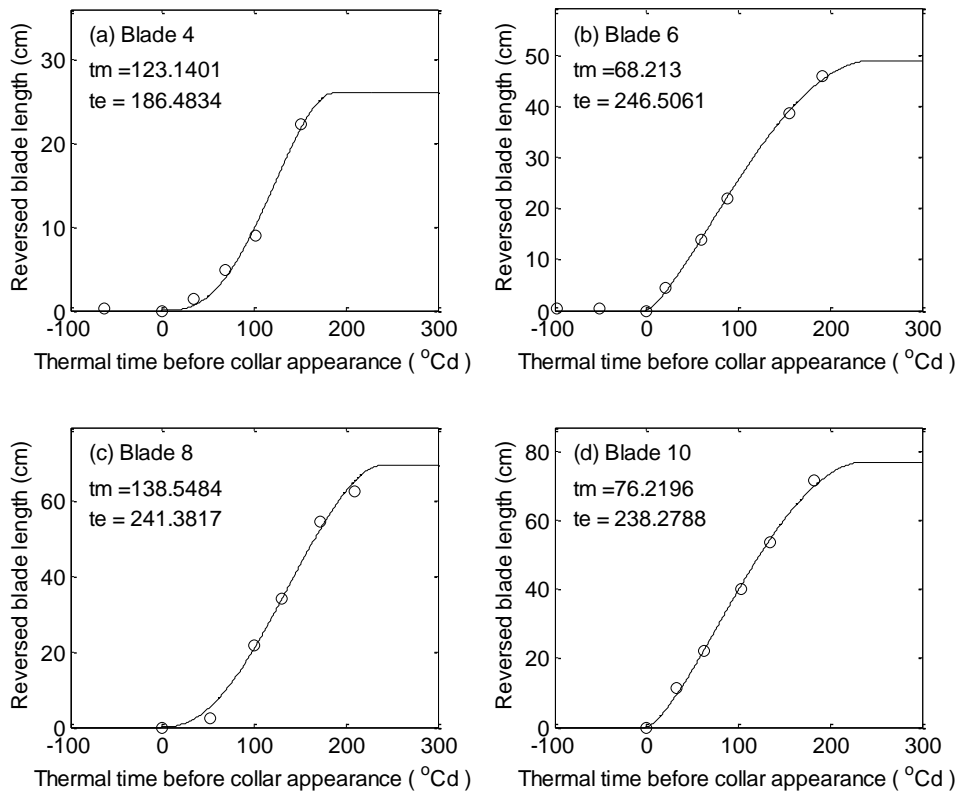


Fig. S3.1: Example of using beta function to derive blade elongation duration for each individual blade (Eq. 3.1)

- Collar emergence time was set to zero  $^{\circ}\text{Cd}$ , because collar emergence was estimated more reliably than tip appearance by the blade dynamics data.
- Subsequently, the curve was reversed by taking final blade length minus measured length versus absolute thermal time.
- Blade elongation duration  $t_e$  was fitted by the beta function (Eq. 3.1 in the main text).

Table S3.1 Fitting parameters for R:FR and PAR dynamic in three planting systems

		$\zeta_{\min}$	$\zeta_{\max}$	$k$ ( $^{\circ}\text{Cd}^{-1}$ )	$t_i$ ( $^{\circ}\text{Cd}$ )
R:FR	Monoculture	0.29	1.13	$-1.1 \cdot 10^{-2}$	420
	Wide intercrop	0.48	1.63	$-5.4 \cdot 10^{-3}$	-43
	Narrow intercrop	0.41	8.68	$-3.0 \cdot 10^{-3}$	-981
PAR	Monoculture	$5.9 \cdot 10^{-2}$	0.97	$-8.4 \cdot 10^{-3}$	486
	Wide intercrop	0.23	0.82	$-1.3 \cdot 10^{-3}$	528
	Narrow intercrop	0.19	0.78	$-1.1 \cdot 10^{-3}$	509

Where  $\zeta$  is the red : far-red ratio.  $\zeta_{\min}$  and  $\zeta_{\max}$  are the lower and upper asymptotes (dimensionless),  $k$  is the slope at the inflection point ( $^{\circ}\text{Cd}^{-1}$ ), and  $t_i$  is the thermal time of the inflection point ( $^{\circ}\text{Cd}$ ).

Table S3.2 Coordination between leaf initiation and leaf appearance

Initiated leaves (#)	8	9	10	11	12	13	14	15
Appeared leaves (#)	3	3.63	4.26	4.89	5.52	6.15	6.78	7.41

Estimation equation is:  $\text{Appeared leaves} = 0.63 * (\text{Initiated leaves} - 8) + 3$ . Initial estimation point was set to 3 appeared leaves and 8 initiated leaves, subsequently 0.63 leaves appeared per initiated leaf (Padilla & Otegui, 2005).



# Appendix III

## Towards modelling the flexible timing of shoot development: simulation of maize organogenesis based on coordination within and between phytomers

Method S4.1: Estimation of the ratio between the final length of internode  $n$  and sheath  $n-1$

To estimate the final length of internode  $n$ , a relationship between the final length of internode  $n$  and the final length of the encapsulating sheath ( $n-1$ ) was set up. The ratio between final length of internode  $n$  and sheath  $n-1$  was fitted according to a quadratic function (Eq. S4.1). Regressions were made using the nonlinear least square function (nls) in the ‘stats’ package of the R programming language (R Core Team, 2014).

Complementary data of normal density 'D  ' in 1996, and 'Nobilis' in 1998 and in 2000 were also used for quantifying the relationship between final length of internode  $n$  and final length of the encapsulating sheath ( $n-1$ ). The agronomic treatments and data collection in these experiments were similar as in the experiment with D   in 2000. Relative rank, defined as the ratio between current rank and final rank, was used since the final leaf number for normal density 'D  ' in 1996 was 17 while all others were 15.

$$ratio_{int/sth} = ratio_{max} * (2 * \rho_{max} - \rho_b - \rho) * \frac{(\rho - \rho_b)}{(\rho_{max} - \rho_b)^2} \quad (Eq. S4.1)$$

where  $ratio_{int/sth}$  is the ratio between final length of internode  $n$  and sheath  $n-1$ ,  $ratio_{max}$  is the maximum ratio,  $Q_{max}$  is the relative phytomer rank where maximum ratio is reached,  $Q_b$  is the relative starting rank where the  $ratio_{int/sth}$  is equal to zero. For model implementation, final leaf number was fixed to 15 and relative ranks was transferred to real ranks. The fitted  $ratio_{max}$  was  $1.29 \pm 0.2$ ,  $Q_{max}$  was  $0.78 \pm 0.03$ ,  $Q_b$  was  $0.24 \pm 0.02$ . The fitting results were shown in Fig. S4.2.

#### Method S4.2: Justification of coordination rules used in the model

The model is based on a detailed consideration of empirical data and proposed mechanisms for coordination of leaf growth in maize and other species in the Poaceae. Here we summarize the main empirical findings supporting our model.

##### *Dynamics of blade extension*

- Blade initiation occurs at a constant thermal time interval. The initiation of a blade is defined as the moment when the length of the blade reaches 0.25 mm (Andrieu *et al.*, 2006).
- The linear phase of blade growth was found to start close to the time of leaf tip emergence for blades of ranks below 10, and before that for higher ranks (Andrieu *et al.*, 2006), which supports the notion that the exponential phase of growth ends at tip emergence.
- Several studies found that the rate of cell division in the blade declined rapidly after tip emergence (Wilson and Laidlaw, 1985; Casey *et al.*, 1999; Parent *et al.*, 2009).
- The growing zone is shorter than the sheath tube and in the exposed section of a leaf, both cell division and cell enlargement have ceased (Begg and Wright, 1962; Davidson and Milthorpe, 1966).
- The extension of the blade and sheath are highly coordinated (Schnyder *et al.*, 1990; Casey *et al.*, 1999; Parent *et al.*, 2009). Once the ligule is differentiated, it propagates passively within the growing zone, delimiting an increasing sheath growing zone (basal) and a decreasing blade growing zone (apical) (Skinner and Nelson, 1994).

##### *Dynamics of sheath extension:*

The extension of the sheath contains three growth phases in this model: an exponential phase, a linear phase, and a decline phase. We distinguish events occurring before and after the switch to the generative phase, i.e. the initiation of the tassel, for sheath dynamics.

##### *Before tassel initiation:*

- In maize and rice (*Oryza spp*), sheath initiation (observable at a minimum length of 1 to 3 mm) was found to occur simultaneously

with tip emergence of the same leaf (Andrieu *et al.*, 2006; Parent *et al.*, 2009).

- The dynamics of sheath extension was described by a model possessing exponential plus linear growth phases (Hillier *et al.*, 2005).
- For phytomers below rank 8, the change to the linear phase of extension took place later (in both time and length) in higher density than in normal density (Andrieu *et al.*, 2006).
- The decline of sheath elongation rate was synchronized with the emergence of the collar of the phytomer in question (Fournier and Andrieu, 2000a).

*After tassel initiation:*

- Two features have been identified for sheath initiation shortly after tassel initiation (Paysant-Leroux, 1998; Andrieu *et al.*, 2006): (a) Collars became distinguishable on several leaves within a short period of time, although the corresponding sheaths had different lengths. (b) After this short period, the rate of emergence of distinguishable collars on leaves at higher ranks was close to that of leaf initiation.
- For phytomers 8-10, early sheath development was delayed in high density compared with normal density but fast extension took place simultaneously in both treatments (Andrieu *et al.*, 2006).
- For phytomers 11 and above, the dynamics of sheath extension were identical in both low and high population density from the first date of accurate measurement up to a size of 5-8 cm, after which sheath expansion took place at a lower rate in the high density treatment (Andrieu *et al.*, 2006).

*Dynamics of internode extension:*

The extension of the internode contains three phases in this model: an exponential phase, a transition phase, and a linear phase.

- Internodes are initiated having one single cell layer (20  $\mu\text{m}$ ), at about half a plastochron after the initiation of the corresponding leaf primordium (Sharman, 1942; Fournier and Andrieu, 2000a).
- Internodes elongate exponentially until the collar emergences of the phytomer in question.
- After collar emergence, the elongation rate of the sheath declines and

the elongation rate of the internode increases rapidly, while their sum was close to the linear elongation rate of the internode for both full light and shade conditions (Fournier and Andrieu, 2000b; Fournier and Andrieu, 2000a). However, such rapid elongation rate increase can only be found from ear initiation onwards defined as the time of lengthening of the axillary meristem (Siemer et al., 1969; Kiesselbach, 1999).

Method S4.3: Calculation of decline coefficient (d) of the elongation rate of sheath

$$\begin{cases} \frac{dE_n}{dt} = \frac{dS_n}{dt} + \frac{dI_n}{dt} \\ \frac{dS_n}{dt} = \frac{dS_n}{dt} - d * E_n \end{cases} \quad (\text{Eq. S4.2})$$

Where  $S_n$  is the length of sheath  $n$  (cm) and  $I_n$  is the length of internode  $n$ .  $E_n$  is the sheath length that out of the sheath tube (cm).  $d$  is the decline coefficient of the elongation rate of sheath, per unit of exposed sheath length ( $^{\circ}\text{Cd}^{-1}$ ).

The criterion for the optimization was to minimize the sum of squared differences between the simulated and observed length of the exposed part of sheaths at the moment when sheath is mature simultaneously for all phytomers. The rate of the length of  $E_n$  increases with time equal to the sum of the elongation rate of sheath and internode of the phytomer in question. Initial sheath elongation rate at collar emergence was set to fitted linear elongation rate for each individual rank, and the length of  $E_n$  at collar emergence was set to 0.1 cm. Average internode elongation rate was used. This average elongation rate of internode is calculated based on the duration between collar emergence and the time when sheath is mature and internode length increase during this period according to the data set based on multi-phase models for the growth of each organ, as parameterized by Andrieu *et al.* (2006). The value was subsequently fine-tuned such that modelled final sheath length approximated observed values at normal density.

Table S4.1: Simulation scenarios for exploring the cause of reduction of final length of blade at high ranks

Scenarios	Standard settings	Replacing $r_{B,n}^1$	Replacing $e^2$
S1	✓		
S2	✓	✓	
S3	✓	✓	✓

<sup>1</sup>For simulations at high density condition, replacing the  $r_{B,n}$  fitted for normal density by the  $r_{B,n}$  fitted for high density for ranks beyond 8.

<sup>2</sup>Replacing the single value of maximum elongation  $e$  by the linear elongation rate estimated for each rank ( $k_{B,n}$ ) in Andrieu *et al.* (2006).

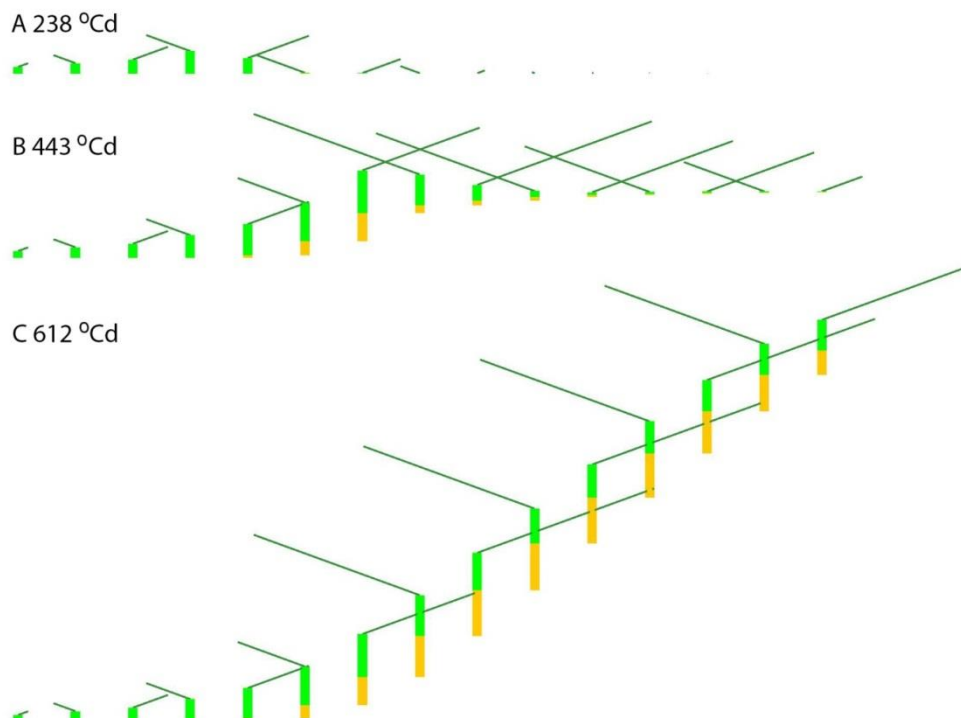


Fig. S4.1: Visualization of the extension of blades (dark green), sheaths (light green) and internodes (orange) for individual maize phytomers 1 to 15 (from left to right) at

### Appendix III

(a) 238 °Cd, (b) 443 °Cd, and (c) 612 °Cd. Maize phytomers have been represented next to instead of on top of each other to clearly show the individual organs and their sizes.

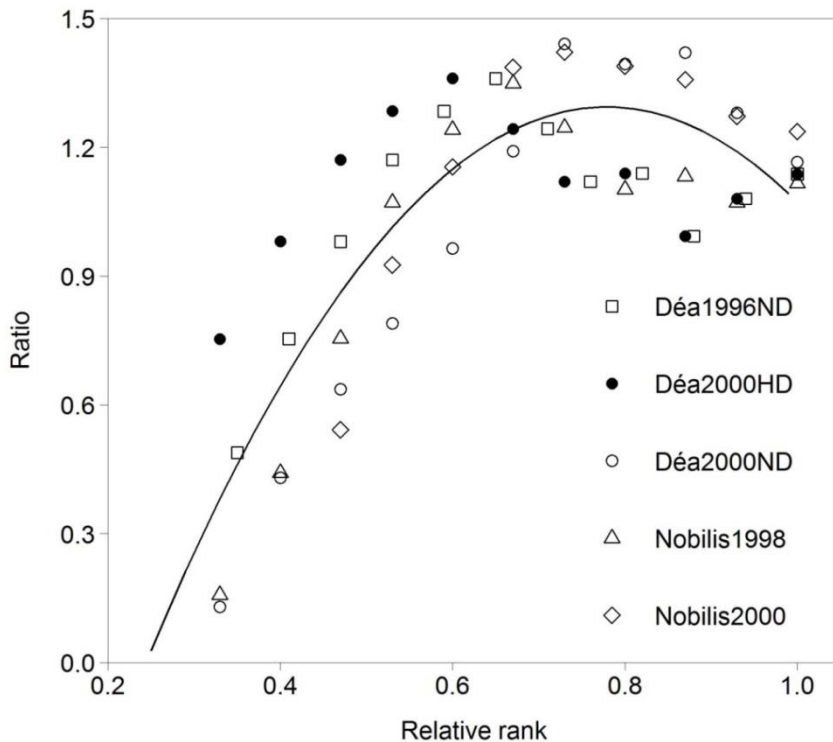


Fig. S4.2: The ratio of final internode length of rank  $n$  and final sheath length of rank  $n-1$  versus the relative rank defined as the current rank divided by the final leaf number. Data are for maize cv. 'D  a' at normal density in 1996 (squares) and in 2000 (open circles), and at high density in 2000 (filled circles), and cv. 'Nobilis' at normal density in 1998 (triangles) and in 2000 (diamonds). The line is the fitted curve of the quadratic function that we used.

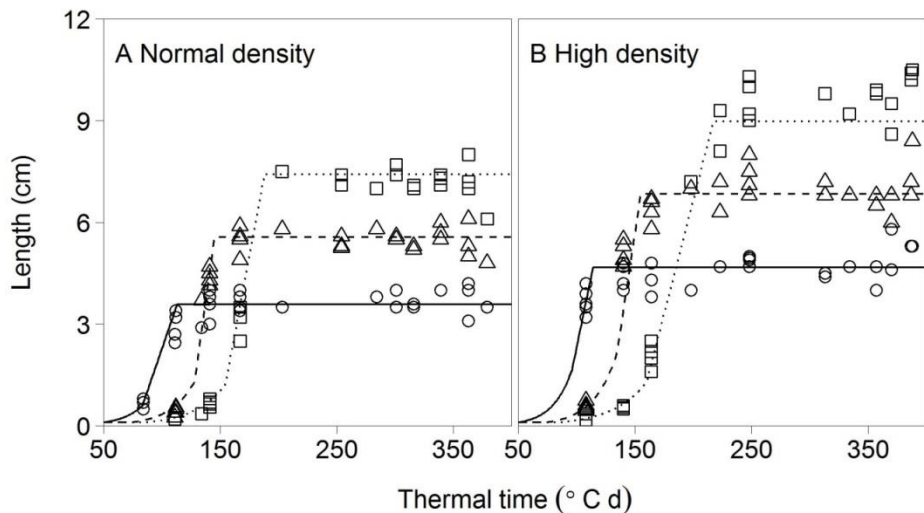


Fig. S4.3: Dynamics of length growth of sheath 1 (circles), 2 (triangles) and 3 (squares) for normal density (A) and high density (B) against thermal time. Symbols are measurements from maize cv. 'D  a' in 2000, and lines are fitted by equation Eq. S4.3 including an exponential phase and a linear phase (Hillier et al., 2005). Fitting was conducted using non-linear least squares optimization was conducted in R, using function optim() with appropriate starting values. The fitting procedure was repeated using different sets of starting values to check robustness of the fitted parameter values.

$$S_{n,t} = \begin{cases} S_0 * e^{R_1(t-T_0)} & T_0 < t \leq T_1 \\ S_{n,T1} + R_2(t-T_1) & T_1 < t \leq T_2 \\ S_{n,fin} & t > T_2 \end{cases} \quad (\text{Eq. S4.3})$$

Where  $S_{n,t}$  is the length of sheath  $n$  at time  $t$ .  $T_0$  ( $^{\circ}\text{Cd}$ ) is the point in thermal time at which the model begins, which corresponds to the moment when  $S = S_0$ .  $S_{n,T1}$  is the sheath length at the end of the exponential phase ( $T_1$ ).  $S_{n,fin}$  is the final length of sheath  $n$  that was reached at the end of linear phase ( $T_2$ ).  $R_1$  is the relative elongation rate at the exponential phase.  $R_2$  is the linear elongation rate at the linear phase.

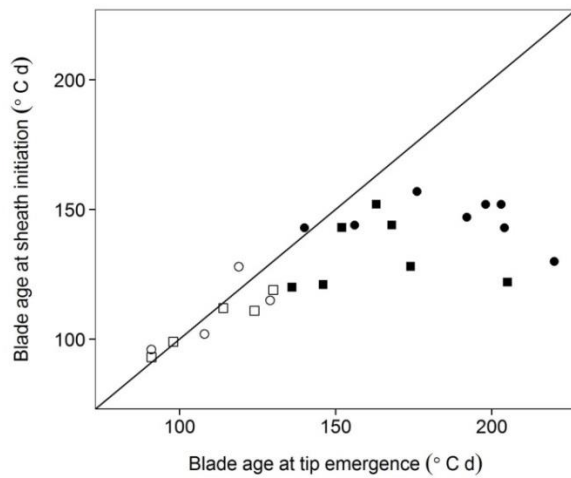


Fig. S4.4: Relationship derived from maize cultivar 'Dea' between blade age at sheath initiation (y-axis) and blade age at tip emergence (x-axis). Blade age was counted from the moment of initiation and expressed in  $^{\circ}\text{Cd}$ . Data represent normal density (squares) and high density (circles). Open symbols represent sheaths that initiated before tassel initiation, and filled symbols represent sheaths that initiated after tassel initiation.

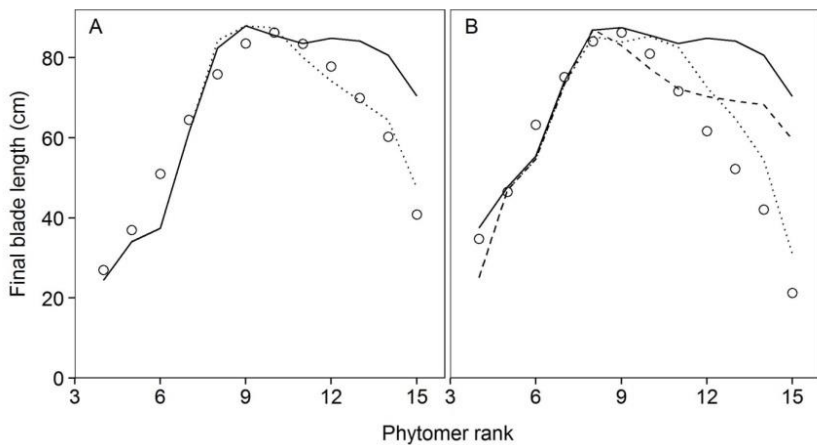


Fig. S4.5: (A) Final blade length of ranks 4-15 at normal density in scenarios S1 (solid line), S3 (dotted line); (B) Final blade length at ranks 4-15 at high density in scenarios S1 (solid line), S2 (dashed line), S3 (dotted line). See Table S1 for a description of the scenarios. Symbols are measurements on maize 'D  a' in 2000.

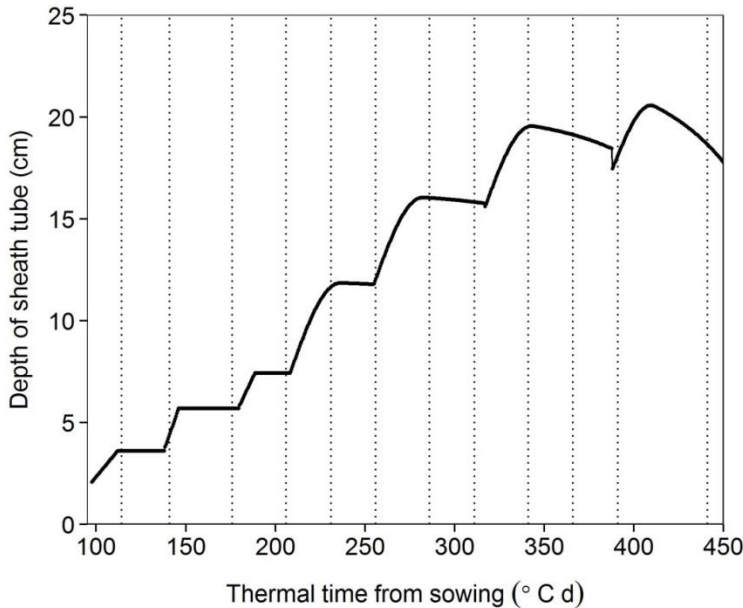


Fig. S4.6: The depth of sheath tube over time at normal density maize 'D  ' in 2000. Vertical dotted lines indicate the collar emergence time of ranks 4-15. The depth of sheath tube in this graph is calculated as the length of the sheath  $n$  which has the highest collar at the plant at that time minus the length of internode  $n+1$ . The gradual decrease of the depth of sheath tube represents the extension of internode  $n+1$ . The rapid drops represent represents the length of internode  $n+2$  at the moment of collar emergence  $n+1$ , which become the highest collar at that moment. Note the depth of sheath tube for all unemerged leaf tips and collars are different even at the same time because of the difference in the position of each leaf. The high rank leaves was elevated by the internode below it. Thus when sheath  $n$  has the highest collar at the plant, the depth of sheath tube for leaf  $n+x$  is  $S_n - \sum_{n+1}^{n+x} I_n$ .

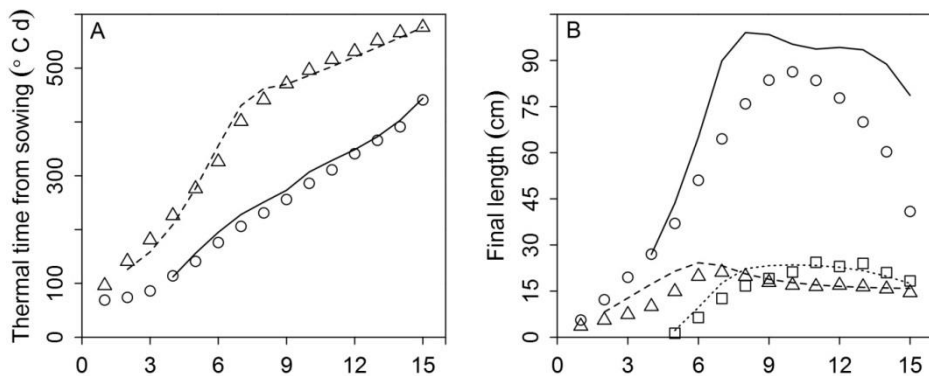


Fig. S4.7: Simulation results of only input the length dynamics of the first sheath. (A) Tip emergence (circles and solid line) and collar emergence (triangles and dashed line), and (B) final length of blade (circles and solid line), sheath (triangles and dashed line) and internode (squares and dotted line) versus phytomer rank. Symbols are measurements from normal density maize 'D  a' in 2000, and lines are simulations with only input the dynamics of first sheath length, collar emergence of first rank and tip emergence of first three ranks. Note with the current parameter settings for all sheaths, the model overestimated the sheath length of rank 2 and 3. This overestimation propagate to blade and sheath of the following phytomers.

## Appendix IV

### The contribution of plastic architectural traits to complementary light capture in plant mixtures

This supplementary material provides information on: (1) leaf geometry properties measurements and analysing methods (Method S5.1 and Fig. S5.11); (2) comparison of field dynamic of wheat-maize intercropping experiment with the simulated architectural development (Fig. S5.1-S5.3); (3) the original data of leaf life, organ size, leaf azimuth and declination angle distribution of wheat and maize for model input (Fig. S5.4-S5.11); (4) the appearance and senescence probability of each tiller type that input in the model (Table S5.1); (5) illustration of the arrangement of direct and diffuse light sources in the model, and verification of global radiation output and fraction of light penetration at the soil level in sole crops and intercrop (Fig. S5.12-5.15). (6) illustration of the leaf area dynamics in the model

#### Method S5.1: Leaf geometry properties measurements and analysing methods

Leaf geometry properties including leaf azimuth, declination angle and leaf curvature were one of the major input for the model. Leaf azimuth was defined as the horizontal angle measured clockwise from a south base line until the projected vector of the leaf at the horizontal plane. Leaf declination angle was defined as the vertical angle measured clockwise from plant shoot until the blade midrib. In order to gather data on leaf geometry of fully grown leaves, individual plants were digitized using a Polhemus Fastrak magnetic digitizer (Polhemus, Colchester, VT, USA). This device records X, Y and Z coordinates of objects relative to a reference point. Digitization of plants was done on three occasions, as it was not possible to digitize all fully grown leaves of wheat and maize at once because of leaf senescence. On the first occasion (May 3), 36 wheat plants in intercrop were digitized when the five main stem leaf was fully grown, twelve in each of rows 6 (border row), rows 5 (inner row I) and rows 4 (inner row II). On the second occasion (July 10), 36 intercropped wheat plants, 12 mono- and 12 intercrop-maize plants were digitized. At this time, wheat was at grain filling stage and maize had eight fully grown leaves. Finally, on the third occasion (September 20), 12 mono- and 12 intercrop-maize plants were digitized. At this time, wheat was harvested and maize is at grain filling stage.

Leaf azimuth for each rank was derived from the digitization database using principle component analysis (PCA). The data were first transformed from three dimension to two dimension by combining the x and y coordinates at horizontal plane into one axis by using function ‘princomp’ in package ‘stats’ in R (R Core Team, 2014). The transformed data were further used in the fitting of leaf curvature). The azimuth for each leaf was derived from loadings of the first component of the PCA analysis and corrected for the location of the leaves in the coordinate plane. The distribution of leaf azimuth of wheat was shown in Fig. S5.7 and maize was shown in Fig. S5.11.

Curvature of the blade midrib was modelled using the method developed by Prévot *et al.* (1991), and applied to maize (Fournier and Andrieu, 1998) and wheat (Fournier *et al.*, 2003; Evers *et al.*, 2005). The model describes a blade as a combination of an ascending parabolic part and a descending elliptic part. A description of the computational procedures and the associated source code are available from Junqi Zhu (junqi.zhu01@gmail.com). In this study, only the parabolic part was considered for wheat blades. See examples of modelled blade curvature in Fig. S5.3. The fitted parameters were gathered in a database specific for ranks. During simulation, parameter sets were chosen randomly from this database according to leaf rank..

Leaf declination angle was determined by taking the derivation of the parabolic part at the starting point. The distribution of leaf declination angle of wheat was shown in Fig. S5.8 and maize was shown in Fig. S5.12.

### Method S5.2: Data input for the model

**Wheat** (1) *leaf life* (Fig. S5.3): mean leaf elongation duration and leaf life span across treatments for each cumulative phytomer rank of wheat were input in the model. Cumulative phytomer rank of main stem and tiller leaves was calculated by counting leaves starting from the bottom of the plant, i.e. from main stem phytomer 1. Elongation duration was calculated as the duration between leaf appearance and collar appearance, and leaf life was calculated as the duration between leaf appearance and leaf senescence. The time of leaf senescence for high ranks were missing for some plants, their leaf life were estimated as the largest leaf life that was recorded for that rank. The life span of sheath and internode were set as 1100 °Cd in the model based on the mean of blade life span for ranks above 5. (2) *final organ size* (Fig. S5.4): raw records of blade length of each rank at main stem and tillers, grouped in plant, were input for different rows in intercrop. Mean leaf width across plants were input for different rows. Mean sheath length, internode length and internode diameter across rows and plants were input for each row. Mean values were calculated across main stem, tiller 1, tiller 2 and tiller 3, for which we have complete records in different rows,

based on cumulative phytomer rank. (3) *leaf azimuth* (Fig. S5.5): leaf azimuth were specified for each cumulative number and grouped in plants. The data were input for different rows in intercrop. (4) *leaf declination angle* (Fig. S5.5): leaf declination angle were specified for each cumulative number but didn't not group in plant due to many leaves senesced and having a declination angle larger than 90 °C when the measurement was done. The data were input for different rows in intercrop.

**Maize** (1) *leaf life* (Fig. S5.7): mean leaf elongation duration and leaf life span, specified for intercrop- and mono-maize, for each phytomer rank of maize were input in the model. For ranks 9 and 10 in intercrop, which were still green at harvest, life span was set to 1200 °Cd which was the maximum life span we observed. The life span of sheath and internode were set as 1100 °Cd in the model based on the mean of blade life span for ranks above 5. Leaf appearance time and mature time have been published in chapter 3. (2) *final organ size* (Fig. S5.8): raw records of blade length which were grouped in plant were input in the model specified for different treatments. Mean leaf width, sheath length, internode length and internode diameter across plants were input in the model specified for different treatments. (3) *leaf azimuth* (Fig. S5.9): leaf azimuth were specified for each rank and grouped in plants, and ere input in the model specified for different treatments. (4) *leaf declination angle* (Fig. S5.10): leaf declination angle were specified for rank but didn't not group in plant due to many leaves senesced and having a declination angle larger than 90 °C when the measurement was done. The data were input were input in the model specified for different treatments.

## Appendix IV

Table S5.1 Appearance and senescence probability of each tiller type

Tiller type	Treatment	T1	T1.1	T1.2	T2	T2.1	T2.1.2	T2.1.4	T2.2	T2.4	T3	T3.1	T3.1.3	T3.2	T3.3	T3.4	T4	T4.1	T4.2	T4.3	T5	T6	T7
	Sole wheat	0	0	0	1	0	0	0	0	0	0	1	0	0	0	0	0	1	0	0	0	0	0
Appearance probability	Border row	0	0	0	1	1	0.1	0.1	0.3	0.2	1	0.8	0.1	0	0.2	0.4	1	0.2	0.1	0.2	0	0	0
	Inner row	0	0	0	1	0.7	0	0	0.1	0	1	0.4	0	0	0	0	0	1	0	0	0	0	0
	Sole wheat	0	0	0	1	0	0	0	0	0	0	1	0	0	0	0	0	1	0	0	0	0	0
Senescence probability	Border row	0	0	0	0	0.4	0	0	0.5	0	0	0.4	0	0	0	0.2	0	0.5	0	0	1	1	0
	Inner row	1	1	1	1	1	0	0	1	0	0	1	0	1	0	0	1	0	0	0	0	0	0

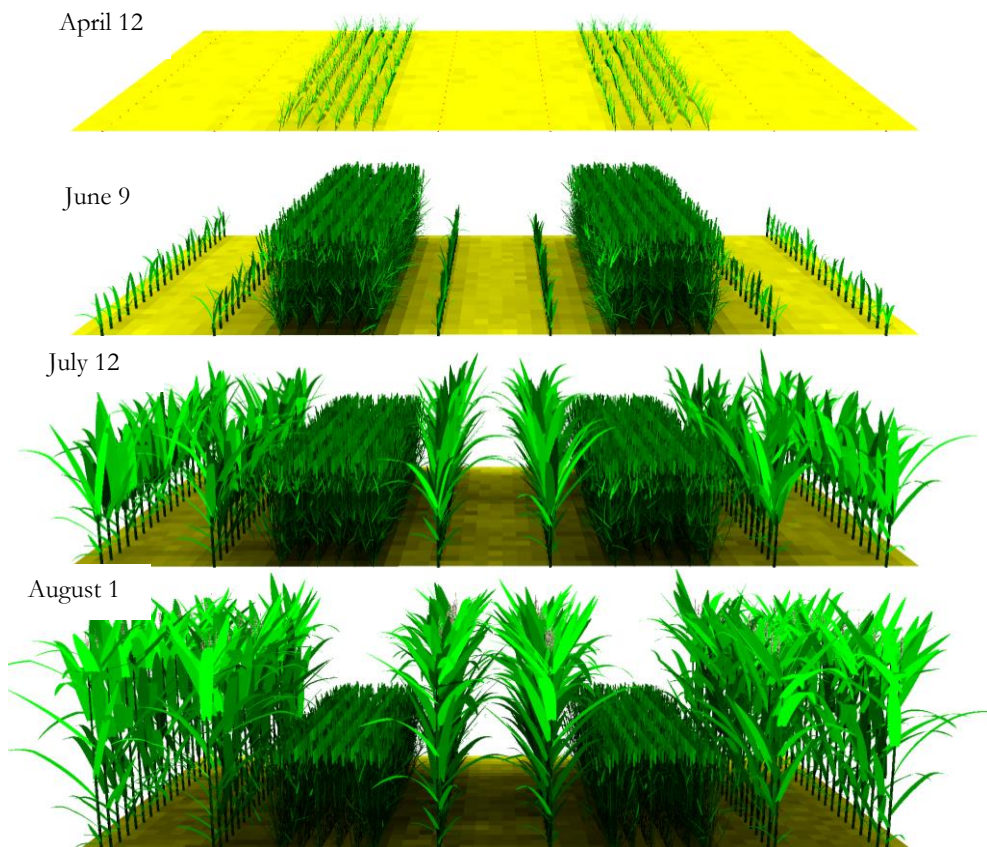


Fig. S5.1 Visualization of wheat-maize intercropping architectural development at 2 mature leaf stage of wheat (April 12), at 9 mature leaf stage (heading stage) of wheat and 3 mature leaf stage of maize (June 9), at milk development stage of wheat and 8 mature leaf stage of maize (July 12) and at ripening stage of wheat and tasseling stage of maize. Left side corresponding to east direction in the field.



Fig. S5.2 Comparison of field observation of monoculture wheat and maize (top panels) with the simulated of monoculture wheat and maize (middle and bottom panels) at jointing stage of wheat (May 10) and at tasseling stage of maize (July 28) respectively.

## Appendix IV

Input data of wheat:

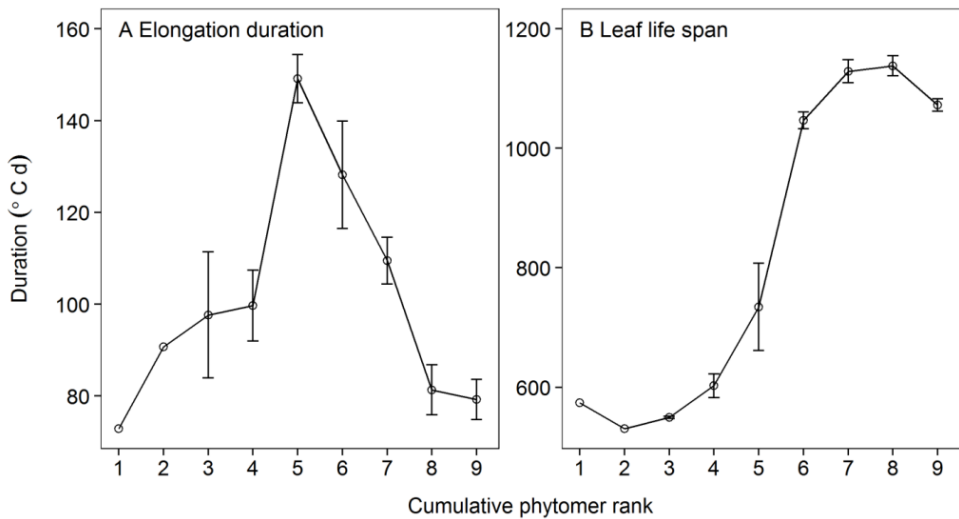


Fig. S5.3 Mean leaf elongation duration and leaf life span versus cumulative phytomer rank in intercrop and monoculture wheat. Cumulative phytomer rank of main stem and tiller leaves was calculated by counting leaves starting from the bottom of the plant, i.e. from main stem phytomer 1. Elongation duration was calculated as the duration between leaf appearance and collar appearance, and leaf life was calculated as the duration between leaf appearance and leaf senescence. Error bars indicate one standard error. Leaf appearance time and mature time have been included in chapter 2.

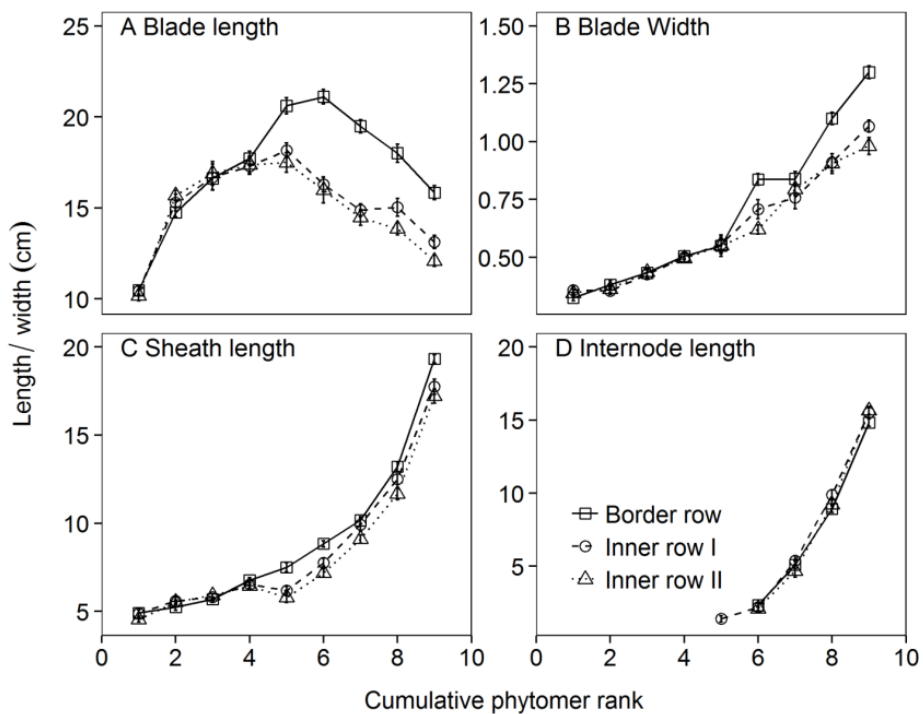


Fig. S5.4 Mean final blade length (A), final blade width (B), final sheath length (C) and final internode length (D) at border rows (squares and solid line), inner rows I (circles and dashed line) and inner rows II (triangles and dotted line) in intercrop. Error bars represent one standard error. Mean values were calculated across main stem, tiller 1, tiller 2 and tiller 3, for which we have complete records in different rows, based on cumulative phytomer rank.

## Appendix IV

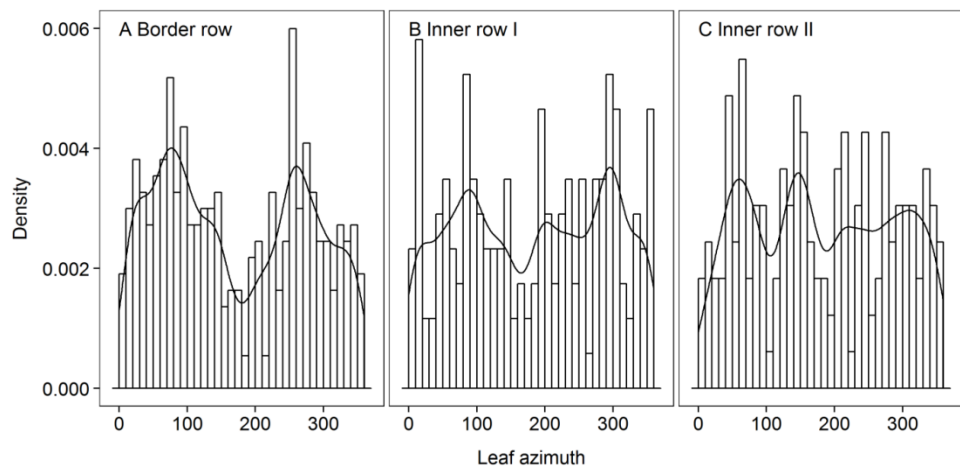


Fig. S5.5 Distribution of leaf azimuth for all available leaves at border rows, inner rows I and inner rows II in intercrop wheat.

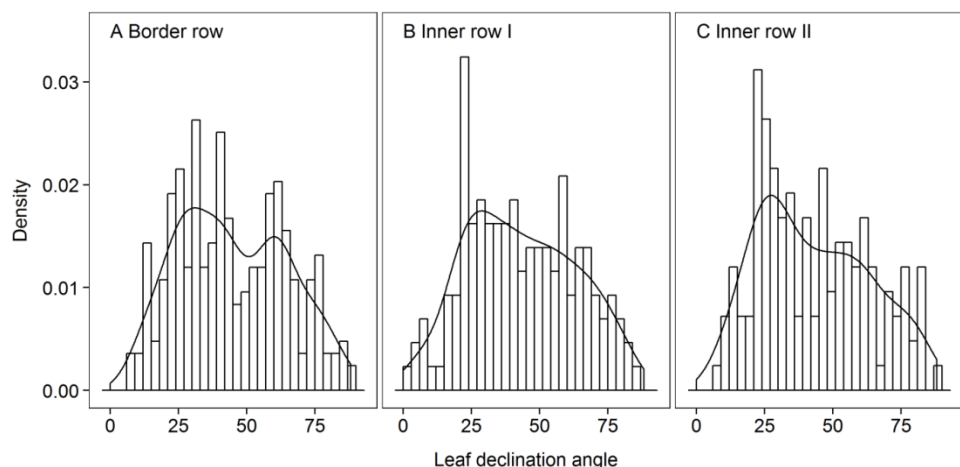


Fig. S5.6 The distribution of leaf declination angles for all available leaves at border rows, inner rows I and inner rows II of intercrop wheat.

Input data of maize:

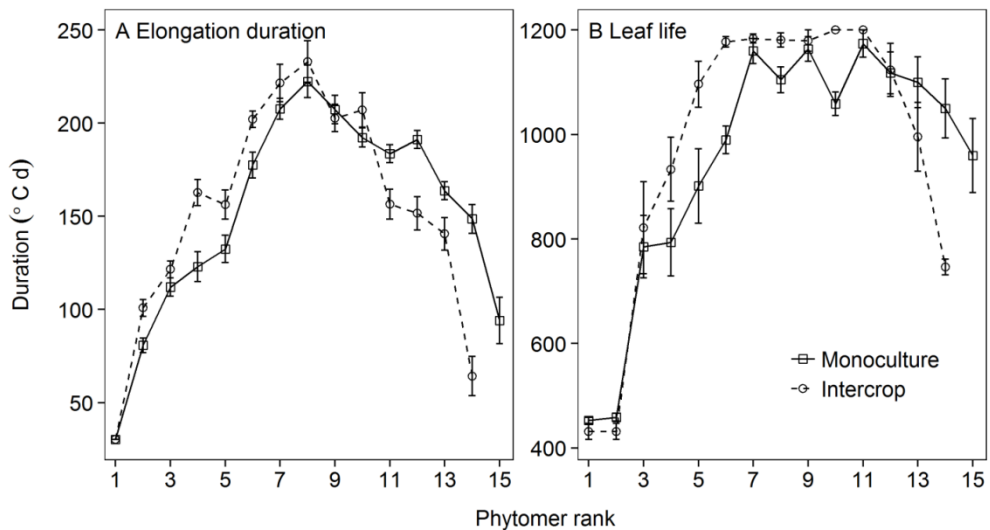


Fig. S5.7 Mean leaf elongation duration and leaf life span versus phytomer rank of intercrop- and mono-maize. Mean elongation and leaf life, specified for different treatments, were input in the model. Error bars indicate one standard error. Leaf appearance time and mature time have been shown in chapter 3.

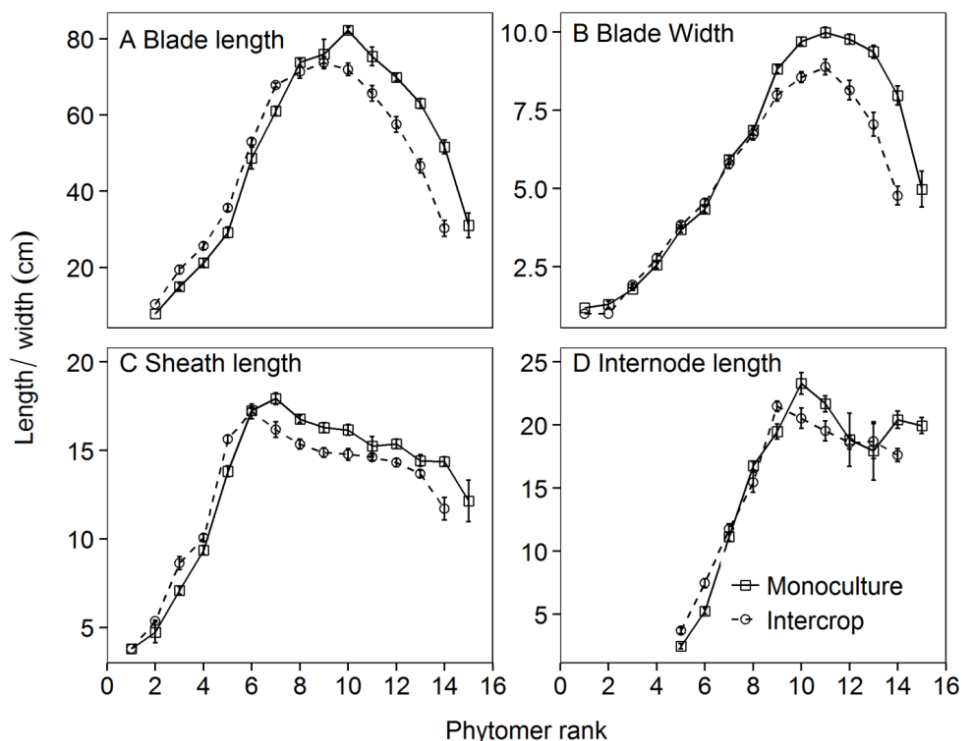


Fig. S5.8 Mean final blade length (A), final blade width (B), final sheath length (C) and final internode length (D) of mono-maize (squares) and intercrop-maize (circles) versus phytomer rank. Error bars indicate one standard error. Blade length and width, sheath length have been shown in chapter 3.

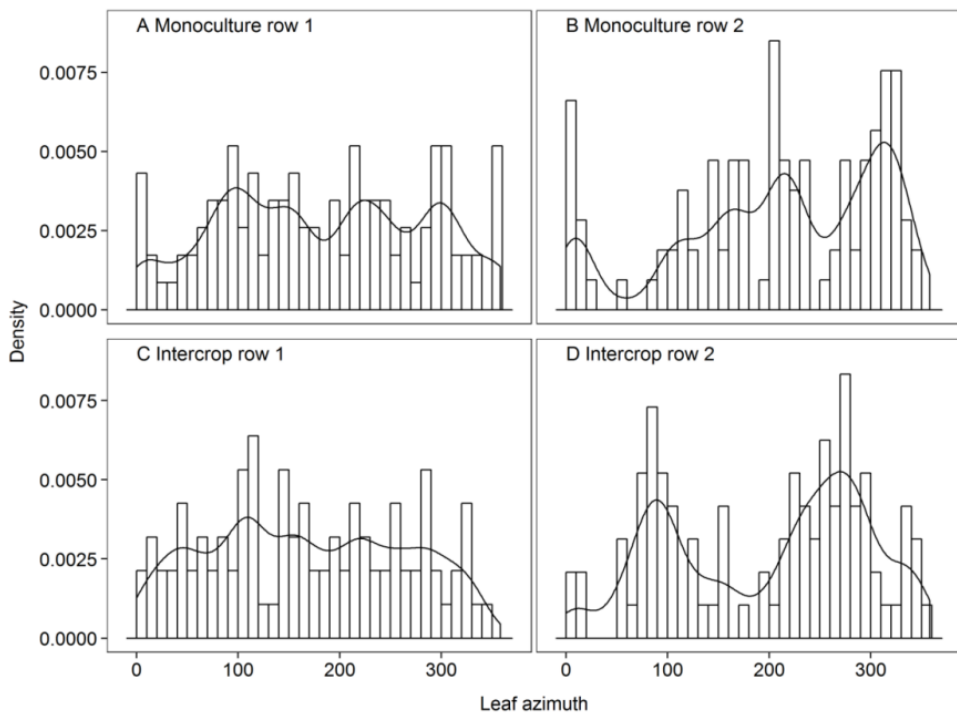


Fig. S5.9 Distribution of leaf azimuth for all available leaves in intercrop- and monoculture maize. Row number was counted from left to right in Fig. S5.2.

## Appendix IV

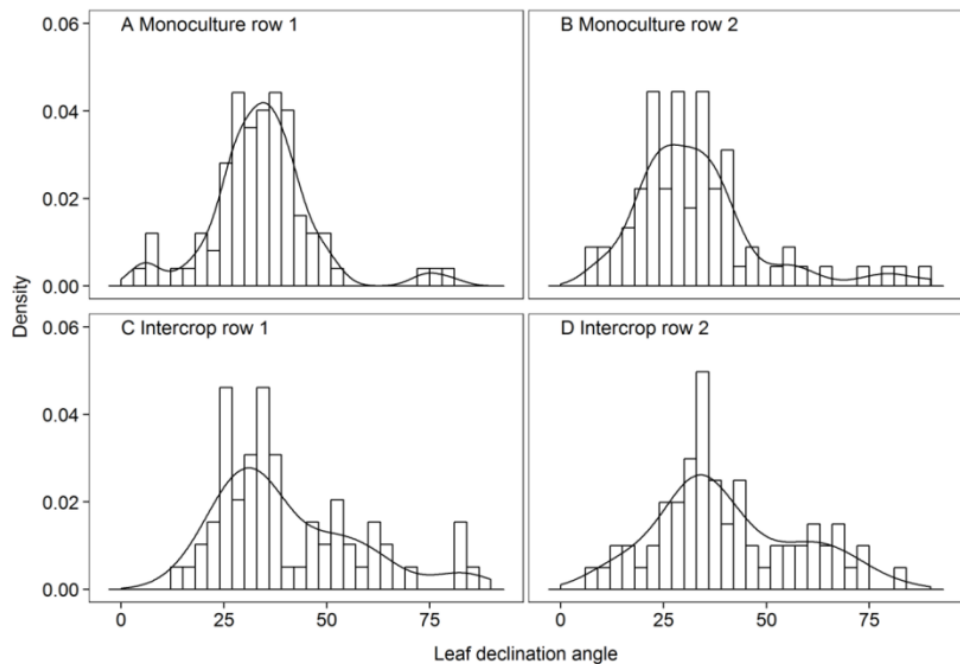


Fig. S5.10 The distribution of leaf declination angles for all available leaves in intercrop- and mono-maize. Row number was counted from left to right in Fig. 5.1.

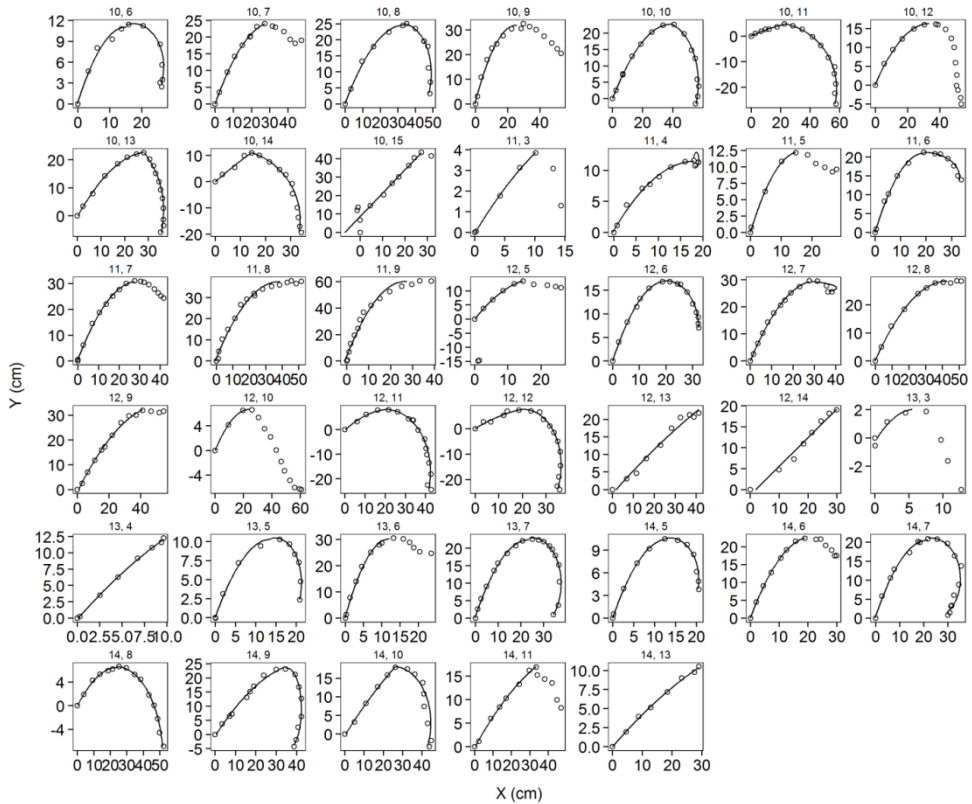


Fig. S5.11 Examples of modelled blade curvature for maize plants. Numbers above the panel denotes the plant number and leaf rank. Dots represent digitized points, lines represent the modelled blade curvature. x- and y-axes represent distance to the blade ‘insertion point’ – the point at which the blade is touching the stem. Only the fitting results with successful parabola part and ellipse part or with successful parabola part and it account for more than 80% of the whole blade length were further used in the model for the visualization of blade curvature.

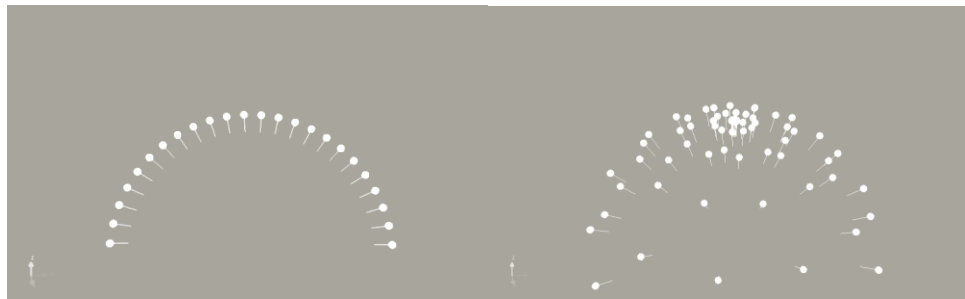


Fig. S5.12 Illustration of the arrangement of direct light and diffuse light sources in a virtual hemisphere.

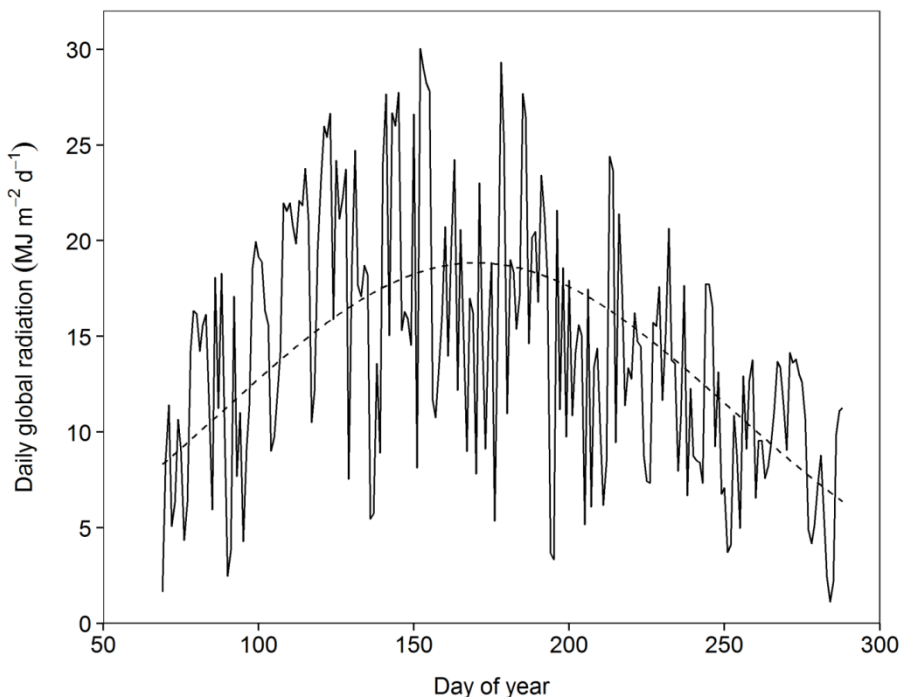


Fig. S5.13 Comparison of the observed (solid line) and simulated daily global radiation. Observed values were the daily global radiation measured at Deelen weather station ( $52^{\circ}3'39''\text{N}$ ,  $5^{\circ}53'17''\text{E}$ ) in 2011. Simulated values were calculated based on (Spitters, 1986) with mean atmospheric transmissivity ( $\tau$ ) of 0.35. The mean transmissivity was calculated based on the global radiation data at Deelen weather station from 2000 to 2010.

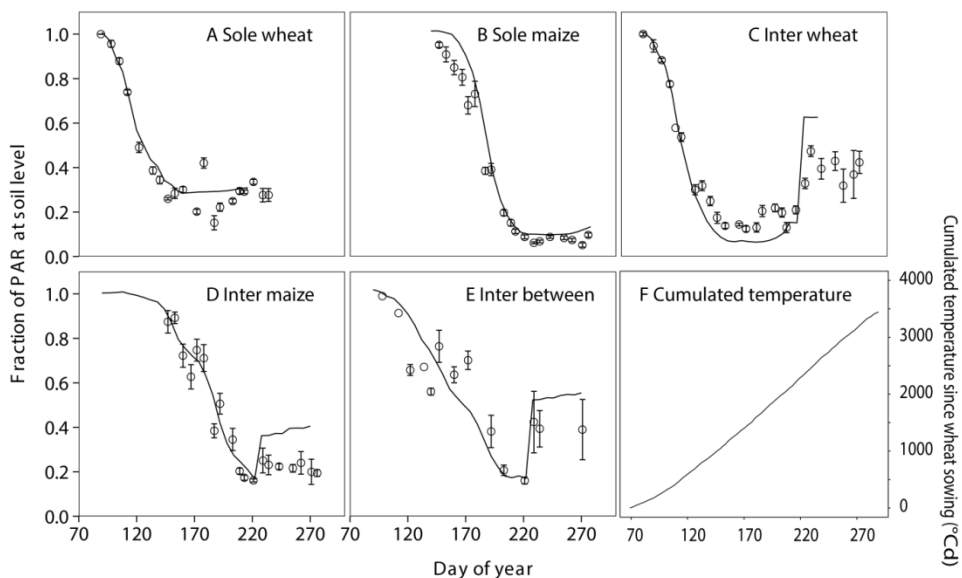


Fig. S5.14 Verification of light penetration at soil level around solar noon in sole wheat (A), sole maize (B), intercrop wheat strip (C), intercrop maize strip (D), and between wheat strip and maize strip (E). Panel F shows the conversion between day of year and cumulated daily mean temperature since wheat sowing. Points are observed mean percentage of fraction of PAR at soil level around solar noon. Lines are means of six simulations. The sudden increase in the fraction of PAR at 222 corresponds to the wheat harvest. The observed fraction of PAR is lower than the simulated value, which is partly because of the influence of stubble and weeds in the field.

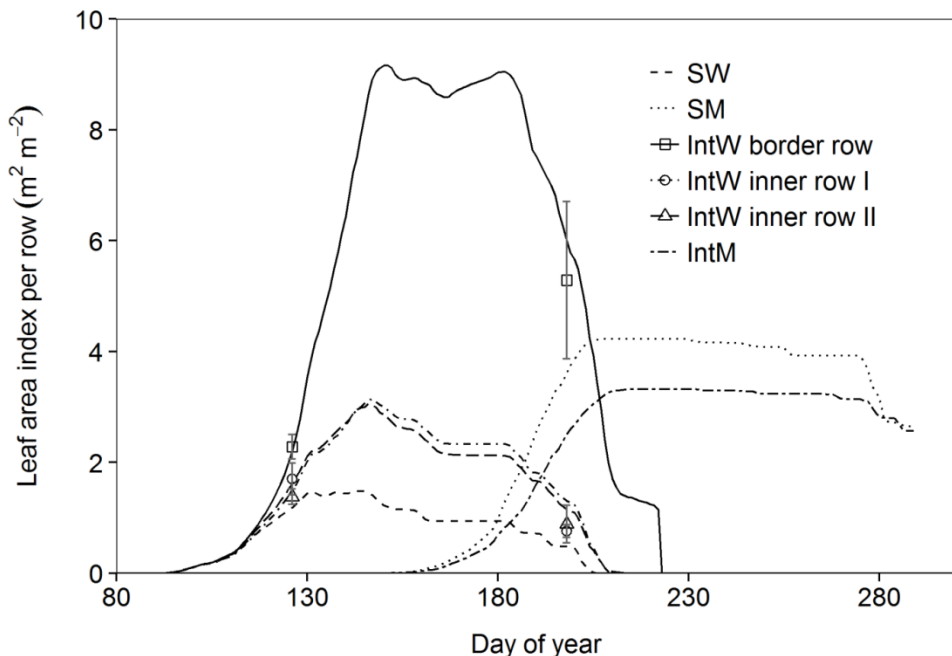


Fig. S5.15 Dynamics of leaf area index along the growing season in sole wheat (dashed line), sole maize (dotted line), border-row wheat (solid line), inner row I (dot-dashed line), inner row II (long-dashed line) and intercrop maize (two-dashed line). The leaf area index here were expressed per unit wheat or maize area, counting a meter row length as an area of  $0.125\text{ m}^2$  or  $0.75\text{ m}^2$ , based on the row distance of sowing. Points were measured leaf area index of wheat derived from the destructive measurements for determining fully-grown organ size and dry matter. 12 plants in each row were used in the measurements. The data for maize were not shown here since for each harvest we were only measured a proportion of leaves in all appeared leaves. Error bars for the simulated values were not shown since they were within one percentage of values.

## Summary

Despite a substantial increase in food production over the past half-century, one of the most important challenges facing the world today is still how to feed a rapidly growing population. However, the need for increased food production should be viewed in relation to the considerable environmental impact of agriculture. Diverse agricultural systems such as intercrops could contribute to sustainable food production, as both ecological and agricultural literature show that productivity, nutrient retention by soil, and resilience to stress (drought, diseases and pests) tend to increase with the number of species in one field. Yet, contrary to decades of crop improvement in sole cropping, little quantitative research has been done to determine the traits of cultivated species that drive the positive effects that have been shown for intercropping. Thus there is ample scope to further increase the advantages of intercropping systems by optimizing crop traits in relation to the specific conditions in intercrop systems. This thesis therefore addresses the following questions: 1). How does plant growth in intercrops differ from that in monocrops?; 2). how are different plastic responses of plants coordinated and regulated at organ level and 3). how does plasticity in plant development and growth contribute to the performance of an intercropping system.

Wheat-maize relay strip intercropping system was used as a case study in this thesis. I hypothesized that the yield advantage of wheat-maize intercropping can largely be explained by the increase in light capture, not by the increase in light-use efficiency. The enhancement in light capture can partly be due to the plant configuration in time and space, and partly be due to plant plastic responses to the intercrop light environment. Based on this hypothesis, we conducted detailed measurements of maize wheat plants grown in a field experiment either in sole crops or in intercrops throughout their life cycle. Furthermore, we obtained data on final organ sizes and yield from all these cropping types as well.

In chapter 2, I assessed the plastic responses of wheat when intercropped with maize, and tested the hypothesis that mixed cultivation triggers plastic responses of wheat that maximize light capture and result in overyielding. Compared to wheat plants in a sole crop and in inner rows of an

intercrop, plants in border rows of an intercrop experienced more favourable light conditions and exhibited the following plastic responses: (i) more tillers due to increased tiller production and survival, (ii) larger top leaves on both the main stem and the tillers, and (iii) higher chlorophyll concentrations. Grain yield per plant was 141% higher in border rows than in sole wheat. Together these results clearly show that plasticity in tillering is the most important trait for the overyielding of wheat in intercrop, and indicate the importance of plasticity in architectural traits for overyielding in multi-species cropping systems in general.

In chapter 3, I assessed the plastic responses of maize when intercropped with wheat. Compared to maize in monoculture, maize in intercrops had lower leaf and collar appearance rates, larger leaf blade and sheath sizes at low ranks and smaller ones at high ranks, increased blade elongation duration, and decreased R:FR and PAR at plant base during early development, and these effects became stronger with decreasing distance between adjacent maize and wheat rows. The data suggest a feedback between leaf initiation and leaf emergence at plant level and coordination between blade and sheath growth at the phytomer level. A conceptual model, based on coordination rules, was proposed to explain the development of the maize plant in pure and mixed stands.

In chapter 4, a model of maize development was constructed based on three coordination rules between leaf emergence events and dynamics of organ extension. The model was parameterized with data from maize grown at a low plant population density and tested using data from maize grown at high population density. The model showed that flexible timing of maize organ development can emerge from a set of coordination rules as well as the distribution of leaf sizes over ranks. In this model, whole-plant architecture was shaped through initial conditions that feed a cascade of coordinated events. Thus, a set of simple rules for coordinated growth of organs was sufficient to simulate the development of maize plant structure when assimilate supply is not a limiting factor.

In chapter 5, I present a novel approach to quantify the role of architectural trait plasticity in light capture in a wheat-maize intercrop, as an elementary example of mixed vegetation. Whole-stand light capture was

simulated for scenarios with and without plasticity based on empirical plant traits data. The plasticity effect was estimated as the difference in light capture between simulations with and without plasticity. Light capture was 23% higher in intercrop with plasticity than expected if each plant in intercrop captured the same amount of light as a plant in the monoculture of the same species. Thirty-six percent of this light increase was due to intercrop configuration alone while the remaining 64% was attributable to plasticity. For wheat the greater light capture in the intercrop was mostly attributed to plasticity in tillering and to a lesser extent to plasticity in leaf size and leaf angle distribution, while the configuration effect was almost negligible. Conversely, in maize the increased light capture in the intercrop was entirely due to the configuration effect and plasticity contributed negatively. The quantitative results clearly show the importance of developmental plasticity in explaining overyielding in this two-species system. It is suggested that in general, plasticity can have a large contribution in driving the potential benefits of niche differentiation in diversified plant systems.

In conclusion, although intercropping has been practiced for thousands of years, the mechanisms that make intercropping advantageous are still poorly understood. This study provided insights on how plants grow in intercrop and on how plastic responses of a plant are regulated. I identified the importance of plant plastic responses in enhancing the performance of the whole system, and present a novel method for quantifying their contribution. While the thesis focuses on a specific C3-C4 plant intercropping system, methods and main conclusions may apply to other intercropping systems and mixed plant communities. More research nevertheless still needs to be done to investigate the mechanisms that drive the advantage of intercropping.



## Samenvatting

Ondanks een aanzienlijke toename van de voedselproductie gedurende de afgelopen halve eeuw, blijft het voeden van een snel groeiende bevolking één van de belangrijkste uitdagingen waar de wereld op dit moment mee wordt geconfronteerd. De noodzaak voor grotere voedselproductie moet echter bezien worden in relatie tot de aanzienlijke invloed op het milieu door de landbouw. Gediversifieerde landbouwsystemen, zoals mengteelten ('intercropping') zouden kunnen bijdragen aan duurzame voedselproductie, daar zowel de ecologische als de landbouwkundige literatuur laat zien dat productiviteit, de capaciteit van de bodem om nutriënten vast te houden, en de mate waarin systemen veerkrachtig reageren op stress (droogte, ziekten en plagen) de neiging hebben toe te nemen met het aantal soorten op een veld. Niettemin, in tegenstelling tot de tientallen jaren waarin gewasmonoculturen werden verbeterd, is er weinig kwantitatief onderzoek gedaan om de eigenschappen van cultuurgewassen te bepalen die ten grondslag liggen aan de positieve effecten die aangetoond zijn voor mengteelten. Er zijn dus ruime mogelijkheden om de voordelen van mengteelten verder te laten toenemen door gewas eigenschappen te optimaliseren in relatie tot de specifieke omstandigheden in deze teeltsystemen. Dit proefschrift gaat hierbij in op de volgende vragen: 1). Hoe verschilt de groei van planten in gemengde systemen van die in monoculturen? 2). Hoe zijn verschillende plastische reacties van planten gecoördineerd op orgaanniveau? 3). Hoe draagt plasticiteit in de ontwikkeling en groei van planten bij aan het functioneren van een gemengd teeltsysteem?

In dit proefschrift wordt een systeem, bestaande uit afwisselende stroken van enkele rijen tarwe en mais, als voorbeeldsysteem gebruikt. Ik stel de hypothese dat het opbrengstvoordeel van het gemengde tarwe-maissysteem grotendeels verklaard kan worden uit de toename van de lichtonderschepping en niet door toename van de lichtbenuttingsefficiëntie. De versterkte lichtonderschepping is daarbij gedeeltelijk te danken aan de configuratie van de planten in ruimte en tijd en gedeeltelijk aan plastische reacties op de lichtverdeling in het gemengde teeltsysteem. Om deze hypothese te testen hebben we gedurende de gehele groeicyclus gedetailleerde metingen verricht

## *Samenvatting*

aan mais- en tarweplanten, die in een veldexperiment in mono- of in mengteelt groeiden. Verder verzamelden we gegevens over de grootte van volgroeide organen en over de opbrengsten van deze teeltwijzen.

In hoofdstuk 2 bepaalde ik de plastische reacties van tarwe, geteeld in mengteelt met mais en testte ik de hypothese dat gemengde teelt plastische reacties van tarwe op gang brengt die de lichtonderschepping maximaliseren en daardoor resulteren in meeropbrengst. vergeleken met tarweplanten in een monocultuur en in de binnenste rijen in een gemengd systeem, ondervonden de planten in de buitenste rijen van de tarwestroken in het gemengde systeem gunstiger lichtomstandigheden en vertoonden de volgende plastische reacties: (i) meer zijspruiten door toegenomen spruitproductie en overleving van spruiten, (ii) grotere bladeren bovenin de scheut bij zowel de hoofdas als de zijspruiten en (iii) hogere chlorofylconcentratie. De korrelopbrengst per plant was in de buitenste rijen 141% van die in monocultuur. Deze resultaten laten duidelijk zien dat plasticiteit in uitstoeeling de meest bepalende eigenschap is voor de meeropbrengst van tarwe in gemengde systemen. Meer in het algemeen wijzen de resultaten op het belang van plasticiteit in architectuurkenmerken voor de meeropbrengst in teeltsystemen met meerdere gewassoorten.

In hoofdstuk 3 bepaalde ik de plasticiteitsreacties van mais in mengteelt met tarwe. vergeleken met mais in monocultuur waren bij mais in de mengteelt de snelheden waarmee bladeren en bladbases verschenen lager, de bladschijven en bladscheden voor de lagere bladrangnummers groter en schijven en scheden voor de hogere rangnummers juist weer kleiner. Tevens nam de groeiduur van de bladschijven toe terwijl de R:FR en PAR aan de voet van de plant tijdens de vroege ontwikkelingsstadia lager was. Deze effecten waren sterker bij een grotere afstand tussen de mais en de aangrenzende tarwerijen. De gegevens suggereren een terugkoppeling tussen bladaanleg en bladverschijning op het niveau van de plant en coördinatie tussen de groei van de bladschijf en de bladschede op het niveau van het phytomeer. Op basis van deze coördinatieregels, is een conceptueel model voorgesteld om de ontwikkeling van maisplanten in mono- en in mengcultuur te verklaren.

In hoofdstuk 4 is een model van de ontwikkeling van mais geconstrueerd, dat gebaseerd is op drie regels die coördinatie tussen

bladverschijningsfasen en de dynamiek van lengtegroei van organen beschrijven. Het model werd geparameteriseerd met gegevens van mais die in lage plantpopulatiedichtheid werd geteeld en getest met gegevens van mais die in hoge plantpopulatiedichtheid werd geteeld. Het model toonde dat de flexibele timing van de ontwikkeling van de organen van mais voortkomt uit een stelsel coördinatieregels alsmede uit de verdeling van bladgrootte over bladnummers. In dit model wordt de architectuur van de plant bepaald door de initiële condities die bepalend zijn voor de daaruit voortkomende reeks van gecoördineerde ontwikkelingsstappen. Een stelsel van eenvoudige regels met betrekking tot gecoördineerde groei van organen was dus voldoende om de ontwikkeling van de structuur van de maisplant te simuleren wanneer assimilatenbeschikbaarheid geen beperkende factor is.

In hoofdstuk 5 presenteert ik een nieuwe benadering om de rol te kwantificeren die plasticiteit in architectuurkenmerken speelt in de lichtonderschepping van een gemengde teelt van tarwe-mais, waarbij dit systeem dienst doet als een elementair voorbeeld van een gemengde vegetatie. De lichtonderschepping van het gehele plantenbestand werd gesimuleerd voor scenario's met en zonder plasticiteit, gebaseerd op empirische gegevens over de betreffende plantkenmerken. Het effect van plasticiteit werd geschat als het verschil in lichtonderschepping tussen simulaties met en zonder plasticiteit. In het gemengde teeltsysteem was de lichtonderschepping 23 % hoger met plasticiteit dan verwacht kon worden indien iedere plant in het gemengde teeltsysteem dezelfde hoeveelheid licht zou onderscheppen als in een monocultuur van de betreffende plantensoort. Zesendertig procent van deze toename in lichtonderschepping was toe te schrijven aan de plantconfiguratie op zich, terwijl de overige 64 % toe te schrijven was aan plasticiteit. Voor tarwe was de grotere lichtonderschepping in gemengde teeltwijze voornamelijk toe te schrijven aan plasticiteit in uitstoeeling en voor een kleiner deel aan plasticiteit in bladgrootte en bladhoekverdeling, terwijl het configuratie-effect vrijwel verwaarloosbaar was. Omgekeerd was in mais de toegenomen lichtonderschepping bij gemengde teeltwijze in zijn geheel te danken aan het configuratie-effect terwijl plasticiteit een negatieve bijdrage had. De kwantitatieve resultaten laten duidelijk het belang zien van plasticiteit in ontwikkeling bij de verklaring van de meeropbrengst in dit systeem met twee

## *Samenvatting*

plantensoorten. De suggestie wordt gedaan dat in het algemeen plasticiteit in hoge mate kan bijdragen aan de voordelen van nichedifferentiatie in gediversifieerde plantsystemen.

Concluderend kan gesteld worden dat hoewel gemengde teelt al duizenden jaren gepraktiseerd wordt, de mechanismen welke gemengde teelt voordelig maken nog niet goed bekend zijn. Deze studie verschaft inzichten in hoe planten in gemengde teeltwijzen groeien en hoe de plasticiteitsreacties van een plant gereguleerd worden. Ik ontdekte het belang van plastische reacties van de plant voor het verbeteren van het functioneren van het systeem als geheel en presenteert een nieuwe methode om hun bijdrage te kwantificeren. Terwijl dit proefschrift zich richt op een specifiek systeem van gemengde teelt van een C3 en een C4 plant zijn de methoden en hoofdconclusies mogelijk ook toepasbaar in andere gemengde teeltsystemen en gemengde plantengemeenschappen. Niettemin is meer onderzoek nodig om de mechanismen te bestuderen die verantwoordelijk zijn voor het voordeel van gemengde teelt.

## 摘要

尽管粮食生产在过去的半个世纪中大幅增加，但要满足快速增长的食物需求仍然是当今世界面临的重要挑战之一。同时随着环境问题日益突显，维持农业生产和环境保护之间平衡也迫不及待。生态学和农学研究都表明多样化的作物生产系统例如间套作，有助于提高粮食生产的可持续性。这是因为多样化的作物生产系统增加了田间尺度上物种的多样性，提高了养分利用效率，土壤养分的固持和系统对干旱和病虫害等环境胁迫的抗性。然而，对比于我们长期对单作植物品种的改良和研究，很少有定量的研究来确定适合于间作种植模式的作物性状。因此，我们仍然有很大的空间来通过优化间作作物性状提高间作系统的生产力。本研究旨在了解：1) 植物生长在间作与单作条件下的区别；2) 植物不同器官的生长可塑性是如何相互联系与调节的；3) 植物生长可塑性在提高间作系统的生产力中的作用。

本论文使用小麦-玉米间作系统作为研究体系。我假设了小麦玉米间作的产量优势在很大程度上可以通过光捕获的增加来解释，而不是通过光利用效率的增加。间作光捕获的增强，部分是由于植物在时间和空间上的配置以及植物本身形态结构间的差异，部分是由于植物对间作光环境的适应。基于这一假设，我设计了一个田间试验来详细测定在不同种植模式下，小麦和玉米在整个生命周期中的发育和生长性状。此外，我还测定了不同种植模式下植物的最终器官大小和产量。

在第二章中，我评估了小麦在与玉米间作条件下对生长环境的响应。同时我检验了小麦生长可塑性可以最大限度地提高自身的光捕获并提高间作系统产量优势的这个假设。相比于单作小麦以及间作的内行小麦，间作边行小麦经历了更好的光照条件并表现出如下的生长反应：(i) 分蘖增多，主要来源于分蘖生产以及存活率的增加；(ii) 主茎和分蘖的顶部叶片增大；(iii) 叶片叶绿素浓度增加。边行小麦的单株产量是单作小麦的2.41倍。这些结果清楚地表明，小麦分蘖生长的可塑性是间作小麦取得产量优势的一个重要因素。这同时也表明植物生长可塑性在多样化的作物生产系统的产量优势中的发挥着重要作用。

在第三章中，我评估了玉米在与小麦间作条件下对生长环境的响应。对比于单作玉米，间作玉米在生长发育前期经历了较低的光照条件，表现出较低的叶片和叶耳出现速率，较长的下部叶片和叶鞘，较短的上部叶片和叶鞘以及较长的叶片伸长时间。这些现象随着玉米和小麦行之间的距离减小而增强。数据表明叶片分化和叶片出现在植株尺度上具有相互反馈作用。同时叶片和叶鞘生长在局部尺度上具有反馈调节作用。根据这个发现，我建立了一个概念模型来解释玉米在间作和单作条件下的生长和形态差异。

在第四章中，我建立了一个单株玉米的结构生长模型。这个模型是基于三个叶片和叶耳出现与器官生长之间的协调规则建立的。模型使用在较低密度的玉米数据来进行参数化，并使用较高密度的玉米数据来进行验证。该模型表明，玉米器官的伸长时间以及叶片大小的分布都可以协调反馈规则中产生。在这种模型中，玉米前期的形态改变

## 摘要

会通过一系列响应改变玉米后期的生长，并塑造玉米全株的形态结构。因此，在同化物质不限制玉米生长时，器官之间简单的生长协调反馈就足以描述玉米形态结构的生长了。

在第五章中，我以小麦-玉米间作为例提出了一个新的方法来量化植物形态结构的可塑性在植物多样性增加系统光捕获中的作用。基于实验测定的小麦玉米性状数据，我模拟了在有形态可塑性和没有形态可塑性两种条件下群体的光捕捉。植物形态可塑性的贡献是根据模拟中具有和不具有可塑性之间的群体光捕获的差异来计算的。在具有形态可塑性的情况下，间作的光捕获约为光捕获期望值的 1.23 倍。间作光捕获的期望值是假设间作中各植物的光捕获量与其在对应单作条件下的光捕获一致而计算得到的。在我们这个小麦玉米间作中，36%的光捕获量的增加是由于间作在时间和空间上作物配置以及植物结构形态之间的差异，而剩余的 64%则来源于植物形态的可塑性。小麦光捕获在间作中的增加大部分来源于小麦分蘖的可塑性，小部分来源于叶片大小和叶片角度分布的改变，而间作植物配置的效果几乎可以忽略不计。相反，玉米在间作中光捕获的增加全部来源于间作在时间和空间上作物配置以及植物形态之间的差异，而植物形态可塑性的贡献为负。定量分析清楚地表明植物形态可塑性在提高小麦玉米间作系统光捕获中的巨大贡献。基于这个发现我提出在广义情况下，植物形态可塑性在推动以及实现植物群体生态位差异中发挥着重要作用。

虽然间作已经实行了几千年，但对我们对间作增产的机制仍知之甚少。本研究详细描述了小麦与玉米在间作条件下形态结构的可塑性，并对不同器官在形态改变时的相互调节作用提出了新的见解。我确认了植物形态可塑性在提高整个系统表现性中的重要作用，并为量化其贡献提出新的方法。虽然本论文着重研究 C3 与 C4 植物之间的间作，但是我的方法和主要结论也可以适用于其他间作系统和混合群落。虽然如此，我们仍需要更多的调查研究来了解不同间作系统增产的机制。

## Acknowledgements

I am very grateful for having this opportunity and experience to do my PhD in Wageningen. I really learned a lot during the past four years. I went through the whole academic training process: hypothesis formulation – experiment design – data collection – data analysis – model set up – writing and publishing. Now finally I arrived at the final stage of my PhD. This is the time to look back and thank many people, who helped and accompanied me in this long and nice journey.

Looking back to the time when I started my PhD in 2010, first of all I would like to express my deepest gratitude to Prof. Fusuo Zhang and Prof. Xiaoguang Yang, and Prof. Lizhen Zhang at China Agricultural University, and to Dr. Wopke van der Werf at Wageningen University who promoted this intercropping project and accepted me as the PhD candidate for this project. Secondly, I would like to express my earnest thanks to my excellent multidisciplinary supervisor team: Prof. Niels P. R. Anten, Dr. Jochem B. Evers, Dr. Wopke van der Werf and Dr. Jan Vos. Without them, I would never finish this PhD thesis.

I am very grateful to my promoter, Prof. Niels P. R. Anten, for stimulating my interest in ecological research and in plant plasticity. Although he only joined my supervision team for one and half years, I strongly feel the change of my minds which become more ecologically oriented than agronomically oriented. I was amazed by his strong ability in linking different research subjects and formulating interesting interdisciplinary research questions. His suggestions for the role of plant plasticity in mixed vegetation was a reliable source of inspiration for me.

I am indebted to Dr. Jochem B. Evers, my first co-promoter, for his scientific guidance, and hands on teaching. His professional skills in functional-structural plant modelling and clear mind for programming have been very valuable to me. I cannot remember how many times I knocked at his door and looked for help in programming and writing. His constructive suggestions, word-by-word correction and strong requirement for short and clear articles shaped my writing style. Besides, I also benefited a lot from his pragmatic and open-minded attitude in dealing with questions and affairs.

## *Acknowledgements*

I am indebted to Dr. Wopke van der Werf, my second co-promoter, for bringing me to Wageningen and for his kind consideration for my daily life and study. He lent many books to me, and stimulated my interest in reading. His scientific discussion spirit and patient for spending several hours in guiding me to articulate clear definitions and questions always make me very gratitude to him. His inspiring ideas, critical comments often greatly improved my manuscript. His laughs and his regular sporting habits also influenced my life style a lot. I am also very grateful to his wife, Ms. Saskia Beverloo, for the warmly invitations and hospitality.

I am very grateful to Dr. Jan Vos, my third co-promoter for many constructive comments and reviewing manuscripts even after his retirement. His encouragement for exploring the nature of plant plasticity stimulated me to finish the work on coordinated plant development. I am also very much moved by Jan and his wife Ada Wolse for serving us many times delicious and traditional food and snacks, and for organising a nice bus trip to northern Netherlands for me and others.

I am very grateful to Ing. Peter E.L. van der Putten. He is very dedicated and responsible. Without him, it would not have been possible for me to run the field experiment smoothly. I am also very grateful to Mrs. Ans Hofman, and the staff members of the Wageningen UR Experimental Centre (Unifarm), for their help in the field experiment.

I wish to express my profound appreciation to Dr. Bruno Andrieu, INRA Thiverval-Grignon, France. When I was puzzling about the nature of plant plasticity, he helped me out. Later I visited him and cooperated with him on writing Chapter 4 about simulating the flexible time of organ development. His inspiring ideas and open mind-set helped me a lot in this work.

I would like to give my earnest thanks to Prof. Fusuo Zhang for letting me joining three intercropping field trips in China, two in Gansu and one in south China, which helped a lot in understanding the real agricultural production condition in China and gain lots of insights about intercropping.

I also would like to thank all the people who made me have an enjoyable time in Wageningen. My special thanks to Mrs. Sjanie van Roekel, Mrs. Wampie van Schouwenburg, Mr. Alex-jan de Leeuw, Mrs. Nicole Wolffensperger, and Mrs. Henriette Drenth of CSA, and Dr. Claudius van de

Vijver and Mr. Lennart Suselbeek of PE&RC graduate school office for their hospitality and excellent organization in courses and other activities. I'm also very grateful for all colleagues in CSA, Plant Production System group, etc. They helped me in one way or another. My profound appreciation thus goes to Prof. Paul Struik, Dr. Xinyou Yin, Dr. Lammert Bastiaans, Dr. Tjeerd-Jan Stomph, Dr. Pepijn van Oort, Dr. Bob Duma, Dr. Peter Vermeulen, Dr. Aad van Ast, Dr. Willemien Lommen, Ir. Joost Wolf, Ir. Mink Zijlstra, Dr. Lenny van Bussel, Mr Michael Henke, prof. Gerhard Buck-Sorlin and many others for useful discussions and suggestions.

I wish to thank all my friends and PhD fellows in Wageningen. Many thanks to Liansun Wu, Zhaohai Bai, Wei Qin, Wenfeng Cong, JingJing Ying, Chunxu Song, Junfei Gu, Yang Yu, Guohua Li, Bin Chen, Lin Ma, Xia Liu, Xinxin Wang, Mingtian Yao, Vivi He, Chidu Huang, Yong Hou, Yu Hong, Jingmeng Wang, Qian Liu, Yunyu Pan, Kailei Tang, Wenjing Ouyang, Chunjie Li, Zheng Huang, Xu Cheng, Xuan Xu, Junyou Wang, Liping Weng, Guiyan Wang, Fulu Tao, Hiroe Zenihiro, Vu Nam, Stella Kibili, Alejandro Morales Sierra, Joao Nunes Vieira da Silva, Marcelo Labra Fernandez, Jan Hüskens, Herman Berghuijs, Andre Braga Junqueira, Marcia T. M. Carvalho, Clara Pena Venegas, Masood Awan, Mazhar Ali, Marloes van Loon, Merel Jansen, Catherine Kiwuka, Giovani Theisen, Jorad de Vries, Franca Bongers, Nageswara Vajaha, Uta Priegnitz, Niel Verhoog, Guillaume Ezui, Aart van der Linden, Maryia Mandryk, Greta van den Brand, Cesar Ospina Nieto, Edvaldo Sagrilo, Vicky Aerts, Adugna Bote, Dennis Tippe, Nynke Lobregt and many others for accompanying me here in Wageningen and making it memorable.

I also would like to give a special thanks to my wife Gou Fang, and my parents for all their understanding and support. My wife Gou Fang came to Wageningen to pursue her PhD together with me in 2012, and gave me lots of mental support to get me through hardship. Her lovely and open characters brought me lots of happiness, and made my life more colourful.

Junqi Zhu  
Wageningen, The Netherlands  
November, 2014



## Publication list

Zhu, J. Andrieu, B., Vos, J., van der Werf, W., Fournier, C., Evers, J. B. 2013. Simulating maize plasticity in leaf appearance and size using regulation rules. *Proceedings of the 7th International Conference on Functional-Structural Plant Models*, 9-14 June, Saariselkä, Finland.

Zhu, J., Vos, J., van der Werf, W., van der Putten, PEL., Evers, JB, 2014. Early competition shapes maize whole plant development in mixed stands. *Journal of Experimental Botany* **65**(2):641-653.

Zhu, J., Andrieu, B., Vos, J., van der Werf, W., Fournier C., and Evers, JB. 2014. Towards modelling the flexible timing of shoot development: simulation of maize organogenesis based on coordination within and between phytomers. *Annals of Botany* **114**(4):753-762.

Zhu, J., van der Werf, W., Vos, J., Anten, NPR., van der Putten, PEL., Evers, JB. 2014. Overyielding of wheat in intercropping is associated with plant architectural responses that enhance light capture (submitted).

Zhu, J., van der Werf, W., Anten, NPR., Vos, J., Evers, JB. 2014. The contribution of phenotypic plasticity to complementary light capture in plant mixtures (submitted).



## **PE&RC Training and Education Statement**

With the training and education activities listed below the PhD candidate has complied with the requirements set by the C.T. de Wit Graduate School for Production Ecology and Resource Conservation (PE&RC) which comprises of a minimum total of 32 ECTS (= 22 weeks of activities)



### **Review of literature (6 ECTS)**

- Wheat and maize development, maize ontogeny and self-coordination, intercropping pros and cons, functional-structural plant modelling, the ecological consequences of phenotypic plasticity (2010-2014)

### **Writing of project proposal (4.5 ECTS)**

- 3-D Structural and functional adaptation of leaf canopies in intercrops (2011)

### **Post-graduate courses (3.9 ECTS)**

- Spatial ecology; PE&RC, SENSE, RSEE (2011)
- Mixed linear models; PE&RC (2012)
- Photosynthesis, climate and change; PE&RC (2013)

### **Laboratory training and working visits (3 ECTS)**

- Modelling and simulation with GroIMP; University of Göttingen (2010)
- Maize development and self-coordination; INRA, Centre de Versailles-Grignon (2012)

### **Invited review of (unpublished) journal manuscript (1 ECTS)**

- PLOS ONE: phenotypic plasticity in plant mixtures (2014)

### **Deficiency, refresh, brush-up courses (3 ECTS)**

- Advanced statistics (2010)
- Systems analysis, simulation and system s management (2011)
- Ecological modelling and data in R (2012)

**Competence strengthening / skills courses (1.8 ECTS)**

- PhD Competence assessments; Wageningen Graduate School (2011)
- Improving your writing; Wageningen Graduate School (2013)
- WGS PhD workshop; Wageningen Graduate School (2014)

**PE&RC Annual meetings, seminars and the PE&RC weekend (3 ECTS)**

- PE&RC Weekend (2010)
- PE&RC Day (2011 & 2014)
- Global soil fertility smart fertilizer (2011)
- Navigating complex socio-environmental processes (2011)
- Introduction to participatory socio-environmental games and simulations (2011)
- Traits as a link between systematics and ecology (2012)

**Discussion groups / local seminars / other scientific meetings (5.5 ECTS)**

- Plant production system seminar series (2010-2014)
- Centre for crop system analysis seminar series (2010-2014)
- Plant science seminar series (2010-2014)
- Plant and soil interaction discussion group (2011-2012)
- Modelling and statistics network (2012-2013)
- Understanding plant shoot development; a computational morphodynamics approach (2013)
- Symposium systems biology for food, feed and health (2013)
- Debate on future agriculture (2013)
- R Users meeting (2013-2014)
- Symposium systems biology for food, feed and health (2014)

**International symposia, workshops and conferences (7.2 ECTS)**

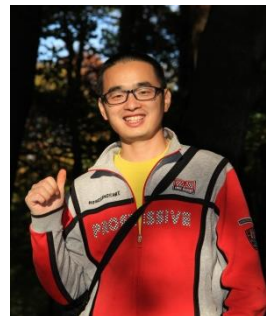
- Intercropping meeting and field trip in South China (2011)
- Can agricultural feed the world (2011)
- Netherlands annual ecology meeting (2013)
- Functional-structural plant modelling 7<sup>th</sup> international conference (2013)

**Lecturing / supervision of practical's / tutorials (1.2 ECTS)**

- Research methods in crop science (2011, 2013, 2014)

## Curriculum vitae

Junqi Zhu was born on 8<sup>th</sup> January, 1986 in Zhejiang Province, China. In 2004, he graduated from Zhejiang Tongxiang Senior High School. At 2008, he finished his Bachelor of Science degree in Agro-meteorology, at the College of Resources and Environmental Sciences, China Agricultural University (CAU), Beijing, China. From 2008 to 2010, he studied in the Department of Applied Agro-meteorology, CAU, for an MSc degree.



During his MSc studies, he worked on a thesis titled “Water use in different crop systems and analysis of regional water balance”. With a scholarship from the China Scholarship Council, he moved to the Netherlands and enrolled to the PhD programme of Wageningen University in September 2010. During his PhD study, he worked on the thesis “Plant plasticity in intercropping: mechanisms and consequences” at the Centre for Crop Systems Analysis.

## **Funding**

The research was funded by the scholarship from China Scholarship Council (CSC). Further support is provided by the grants from Natural Science Foundation of China: The Key Sino-Dutch Joint Research Project (Project No.31210103906).

**Cover design**

Junqi Zhu

**Printing**

GVO drukkers & vormgevers B.V., Ede







